

Optimization of Continuous Counter Current Adsorption Systems

by

Mohammad Elias Biswas

A Thesis Presented to the

FACULTY OF THE COLLEGE OF GRADUATE STUDIES
KING FAHD UNIVERSITY OF PETROLEUM & MINERALS
DHAHRAN, SAUDI ARABIA

In Partial Fulfillment of the
Requirements for the Degree of

MASTER OF SCIENCE

In

CHEMICAL ENGINEERING

December, 1995

INFORMATION TO USERS

This manuscript has been reproduced from the microfilm master. UMI films the text directly from the original or copy submitted. Thus, some thesis and dissertation copies are in typewriter face, while others may be from any type of computer printer.

The quality of this reproduction is dependent upon the quality of the copy submitted. Broken or indistinct print, colored or poor quality illustrations and photographs, print bleedthrough, substandard margins, and improper alignment can adversely affect reproduction.

In the unlikely event that the author did not send UMI a complete manuscript and there are missing pages, these will be noted. Also, if unauthorized copyright material had to be removed, a note will indicate the deletion.

Oversize materials (e.g., maps, drawings, charts) are reproduced by sectioning the original, beginning at the upper left-hand corner and continuing from left to right in equal sections with small overlaps. Each original is also photographed in one exposure and is included in reduced form at the back of the book.

Photographs included in the original manuscript have been reproduced xerographically in this copy. Higher quality 6" x 9" black and white photographic prints are available for any photographs or illustrations appearing in this copy for an additional charge. Contact UMI directly to order.

UMI

A Bell & Howell Information Company
300 North Zeeb Road, Ann Arbor MI 48106-1346 USA
313/761-4700 800/521-0600





**Optimization of Continuous Counter Current
Adsorption Systems**

BY

Mohammad Elias Biswas

A Thesis Presented to the
FACULTY OF THE COLLEGE OF GRADUATE STUDIES
KING FAHD UNIVERSITY OF PETROLEUM & MINERALS
DHAHRAN, SAUDI ARABIA

In Partial Fulfillment of the
Requirements for the Degree of

MASTER OF SCIENCE
In
CHEMICAL ENGINEERING

December, 1995

UMI Number: 1380774

UMI Microform 1380774
Copyright 1996, by UMI Company. All rights reserved.
This microform edition is protected against unauthorized
copying under Title 17, United States Code.

UMI
300 North Zeeb Road
Ann Arbor, MI 48103

**KING FAHD UNIVERSITY OF PETROLEUM & MINERALS
DHAHRAN, SAUDI ARABIA**

This thesis, written by
Mohammad Elias Biswas

*under the direction of his thesis advisor, and approved by his thesis committee,
has been presented to and accepted by the Dean, College of Graduate Studies, in
partial fulfillment of the requirements for the degree of*

MASTER OF SCIENCE IN CHEMICAL ENGINEERING

Thesis Committee:

Mirza Manirul Hassan
Chairman (Dr. M. M. Hassan)

Kevin F. Loughlin
Co-Chairman (Dr. K. F. Loughlin)

A. I. Fatehi
Member (Dr. A. I. Fatehi)

Dr. Dulaihan K. Al-Harbi
Department Chairman

Dr. Ala H. Rabeh
Dean, College of Graduate Studies

Date: 23/12/95



*To the memory of my mother
to my parents
to my wife
&
to my loving son*

ACKNOWLEDGMENTS

All praise to Allah for He is truly the One and only source of all knowledge. Peace and blessings of Allah be upon His Prophet.

I would like to express my profound and heartiest gratitude and sincerest appreciation to my advisor, Dr. Mirza M. Hassan, Associate Professor of Chemical Engineering Department, for his careful guidance and patience throughout this research. His continuous support and encouragement can never be forgotten.

I would also like to thank my co-chairman Dr. Kevin F. Loughlin, Associate Professor of Chemical Engineering Department, for his contribution and constant help. Appreciation is also extended to my committee member Dr. A. I. Fatehi, Assistant Professor of Chemical Engineering Department, for his valuable suggestions and interest in this work.

Acknowledgement is due to Chemical Engineering Department, King Fahd University of Petroleum & Minerals (KFUPM), Dhahran, Saudi Arabia, for the generous help and support for this research.

Special thanks must be given to my parents, wife, brothers, and sisters for their love and affection. Their sacrifices and foresightedness made this work possible.

Finally, I would like to thank all of my friends and relatives inside and outside this kingdom, for their encouragement and moral support.

CONTENTS

Chapter	Title	Page
	ACKNOWLEDGMENT	iii
	LIST OF FIGURES	viii
	LIST OF TABLES	xi
	ABSTRACT	xiv
	ARABIC ABSTRACT	xvi
1	INTRODUCTION	1
1.1	INTRODUCTION	1
1.2	ADSORPTION AS A SEPARATION TOOL	2
1.3	SELECTIVITY OF ADSORPTION SYSTEM	3
1.4	POROUS ADSORBENTS	3
	1.4.1 Activated Carbon and Carbon Molecular Sieves	4
	1.4.2 Silica Gel	4
	1.4.3 Activated Alumina	4
	1.4.4 Zeolites	5
	1.4.5 Ion exchange Resins	5
1.5	ADSORPTION EQUILIBRIUM	6
	1.5.1 Henry's Law	6
	1.5.2 Brunauer's Classification	6
	1.5.3 "Favorable" & "Unfavorable" equilibria	7
	1.5.4 Langmuir Isotherm	7
	1.5.5 Freundlich and Langmuir-Freundlich Isotherm	8
	1.5.6 BET Isotherm	8
1.6	ADSORPTION SEPARATION PROCESSES	8
	1.6.1 Cyclic Batch Systems	9

Chapter	Title	Page
	<i>1.6.2 Continuous Counter Current Systems</i>	<i>10</i>
	<i>1.6.3 Simulated Counter Current Adsorption Systems</i>	<i>11</i>
1.7	INDUSTRIAL SCALE COUNTER CURRENT ADSORPTION FRACTIONATION PROCESSES	12
	<i>1.7.1 "Sorbex" Process</i>	<i>12</i>
	<i>1.7.2 Parex and Ebex Processes</i>	<i>13</i>
	<i>1.7.3 Sarex Process</i>	<i>13</i>
	<i>1.7.4 Molex Process</i>	<i>14</i>
1.8	SCOPE AND OBJECTIVES OF PRESENT STUDY	14
	<i>1.8.1 Scope of Present Study</i>	<i>14</i>
	<i>1.8.2 Objectives of Present Study</i>	<i>14</i>
	REFERENCES	16
	NOMENCLATURE	17
2	LITERATURE REVIEW	29
	2.1 INTRODUCTION	29
	<i>2.1.1 Graphical (Mc-Cabe-Thiele Analysis)</i>	<i>29</i>
	<i>2.1.2 Numerical Simulation</i>	<i>31</i>
	2.2 REVIEW OF PREVIOUS WORK	33
	2.3 CONCLUSIONS	38
	REFERENCES	39
	NOMENCLATURE	43
3	THEORETICAL MODEL	50
	3.1 INTRODUCTION	50
	3.2 MODELING AND SIMULATION OF SMB PROCESSES	50

Chapter	Title	Page
	3.2.1 <i>Equivalent Counter Current Model : Dispersed Plug Flow Model</i>	50
	3.2.2 <i>Equivalent Counter Current Model: Equilibrium Stage Mode</i>	53
	3.2.3 <i>Equivalent Counter Current Model: A More Precise Approach</i>	54
3.3	OPTIMIZATION METHODS	57
	3.3.1 <i>Introduction</i>	57
	3.3.2 <i>The Objective Function</i>	57
	3.3.3 <i>Constraints</i>	58
	3.3.4 <i>Classification of Optimization Problem</i>	58
3.4	OPTIMALITY CONDITIONS	59
3.5	SOLUTION OF AN OPTIMIZATION PROBLEM	61
	3.5.1 <i>Solution of a nonlinearly inequality constrained Optimization problem</i>	61
	REFERENCES	64
	NOMENCLATURE	66
4	OPTIMIZATION OF CONTINUOUS COUNTER CURRENT ADSORPTION SYSTEM WITH NON-LINEAR ADSORPTION ISOTHERM	70
	4.1 INTRODUCTION	70
	4.2 THEORY	72
	4.2.1 <i>The Theoretical Model</i>	72
	4.2.2 <i>Optimization of Process Variables</i>	74
	4.3 RESULTS AND DISCUSSION	75
	REFERENCES	79
	NOMENCLATURE	81

Chapter	Title	Page
5	OPTIMIZATION OF "SORBEX" SYSTEM WITH NON-LINEAR ADSORPTION ISOTHERM	99
5.1	INTRODUCTION	99
5.2	THEORY	102
	5.2.1 <i>The Theoretical Model</i>	102
	5.2.2 <i>Optimization of Process Variables</i>	104
5.3	RESULTS AND DISCUSSION	106
	REFERENCES	111
	NOMENCLATURE	114
6	CONCLUSIONS AND RECOMMENDATIONS	134
6.1	CONCLUSIONS	134
6.2	RECOMMENDATIONS FOR FURTHER STUDY	135
	APPENDICES	
A	<i>Computer Program for Optimization for Two-section Model</i>	137
B	<i>Computer Program for Optimization for Four-section Model</i>	157
	VITAE	173

LIST OF FIGURES

Figure		Page
1.1	The Brunauer classification of isotherms	18
1.2	Dimensionless equilibrium isotherm showing the meaning of the terms "favorable," "linear," and "unfavorable."	19
1.3	Schematic diagram showing two basic mode of operation a) Cyclic batch b) Continuous countercurrent	20
1.4	Schematic diagram of the physical arrangement of columns and switch valves	21
1.5	Schematic diagram of a) the equivalent countercurrent system b) the notation used in describing the profile within an individual section	22
1.6	Two-section equivalent countercurrent arrangement	23
1.7	Four-section equivalent countercurrent arrangement	24
1.8	Schematic diagram of an industrial scale "SORBEX" system	25
2.1	McCabe-Thiele analysis of a countercurrent system.	44
2.2	McCabe-Thiele analysis of "SORBEX" system	45
3.1a	Schematic diagram of the physical arrangement of columns and valves for the precise model	69
3.1b	Schematic diagram of the mass balances of the jth bed for this model.	69
4.1	Schematic diagram of two section simulated moving bed	83
4.2a	Schematic diagram of two section equivalent countercurrent system	84
4.2b	Schematic diagram of the mass balance of jth section for two section equivalent countercurrent system	84
4.3	Flowsheet showing the algorithm of optimization procedure	85
4.4	Concentration profile for the base case (Run 2 in Table 1)	86

Figure	Page	
4.5	Plot of Recovery and Purity at various dimensionless Fructose concentrations in the raffinate for fixed length and diameter for (a) $\lambda_A = \lambda_B = 0$; (b) $\lambda_A = 0.1$ and $\lambda_B = 0.17$; and (c) $\lambda_A = 0.2$ and $\lambda_B = 0.345$	87
4.6	Concentration profile for optimal choice of operation (Run 6 in Table 4.1)	88
4.7	Concentration profile for general case (Run 2 in Table 4.4)	89
4.8	Plot of Recovery and Purity at various dimensionless Fructose concentrations in the raffinate for general case for (a) $\lambda_A = \lambda_B = 0$; (b) $\lambda_A = 0.1$ and $\lambda_B = 0.17$; and (c) $\lambda_A = 0.20$ and $\lambda_B = 0.345$	90
4.9	Concentration profile for MEA-MOH system (Run 4 in Table 7)	91
5.1	Flowsheet showing algorithm of optimization scheme	116
5.2	Recovery vs. purity plot considering scheme(a) for glucose-fructose system with fixed column length and diameter. ---- Model tie lines	117
5.3	Recovery vs. purity plot considering scheme(a) for glucose-fructose system for general case. ---- Model tie lines	118
5.4	Recovery vs. purity plot considering scheme(b) for glucose-fructose system with fixed column length and diameter. ---- Model tie lines	119
5.5	Recovery vs. purity plot considering scheme(b) for glucose-fructose system for general case. ---- Model tie lines	120
5.6	Concentration profiles for glucose fructose system for best case	121
5.7	Recovery vs. purity plot considering scheme(a) for nonlinear MEA-MOH system with fixed column length and diameter. ---- Model tie lines	122
5.8	Recovery vs. purity plot considering scheme(a) for nonlinear MEA-MOH system for general case. ---- Model tie lines	123

Figure		Page
5.9	Recovery vs. purity plot considering scheme(b) for nonlinear MEA-MOH system with fixed column length and diameter. ----- Model tie lines	124
5.10	Recovery vs. purity plot considering scheme(a) for nonlinear MEA-MOH system for general case. ----- Model tie lines	125

LIST OF TABLES

Table	Page
1.1	Examples of Cyclic adsorption separation processes 26
1.2	Countercurrent adsorption fractionation processes 27
2.1	Classification of models for countercurrent processes 46
2.2	Examples of the application of various countercurrent models 47
2.3	Summary of the published work 49
4.1	Optimized parameters for glucose (A)-fructose (B) system for linear case ($\lambda_A = \lambda_B = 0$) with fixed column diameter (5.1 cm) length (100.00 cm): Feed composition: 5 % A, 5 % B; $K_A = 0.51$; $K_B = 0.88$; Configuration- Prefeed, Postfeed (6,5) 92
4.2	Optimized parameters for glucose (A)-fructose (B) system for non-linear case ($\lambda_A = 1.0$ and $\lambda_B = 0.17$) with fixed column diameter (5.1 cm) length (100.00 cm): $K_A = 0.51$; $K_B = 0.88$; Configuration- Prefeed, Postfeed (6,5) 93
4.3	Optimized parameters for glucose (A)-fructose (B) system for non-linear case ($\lambda_A = 0.20$ and $\lambda_B = 0.345$) with fixed column diameter (5.1 cm) length (100.00 cm): $K_A = 0.51$; $K_B = 0.88$; Configuration- Prefeed, Postfeed (6,5) 94
4.4	Optimized parameters for glucose (A) - fructose (B) system for general case with linear isotherm ($\lambda_A = \lambda_B = 0$) Feed composition: 5 % A, 5 % B; $K_A = 0.51$; $K_B = 0.88$; Configuration- Prefeed, Postfeed (6,5) 95

Table	Page
4.5 Optimized parameters for glucose (A)-fructose (B) system for general case with non-linear isotherm ($\lambda_A = 0.10$ and $\lambda_B = 0.17$) $K_A = 0.51$; $K_B = 0.88$; Configuration- Prefeed, Postfeed (6,5)	96
4.6 Optimized parameters for glucose (A)-fructose (B) system for general case with non-linear isotherm ($\lambda_A = 0.20$ and $\lambda_B = 0.345$) $K_A = 0.51$; $K_B = 0.88$; Configuration- Prefeed, Postfeed (6,5)	97
4.7 Optimized parameters for MOH (A) - MEA (B) system for non-linear isotherm ($\lambda_A = 0$ and $\lambda_B = 0.435$) with fixed column diameter (5.5 cm), length (100.00 cm): Feed composition: 10 % A, 20 % B; $K_A = 0.63$; $K_B = 1.24$; Configuration- Prefeed, Postfeed (6,5)	98
5.1 Optimized parameters for glucose (A)-fructose (B) system for ($\lambda_A = \lambda_B = 0$) (raffinate optimization); column diameter (5.1 cm) length (100.00 cm); Feed composition: 5 % A, 5 % B; $K_A = 0.51$; $K_B = 0.88$; Configuration-(4, 3, 3, 2)	126
5.2 Optimized parameters for glucose (A)-fructose (B) system for ($\lambda_A = \lambda_B = 0$) (raffinate optimization); general case; Feed composition: 5 % A, 5 % B; $K_A = 0.51$; $K_B = 0.88$; Configuration-(4, 3, 3, 2)	127
5.3 Optimized parameters for glucose (A)-fructose (B) system for ($\lambda_A = \lambda_B = 0$) (extract optimization); column diameter (5.1 cm) length (100.00 cm); Feed composition: 5 % A, 5 % B; $K_A = 0.51$; $K_B = 0.88$; Configuration-(4, 3, 3, 2)	128
5.4 Optimized parameters for glucose (A)-fructose (B) system for ($\lambda_A = \lambda_B = 0$) (extract optimization); general case; Feed composition: 5 % A, 5 % B; $K_A = 0.51$; $K_B = 0.88$; Configuration-(4, 3, 3, 2)	129

Table	Page
5.5 Optimized parameters (raffinate optimization) for MOH (A) - MEA (B) system ($\lambda_A = 0$ & $\lambda_B = 0.435$); column diameter (5.5 cm) length (100.00 cm); Feed composition: 10 % A, 20 % B; $K_A = 0.63$; $K_B = 1.24$; Configuration-(4, 3, 3, 2)	130
5.6 Optimized parameters (raffinate optimization) for MOH (A) - MEA (B) system ($\lambda_A = 0$ & $\lambda_B = 0.435$); for general case; Feed composition: 10 % A, 20 % B; $K_A = 0.63$; $K_B = 1.24$; Configuration-(4, 3, 3, 2)	131
5.7 Optimized parameters (extract optimization) for MOH (A) - MEA (B) system ($\lambda_A = 0$ & $\lambda_B = 0.435$); column diameter (5.5 cm) length (100.00 cm); Feed composition: 10 % A, 20 % B; $K_A = 0.63$; $K_B = 1.24$; Configuration-(4, 3, 3, 2)	132
5.8 Optimized parameters (extract optimization) for MOH (A) - MEA (B) system ($\lambda_A =$ & $\lambda_B = 0.435$); for general case; Feed composition: 10 % A, 20 % B; $K_A = 0.63$; $K_B = 1.24$; Configuration-(4, 3, 3, 2)	133

THESIS ABSTRACT

NAME OF STUDENT	Mohammad Elias Biswas
TITLE OF STUDY	Optimization of Continuous Counter Current Adsorption Systems
MAJOR FIELD	Chemical Engineering
DATE OF DEGREE	December, 1995

The operation of continuous countercurrent adsorption systems are optimized for two different configurations. For the two-section configurations, the objective is to maximize the recovery of the less strongly adsorbed species in the raffinate for a specified purity of the product. The optimization results indicate that the optimum values of parameters are significantly different for linear and nonlinear isotherms. An optimal choice of operating variables corresponding to a compromise between recovery and purity is also suggested. For the four section (SORBEX) configuration, the optimization is carried out independently for raffinate and extract streams. In the case of raffinate optimization, the recovery of the relatively less strongly adsorbed species is maximized for a specified concentration of the other component, while for the case of extract optimization the recovery of the more strongly adsorbed species is maximized for a specified concentration of the less strongly adsorbed species. These schemes are applied to systems with linear (Glucose-Fructose) and nonlinear (MEA-MOH) isotherms. In all cases the optimized recovery increases with purity up to a maximum level, which is considered the best of all the optimum sets, beyond which the recovery decreases. The optimum results obtained for maximum recovery are identical for both raffinate and extract optimizations.

MASTER OF SCIENCE DEGREE

KING FAHD UNIVERSITY OF PETROLEUM & MINERALS

Dhahran, Saudi Arabia

December, 1995

خلاصة

إسم الطالب : محمد إلياس بسواس
عنوان الدراسة : نمذجة أنظمة الإمتزاز المستمر ذات الإتجاه المعاكس
التخصص : هندسة كيميائية
تاريخ الشهادة : ديسمبر ١٩٩٥م

في هذا البحث تم نمذجة عملية الأتزاز المستمر لشكلين مختلفين بهدف الحصول على أكبر زيادة ممكنة من المستخلصات الأقل إمتزازاً في الجزء المصفى لمنتج معين ونتائج هذه النمذجة تشير إلى أن النتائج المثلى لمعطيات متغيرة هي بالضرورة تختلف من الـ (Isotherm) الخطي وغير الخطي ولقد أقترح أن النموذج الأمثل لمتغيرات العمليات يتفق مع الموازنة من المركبات المستخلصة وتلك الصافية وأما بالنسبة لأنظمة الإمتزاز ذات الأربع قطاعات (SORBEX) فإن النمذجة قد أجريت لكل من الجزء المنقى والمستخلص من المجرى كلاً على حدى . فأما من ناحية نمذجة الجزء المنقى فإن المركبات المستخلصة والتي تتميز لقوة أقل على الإمتزاز قد تم زيادتها زيادة قصوى وذلك لتركيز المركب الآخر بينما في حالة نمذجة الأجزاء المستخلصة (Extract) فإنه تم زيادة المركبات المستخلصة ذات الإمتزاز القوي وذلك للمركبات ذات الأقل إمتزازاً وهذه الطرق تنطبق على الأنظمة الخطية (Glucose-fructose) وغير الخطية (MEA-MOH) الـ (Isotherms) وفي كل الحالات فإن المستخلص الأمثل يزيد مع النقاء إلى حد الزيادة القصوى والتي تعتبر الأحسن ضمن كل المجموعات النمذجية وغير ذلك فإن هذه المستخلصات تقل . والنتائج المثلى المحصلة لمستخلص عالي الإنتاج تعتبر مطابقة لكل من الجزء المنقى (Raffinate) والجزء المستخلص (Extract) .

درجة ماجستير العلوم
جامعة الملك فهد للبترول والمعادن
قسم الهندسة الكيميائية
الظهران - المملكة العربية السعودية

Chapter 1

Introduction

1.1 INTRODUCTION

A gas molecule near a solid surface experiences a reduction in potential energy as a consequence of interaction with the atoms (or molecules) in the solid. The result is that gas molecules tend to concentrate in this region so that the molecular density in the vicinity of the surface is substantially greater than in the free-gas phase. The strength of the surface forces depends on the nature of both the solid and the sorbate. If the forces are relatively weak, involving only van der Waals interactions supplemented in the case of polar or quadrupolar species by electrostatic forces (dipole or quadrupole interactions), we have what is called “physical adsorption” or “physisorption”. By contrast, if the interaction forces are strong, involving a significant degree of electron transfer, we have “chemisorption.” Chemisorption is limited to a monolayer, whereas, in physical adsorption, multiple molecular layers can form. Since the adsorption forces depend on the nature of the adsorbing molecule as well as on the nature of the surface, different substances are adsorbed with different affinities. It is this “selectivity” that provides the basis for adsorption separation processes [1].

1.2 ADSORPTION AS A SEPARATION TOOL

The practical application of adsorption to the large-scale separation and purification of industrial process streams is relatively recent. Perhaps the most familiar example of such a process is the use of an adsorbent column, packed with a suitable hydrophilic adsorbent, as a drier for the removal of traces of moisture from either gas or liquid streams. Similar processes are also in common use on a large scale for the removal of undesirable impurities such as H_2S and mercaptans from natural gas and organic pollutants from water. Such processes are conveniently classified as purification processes since the adsorbable components are present at low concentrations and have little or no economic value, and therefore are not frequently recovered. The economic benefit of the process is derived entirely from the increase in the purity and value of the stream containing the major component.

The application of adsorption as a means of separating mixtures into two or more streams, each enriched in a valuable component which is to be recovered, is a more recent development [2]. Early examples include the Arosorb process for recovery of aromatic hydrocarbons which was introduced in the early 1950s and a variety of processes, first introduced in the early 1960s, for the separation of linear paraffins from branched and cyclic isomers. During the 1970s there has been a significant increase in both the range and scale of such processes. The economic incentive has been the escalation of energy prices, which has made the separation of close boiling components by distillation a costly and uneconomic process. For such mixtures it is generally possible to find an adsorbent for which the adsorption separation factor is much greater than the relative volatility, so that a more economic adsorptive separation is in principle possible. However for an adsorption process to be developed on a commercial scale, the availability of a suitable

adsorbent in tonnage quantities at economic cost is required. This has stimulated fundamental research in adsorption and led to the development of new adsorbents .

1.3 SELECTIVITY OF ADSORPTION SYSTEM

The primary requirement for an economic separation process is an adsorbent with sufficiently high selectivity, capacity, and life. The selectivity may depend on a difference in either adsorption kinetics or adsorption equilibrium. A Separation factor may be defined as:

$$\alpha = \frac{X_A / X_B}{Y_A / Y_B} \quad (1. 1)$$

The definition of separation factor is analogous to the relative volatility, which measures the ease with which the components may be separated by distillation. The analogy is, however, purely formal and there is no quantitative relationship between the separation factor and relative volatility. For two given components the relative volatility is fixed whereas the separation factor varies widely depending on the adsorbent.

1.4 POROUS ADSORBENTS

The requirement for adequate adsorptive capacity restricts the choice of adsorbents for practical separation processes to microporous adsorbents with pore diameters ranging from a few Angstroms to few tens of Angstroms. This includes both the traditional microporous adsorbents such as silica gel, activated alumina, and activated carbon as well as the more recently developed crystalline aluminosilicates or zeolites.

1.4.1 Activated Carbon and Carbon Molecular Sieves

Activated carbon is produced in many different forms that differ mainly in pore size distribution and surface polarity. The nature of the final product depends on both the starting material and activation procedure. The activation process involves essentially the removal of tarry carbonization products formed during the pyrolysis, thereby opening the pores.

By an additional treatment with benzene or acetylene in the activation procedure, it is possible to prepare carbon adsorbents with a very narrow distribution of micropore size and which therefore behave as molecular sieves.

1.4.2 Silica Gel

A pure silica surface is inactive and "hydrophobic," but if hydroxyl groups are present the surface becomes hydrophilic as a result of the possibilities for hydrogen bond formation. Silica "gel" is formed as colloidal precipitate when a soluble silicate is neutralized by sulfuric acid. The size of the colloidal particles and the nature of their surface are strongly influenced by trace components present in the solution. When water is removed from the "gel," an amorphous microporous solid is formed, but the size of the silica particles and therefore the pore size depends on the conditions during the water removal step.

1.4.3 Activated Alumina

Activated alumina is a porous high-area form of aluminum oxide, prepared either from bauxite ($\text{Al}_2\text{O}_3 \cdot 3\text{H}_2\text{O}$) or from the monohydrate by dehydration and

recrystallization at elevated temperature. The surface is more strongly polar than that of silica gel and has both acidic and basic characteristic, reflecting the amphoteric nature of the sorbent.

1.4.4 Zeolites

In contrast to the other adsorbents so far considered, the zeolites are crystalline rather than amorphous, and the micropores are actually intracrystalline channels with dimensions precisely determined by the crystal structure. There is therefore virtually no distribution of micropore size, and these adsorbents show well-defined size-selective molecular sieve properties- exclusion of molecules larger than a certain critical size and strong steric restriction of diffusion for molecules with dimensions approaching this limit.

1.4.5 Ion exchange Resins

Ion exchange is the reversible interchange of ions between a liquid and solid, in which there are no permanent changes in the structure of the solid. Since the transfer of ions between phases occurs at a solid surface, ion exchange can be considered as a sorption process and has many similarities with adsorption.

Ion exchange materials consist of an inorganic network structure with attached functional groups. Most ion exchange materials used in adsorption are synthetic resins made by polymerization of organic compounds into a porous three-dimensional structure. Ion exchange resins are called cationic if they exchange positive ions and anionic if they exchange negative ions. Cation exchange resins have acidic functional groups, such as sulfonic, whereas anion exchange resins contain basic functional groups, such as amine. Ion exchange resins act as adsorbents for many chemicals such as phenol, methanol etc.

1.5 ADSORPTION EQUILIBRIUM

1.5.1 Henry's Law

The adsorbed layer at the surface of a solid may be regarded as a distinct "phase" in the thermodynamics sense. Equilibrium with the surrounding gas (or liquid) is governed by the ordinary laws of thermodynamics. Physical adsorption from the gas phase is an exothermic process; so equilibrium favors adsorption at lower temperatures and desorption at higher temperatures. At sufficiently low concentration the equilibrium relationship generally approaches a linear form (Henry's Law)

$$q = Kc \quad (1. 2)$$

It is evident that the Henry constant is simply the adsorption equilibrium constant.

1.5.2 Brunauer's Classification

At higher concentrations the equilibrium relationship becomes curved. Brunauer classified the commonly observed forms of isotherm into five types, as shown in Figure 1.1.

The isotherms for true microporous adsorbents, in which the pore size is not very much greater than the molecular diameter of the sorbate molecule, are normally of type I. This result arises in such adsorbents because there is a definite saturation limit corresponding to complete filling of the micropores. If there is any intermolecular attraction effects, an isotherm of type V is observed. In the case of formation of two surface layers either on a plane surface or on the wall of a pore very much wider than the molecular diameter of sorbate, an isotherm of type IV is seen. Isotherms type II and III are generally observed only in adsorbents in which there is a wide range of pore sizes.

Although there are five different classes of isotherms, normally only two types of isotherms, type I and II, are encountered in most practical situations.

1.5.3 "Favorable" & "Unfavorable" equilibria

In the analysis of adsorption column dynamics it is convenient to classify adsorption equilibria as "favorable," "linear," or "unfavorable" depending on the shape of the dimensionless (x-y) equilibrium diagram. The meaning of these terms is evident from Figure 1.2 [1]. In the "favorable" case the dimensionless adsorbed phase concentration is always greater than the dimensionless fluid phase concentration. This classification assumes that the direction of mass transfer is from fluid phase to adsorbed phase (i.e., an adsorption process). Since for desorption the initial and final states are reversed, an isotherm that is "favorable" for adsorption will be "unfavorable" for desorption and vice versa.

1.5.4 Langmuir Isotherm

For microporous adsorbents the simplest theoretical model for monolayer adsorption is due to Langmuir. According to this model, the equilibrium relationship is given by

$$\frac{q}{q_s} = \frac{bc}{1+bc} \quad (1.3)$$

This form may be derived from simple mass action considerations by considering the balance between occupied and unoccupied sites.

1.5.5 Freundlich and Langmuir-Freundlich Isotherm

An alternative expression that is sometimes used to represent a favorable (type I) isotherm is the Freundlich equation:

$$q = bc^{1/n} \quad n > 1.0 \quad (1.4)$$

To obtain greater flexibility as an empirical correlation the Langmuir and Freundlich forms are sometimes combined:

$$\frac{q}{q_s} = \frac{bc^{1/n}}{1 + bc^{1/n}} \quad (1.5)$$

1.5.6 BET Isotherm

Materials such as activated alumina and silica gel commonly show type II behavior. This form is commonly represented by the BET equation:

$$\frac{q}{q_s} = \frac{b(p/p_s)}{(1 - p/p_s)(1 - p/p_s + bp/p_s)} \quad (1.6)$$

all the symbols used through equation (1.1)-(1.6) are defined in the nomenclature.

1.6 ADSORPTION SEPARATION PROCESSES

Adsorption separation processes depend on the preferential adsorption of one component (or a family of similar components) from a mixed feed. The selectivity of the adsorbent, which may depend on differences in sorption equilibrium, or, less commonly,

on a difference in sorption kinetics, is therefore a key factor in determining the viability of any such process.

Large-scale adsorptive separation processes may be conveniently divided into two broad classes: cyclic batch systems, in which the adsorbent bed is alternatively saturated and regenerated in a cyclic manner, and continuous flow systems, generally involving continuous countercurrent contact between feed and adsorbent. Wankat [3] has given a useful review of adsorption technology. The distinction between these two basic modes of operation is shown schematically in Figure 1.3.

1.6.1 Cyclic Batch Systems

In cyclic batch systems, adsorbent bed is alternatively saturated and regenerated in a cyclic manner as shown in Figure 1.3(a). Based on the methods of regeneration, cyclic batch processes differ from each other as reported in Table 1.1. Four basic methods are in common use although combination of two or more methods may be used with advantage in particular situations.

Thermal Swing: In thermal swing operation the bed is regenerated by heating, usually with a stream of hot gas (or less commonly with hot liquid), to a temperature at which the adsorbed species are desorbed and removed from the bed in the fluid stream.

Pressure Swing: In a pressure swing process desorption is accomplished by reducing the pressure at essentially constant temperature and then purging the bed at low pressure. This mode of operation is obviously restricted to gaseous systems.

Purge gas stripping: The bed is regenerated at essentially constant pressure and temperature by purging with a nonadsorbing inert gas as in elution chromatography.

Displacement Desorption: The temperature and pressure are maintained essentially constant, as in purge gas stripping, but instead of an inert purge the adsorbed species are displaced by a stream containing a competitively adsorbed species, as in displacement chromatography.

1.6.2 Continuous Counter Current Systems

Countercurrent contact maximizes the driving force for mass transfer and therefore provides, in principle, more efficient utilization of the adsorbent capacity [4] than is possible in a simple batch-contacting system. However, for countercurrent contact it is necessary to either circulate the adsorbent, as shown in Figure 1.3(b), or, by approximate design of fluid flow system, to simulate adsorbent circulation. This makes the design of countercurrent processes more complex and reduces operational flexibility. It is evident that for relatively easy separations (high separation and adequate mass transfer rates) the balance of advantage will lie with a simple batch system; but for difficult separations in which selectivity is limited or mass transfer is slow, the advantage of a continuous countercurrent system in reducing the required inventory of adsorbent must eventually outweigh the disadvantages of the more complex engineering. Continuous countercurrent adsorption processes are, however, widely used on an industrial scale for several important separations and it seems probable that such processes will become increasingly common in future.

1.6.3 Simulated Counter Current Adsorption Systems

Most of the benefit of countercurrent operation can be achieved without the problems associated with moving the solid adsorbent by using a multiple column (or multiple section) fixed-bed system, with an appropriate sequence of column switching designed to simulate a counter flow system. The basic principle is illustrated in Figure 1.4, although obviously many variants are possible. At each switch time a fully regenerated column is added at the outlet of the adsorption side which is approaching breakthrough while the fully loaded column at the feed end of the adsorption side is switched to the outlet end of the regeneration train. In this way the adsorbent is seen to be in effect moving counter current to the fluid flow direction in both adsorption and regeneration trains. With sufficiently small elemental beds switched with appropriate frequency, such a system becomes a perfect analog of a countercurrent flow system.

In this process the adsorbent is contained in a number of identical column connected in series through pneumatically controlled switch valves which allow the introduction of feed or eluent or withdrawal of product between any pair of columns. The cascade is divided into four sections; section I between desorbent inlet and extract withdrawal, section II between extract withdrawal and feed inlet, section III between feed inlet and raffinate withdrawal points section IV between raffinate withdrawal and the desorbent recirculation point. The countercurrent flow is simulated by advancing the desorbent, extract, feed raffinate and recirculation points at specified time intervals by one column in the direction of fluid flow. The system is thus formally equivalent to the true counter current system sketched in Figure 1.5. Every time the feed location will be advanced by one column, and when the feed location appears again in its initial point, the whole system is considered to have completed one cycle. Depending upon the number of

columns we will have different cycle times. It is evident that a steady state simulated moving bed (SMB) process can be approximated by a continuous countercurrent process.

1.7 INDUSTRIAL - SCALE COUNTER CURRENT ADSORPTION FRACTIONATION PROCESSES

A summary of some of the more important counter-current adsorption fractionation processes which have been operated commercially is given in Table 1.2. Except for the hypersorption process, which is no longer in operation, all these processes operate on the SMB principle using either the cascade arrangement shown in Figure 1.5 or simplified three-section unit shown in Figure 1.6. All these processes operate in the liquid phase although, in principle, either liquid or vapour phase operation is possible [5,6,7].

1.7.1 "Sorbex" Process

The Sorbex family of processes which have been developed by UOP for a variety of industrially important separations operate on the same principle as SMB system shown in Figure 1.7. The actual configuration is however somewhat different as shown in Figure 1.8. Instead of being contained in discrete beds separated by switch valves the adsorbent is contained in a single bed which is divided into a number of sections. Specially designed flow distributors allow fluid to be introduced (or withdrawn) at each section. The flow circuit is completed by a pump which recirculates fluid from the bottom to the top of the column. At any time only four of the connections to the column are utilized. Switching of the flows is accomplished by a single complex rotary valve which, at each switch, advances the desorbent extract, feed and raffinate points by one section in the direction of fluid flow and at the same time passes the extract and raffinate stream to the ancillary distillation column.

The choice of both adsorbent and desorbent is crucial to the economic viability of the process. In this type of process, a difficult separation (A-B) is replaced by a Sorbex unit, which produces A-D and B-D streams, together with ancillary distillation columns to separate the A-D and B-D products and return the desorbent for reuse.

A summary of the more important commercial processes which operate under the same principle as 'SORBEX' system are given in Table 1.2 [8] and brief details of some of these processes are discussed below. The economic advantages of the Sorbex type of processes is greatest for the separation of similar sorbates, often isomers, where differences in physical properties are too small to permit the economic application of more conventional processes such as distillation.

1.7.2 Parex and Ebex Processes

The xylene isomers (including ethylbenzene) have very similar volatilities making distillation uneconomic, except perhaps for production of o-xylene. The Parex process which produces high-purity p-xylene from a mixed feed has been one of the most successful applications of this type of process. The Ebex process for ethyl benzene recovery was developed more recently.

1.7.3 Sarex Process

The Sarex process uses the Sorbex principle with a CaY adsorbent to separate aqueous mixtures of fructose and glucose using water as both solvent and eluent.

1.7.4 Molex Process

In the Molex process the Sorbex system is used to separate linear from branched and cyclic hydrocarbon isomers using a 5A zeolite as the size-selective adsorbent.

1.8 SCOPE AND OBJECTIVES OF PRESENT STUDY

1.8.1 Scope of Present Study

Modelling and simulation of continuous counter-current adsorption system is well established in the literature and has been shown to provide good representation of experimental data. In both two section and four section models, the independent and dependent variables need to be identified. The effects of changes in the independent (manipulating) variables on the performance of the process are very strongly coupled thereby making it difficult to make intuitive predictions. The literature search reveals that there exists an optimum set of these independent variables. Experimental determination of this optimum set requires trial and error procedure which is time consuming and uneconomical. A systematic theoretical evaluation of these optimum set of values is yet to be accomplished.

1.8.2 Objectives of Present Study

The overall objective of the present study is to develop an optimization scheme for the model equations of continuous counter-current system to evaluate the optimum set of parameter values which will maximize the recovery of product or products. The specific objectives are:

- (i) Prepare an optimization scheme for continuous counter-current adsorption system with linear isotherm using the dispersed plug flow model equations for two and four section configurations.
- (ii) For two section configuration the optimum sets of parameter values are found by maximizing the recovery of the less strongly adsorbable species at the raffinate subject to the specified purity.
- (iii) For four section configuration the optimum sets of parameter values are found by defining the objective functions for two different cases:
 - (a) Maximization of recovery of less strongly adsorbable species at the subject to a specified purity raffinate and
 - (b) Maximization of recovery of more strongly adsorbable species at the extract subject to a specified purity.
- (iv) The above optimization scheme is repeated for systems with non-linear and interacting adsorption isotherm.

REFERENCES

- (1) Ruthven, D. M., Farooq, S., and Knaebel, K. S., Pressure Swing Adsorption, VCH Publishers, New York (1995)
- (2) Ruthven, D. M., Principles of Adsorption and Adsorption Processes, John Wiley, New York (1984)
- (3) Wankat, P. C., Large Scale Adsorption and Chromatography, CRC Press, Boca Raton, Florida (1986)
- (4) Lerch, R. G., and Ratowsky, D. A., Optimum allocation of adsorbent in stage wise adsorption applications, Ind. Eng. Chem. Fundamental. 6, 308-310 and 408 (1967)
- (5) Broughton, D. B., and Berg, R. C., Hydrocarbon Processing, 48(6), 115-120 (1969).
- (6) Broughton, D. B., and Gembicki, S. A., Fundamentals of adsorption, pp.115-124, Engineering Foundation, New York (1984).
- (7) de Rosset, A. J., Neuzil, R. W., and Broughton., Percolation Processes, NATO ASI no. 33, 249-281, Noordhoff, Holland (1981).
- (8) Ruthven, D. M., and Ching, C. B., Chem. Eng. Sci., 44(5), 1011-1038 (1989).

NOMENCLATURE

b	Langmuir equilibrium parameter
c	concentration of the adsorbate in the fluid phase
K	Henry or equilibrium constant
n	non-linearity constant
p	partial pressure
p_s	saturation pressure
q	solid phase concentration
q_s	saturated solid phase concentration
q^*	equilibrium solid phase concentration
X_A	mole fraction of component A in adsorbed phase
X_B	mole fraction of component B in adsorbed phase
Y_A	mole fraction of component A in fluid phase
Y_B	mole fraction of component B in fluid phase

Greek symbol

α	separation factor
----------	-------------------

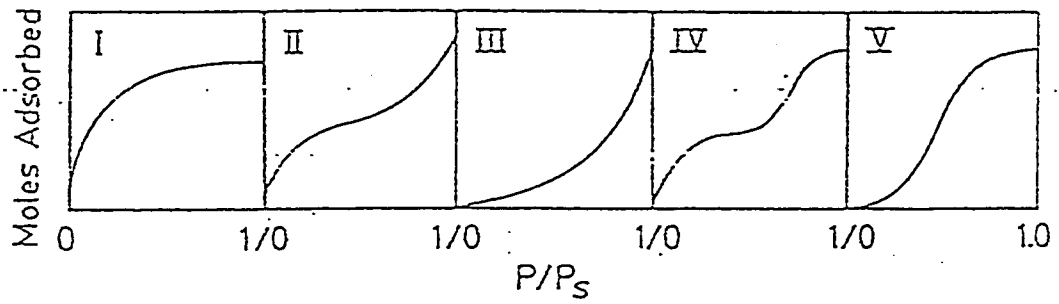


Figure 1.1 The Brunauer classification of isotherm

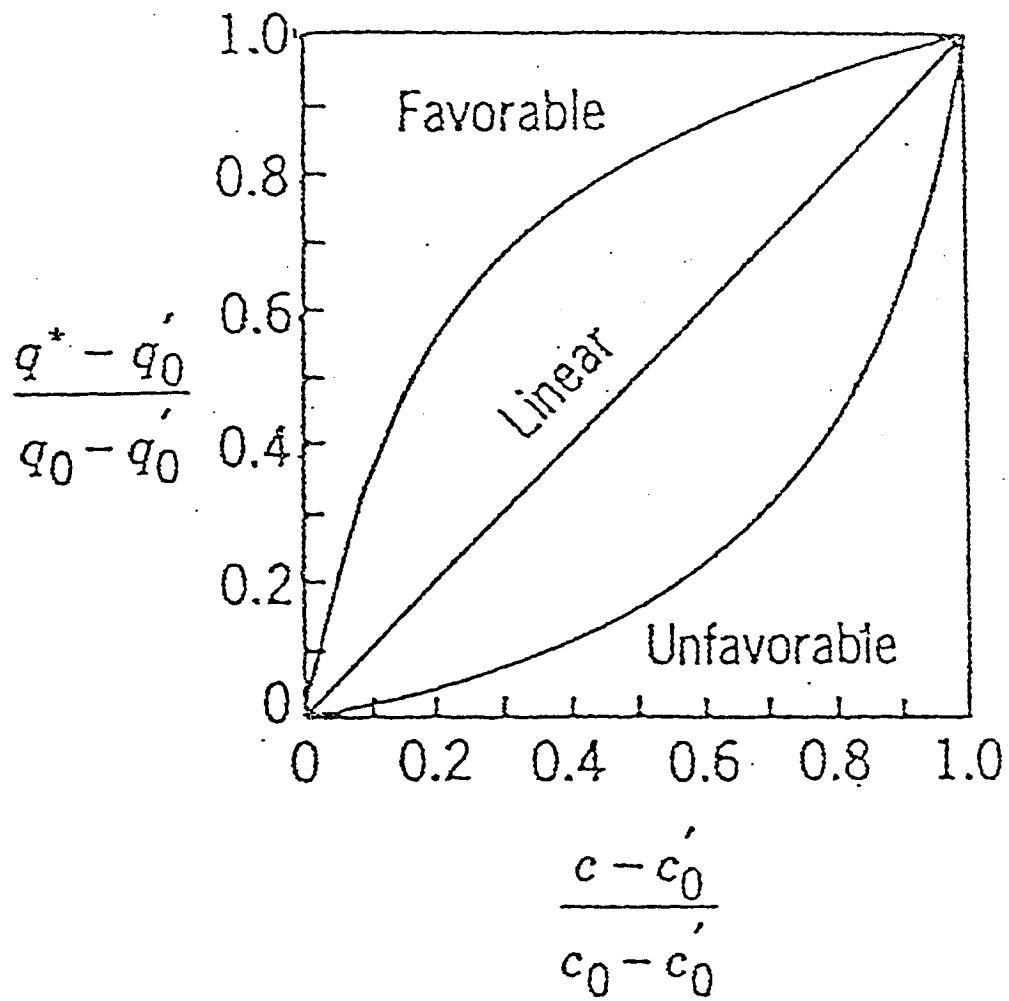


Figure 1.2 Dimensionless equilibrium isotherm showing the meaning of the terms "favorable," "linear," and "unfavorable."

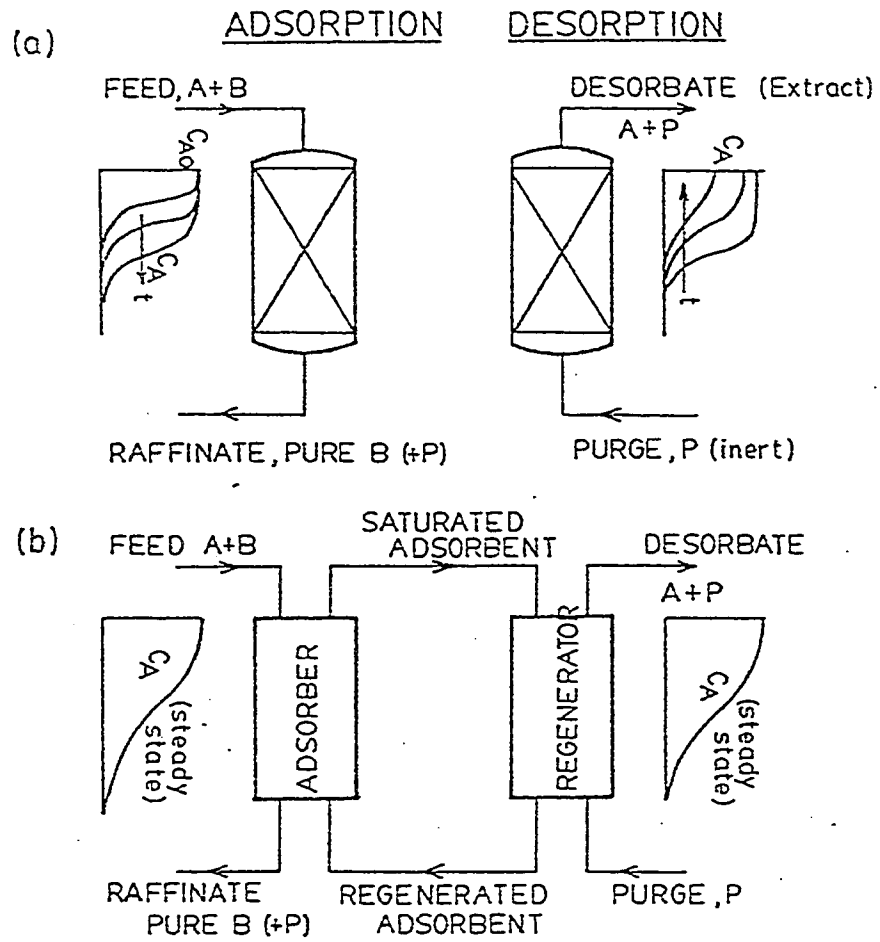


Figure 1.3 Schematic diagram showing two basic mode of operation a) Cyclic batch b) continuous countercurrent

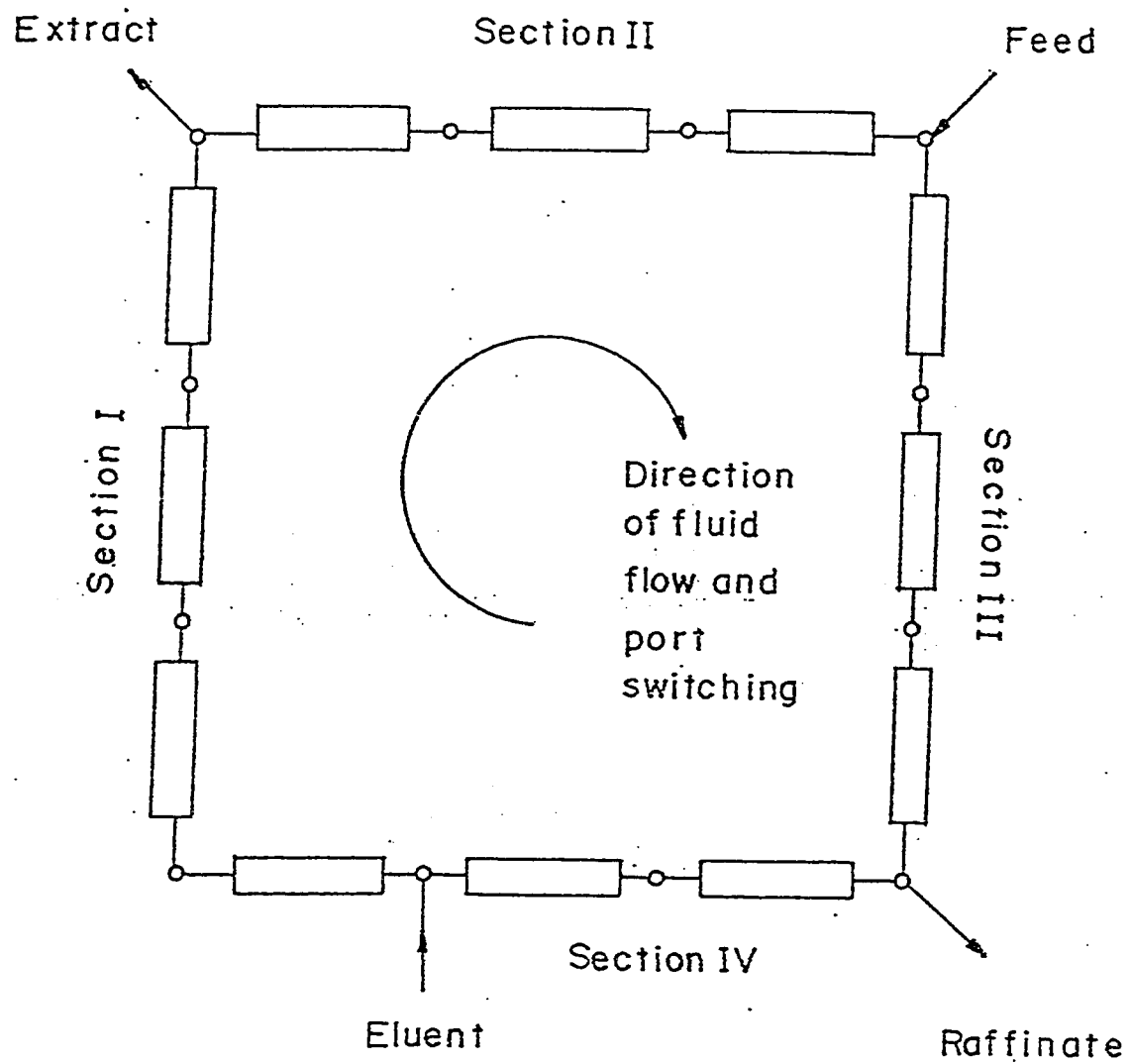


Figure 1.4 Schematic diagram of the physical arrangement of columns and switch valves.

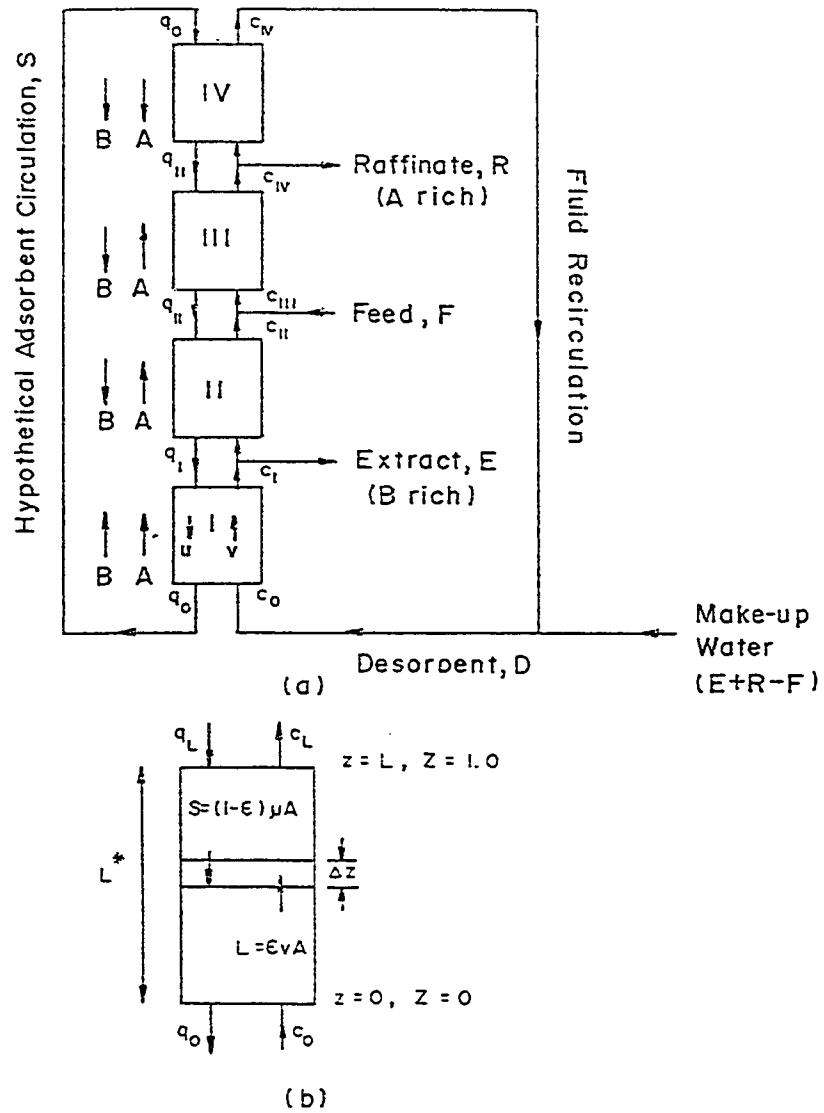


Figure 1.5 Schematic diagram of a) the equivalent countercurrent system b) the notation used in describing the profile within an individual section.

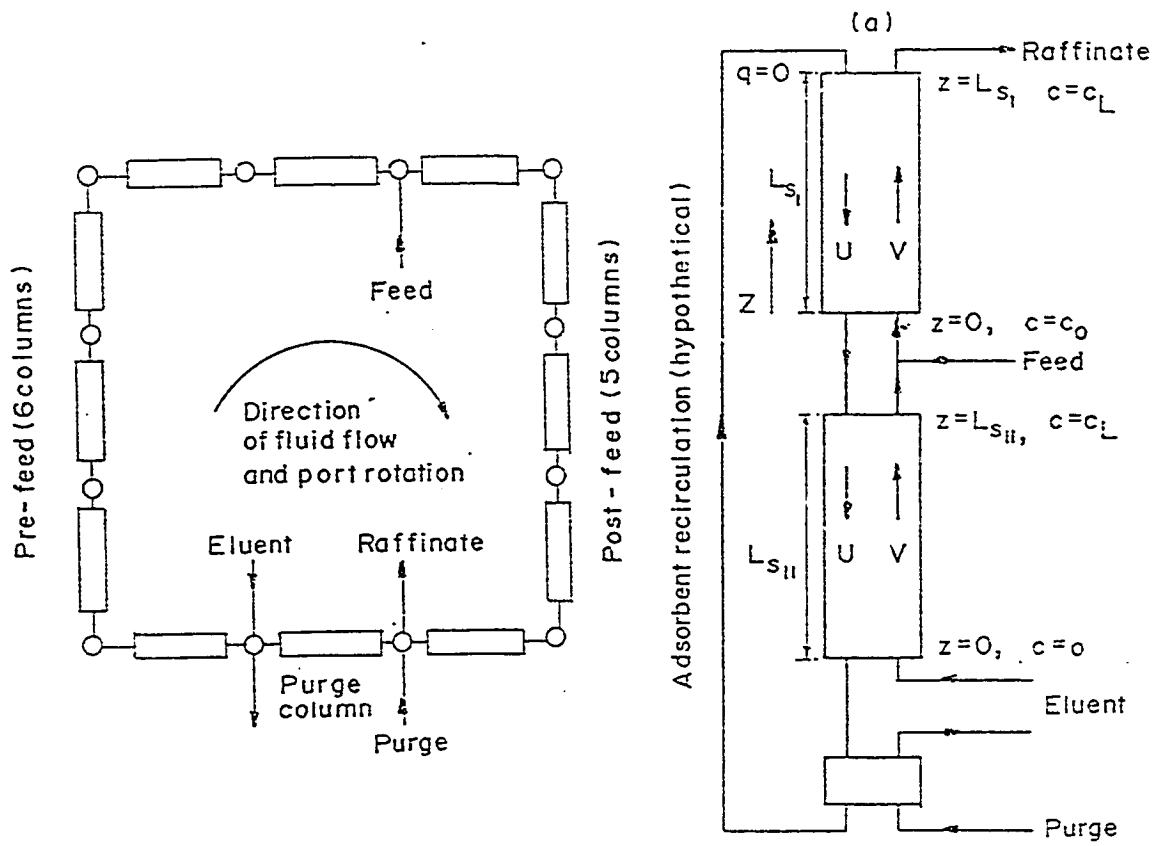


Figure 1.6 Two-section equivalent countercurrent arrangement

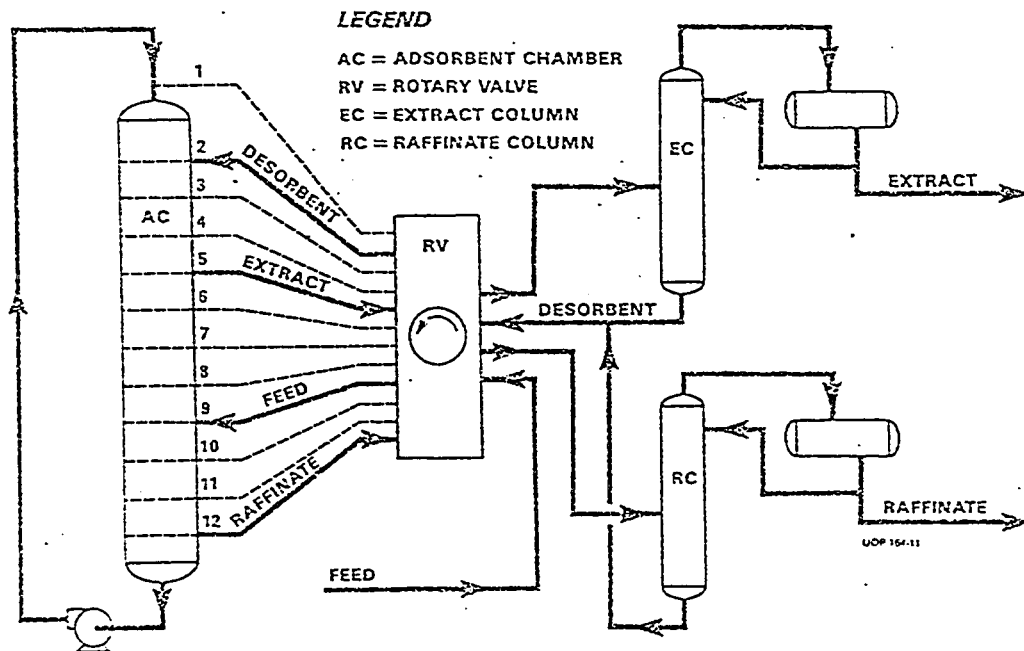


Figure 1.8 Schematic diagram of an industrial scale 'SORBEX' system.

Table 1.1: Examples of Cyclic Adsorption Separation Processes [1]

Process	Liquid (L) or Gas Phase (G)	Adsorbent	Selectivity	Regeneration Method
Drying of gas stream	G	13X, 4A, or 3A mol. sieve	Equilibrium	T swing or P swing
Drying of solvents	L	4A sieve	Equilibrium	T swing
Solvent recovery	G	Activated carbon	Equilibrium	Steam stripping
H ₂ recovery	G	Molecular sieve	Equilibrium	P swing
Air separation	G	Carbon mol.sieve Zeolite	Kinetic	P swing
Linear parafins separation	G	5A mol. sieve	Shape selective sieving	Displacement or vacuum
Waste water purification	L	Activated carbon	Equilibrium	Steam stripping

Table 1.2: Countercurrent adsorption fractionation processes [1]

Process	Separation	Adsorbent	Contacting system	Regeneration
Hypersorption	C ₂ H ₄ from refinery gas	Activated carbon	Dense moving bed	Steam stripping
Arosorb	Separation of aromatics and saturates from cracked naphtha	Silica gel	SMB (eight column)	Displacement (Pentane desorbent)
Aromax	p-Xylene from C ₈ aromatics	X or Y zeolite	Three section SMB cascade	Heavy aromatic desorbent
Adseo(IWT)	Fructose from fructose-glucose	Ca ⁺ resin	Eight column four section SMB	Water desorbent
Molex	Linear/ branched paraffins	5A zeolite	Sorbex	Light naphtha desorbent
Olex	Olefins from saturated isomers	CaX or SrX	Sorbex	Heavy naphtha
Parex	p-Xylene from C ₈ aromatics	Sr-BaY K-BaX	Sorbex	P- Diethylbenzene Toluene

Ebex	Ethylbenzene from C ₈ aromatics	NaY	Sorbex	Toluene
Sarex	Fructose from fructose- glucose	CaY	Sorbex	Water
SCCR4	Fructose from fructose- glucose	Ca ⁺ resin	Three-section SMB	Water
SCCR5	Clinical dextran	Ca ⁺ resin	Three -section SMB	Water

Chapter 2

Literature Review

2.1 INTRODUCTION

From the early 1950's to date researchers have contributed a great deal of work in the field of continuous countercurrent adsorption systems. Various models are available regarding this adsorption separation process. These models were developed considering different types of physical phenomena that are encountered in adsorption separations.

Modelling in continuous countercurrent adsorption can be divided into two broad groups; graphical and numerical simulation. In graphical methods a McCabe-Thiele approach to separating components is adopted. Though this procedure is very simple and quick, the scope of this method is limited. This analysis is only possible for very simple systems, viz., linear equilibrium isotherm with plug flow model. When systems become complex, a more practical numerical simulation is the only choice. In numerical simulation various models are possible depending upon the system complexity.

2.1.1 Graphical (McCabe-Thiele Analysis)

Design procedures for countercurrent systems are basically similar to the elementary procedures used to design any steady state countercurrent mass transfer

operation such as gas absorption. The main difference is that in absorption systems the equilibrium isotherm is generally curved whereas for many gas adsorption systems, at least at low concentration levels, the isotherm is essentially linear. That is why it is possible to represent these adsorption systems using a McCabe-Thiele diagram.

The McCabe-Thiele operating diagram for a simple system with isothermal purge regeneration is shown in Figure 2.1. The equilibrium line is shown as straight line to avoid complexity, although in most real adsorption systems the isotherms are curved except at very low concentrations. The equations of the operating lines can be obtained simply by mass balance.

$$x = x_F + \left(\frac{F}{S}\right)(y - y_F) \quad (2.1)$$

$$x = x_D + \left(\frac{D}{S}\right)(y - y_D) \quad (2.2)$$

If both adsorption and desorption sections operate under the same thermodynamic conditions (same pressure and temperature), the equilibrium lines will be the same. For an operable process the net flow of solute must be up in the desorption section and down in the adsorption section. This requires $D/S > K$, $F/S < K$, implying that the desorbent flowrate must be higher than the feed flowrate. To achieve the required directions of mass transfer the operating lines in the adsorption and desorption sections must lie on opposite sides of the equilibrium line. It follows that $y_D < y_E$ and $y_E < y_F$, i.e., the concentration of the adsorbable species in the purge stream must be lower than in the raffinate product and the concentration in the extract must be lower than that of the feed. Such a process would only be economical in exceptional circumstances, e.g. for removal of an undesirable impurity, without recovery, when a plentiful supply of cheap purge is available.

The McCabe-Thiele analysis of the more commonly used SORBEX system is shown in Figure 2.2. This type of system is used in most commercial adsorptive fractionation processes. An additional component which is competitively adsorbed (the eluent or desorbent) is introduced into the system. The flowrates in each section are adjusted so that, for both components A and B, desorption occurs in sections I and II and adsorption in sections III and IV. The net flow of A (the more strongly adsorbed component) should be downwards in sections II, III and IV and upwards in section I, so that this species moves continuously to the extract point. Similarly the net flow of B should be downwards in section IV and upwards in sections I, II and III, so that it moves towards the raffinate withdrawal point.

Since the system operates isothermally or near isothermally, the equilibrium lines are the same throughout. The operating lines, in the McCabe-Thiele representation can cross the equilibrium lines only at the feed point and at the eluent recirculation point where there are sudden changes in liquid composition as a result of the introduction of feed or eluent. To achieve a satisfactory separation, the operating diagrams for the two components must lie as sketched in Figure 2.2 so that the extract product contains a high concentration of A and a low concentration of B while the raffinate product contains a high concentration of B and a low concentration of A. The flow constraints referred to above require that the slope of the operating line in section I is greater than that for section II while the slope of the operating line for section III must be greater than for section IV.

2.1.2 Numerical Simulation

The problem of modelling a simulated countercurrent adsorption separation process has attracted a great deal of attention in recent years. The approaches which have

been followed may be classified according to whether the system is simulated directly or represented in terms of an equivalent true countercurrent system and whether the bed elements are represented by a continuous flow model (plug flow or axial flow) or as a cascade of mixing cells. The models for simulated moving bed (SMB) countercurrent processes may be classified into four categories as given in Table 2.1 [1].

Each of these four models may be treated either according to equilibrium theory (I) or by including an appropriate rate expression to account for mass transfer resistance, generally in terms of a linear driving force model (II). Examples of application of these models are given in Table 2.2 [1].

For linear equilibrium systems all four modelling approaches are viable. The simplest representation of the fundamental theory of continuous countercurrent "SORBEX" system was developed from the basic principle of McCabe-Thiele analysis (a.1.I) for plug flow and constant separation factor. The equivalent countercurrent model with linearized mass transfer rate expression (model a.1.II) leads to fairly simple expressions for the steady state concentration profile. The linear driving force model together with the simple McCabe-Thiele analysis of the overall process provides all that is needed to design and optimize the system. The same general approach may be extended to nonlinear binary systems though an analytical solution of the equivalent countercurrent model equation can no longer be obtained. Alternatively one may choose to use the mixing cell model with either the equivalent countercurrent representation (model a.2.I) or with direct simulation of the SMB system (b.2.I). For either linear systems or nonlinear binaries these approaches are computationally straightforward.

For more complex nonlinear systems with coupling between the components (ternary and higher order) a more sophisticated approach is needed. The equivalent

countercurrent mixing cell model (a.2.I) may still be used but it is now necessary to solve simultaneously the mass balance equations for all components for each theoretical stage, in order to allow for the coupling of the equilibrium relationships. A similar computational approach is commonly used in modern multicomponent distillation design codes in order to allow for variation of volatility with composition. Initial estimates of appropriate flowrates and switch times may still be obtained from the McCabe-Thiele approach but this is no longer quite so straightforward since a trial and error solution using the full numerical simulation is needed in order to establish the appropriate equilibrium curves (which depend on the concentrations of all components in the system). Alternatively, initial estimates of the appropriate flow parameters may be derived from the equivalent countercurrent model using equilibrium theory, followed by detailed numerical simulation according to any of the models a.1, a.2, b.1 or b.2. This approach, which is particularly useful when the multicomponent equilibria can be represented in terms of the constant separation factor (multicomponent Langmuir) model, has been developed by Storti et al. [2] and applied to the optimization of a multicomponent "SORBEX" separation system.

2.2 REVIEW OF PREVIOUS WORK

Amundson and Kasten [3] developed the analytical solution for single-component adsorption assuming a linear isotherm and film resistance as the mass transfer resistance only. Neretnieks [4] represented analytical solutions of continuous countercurrent adsorption for single component with film plus pore resistance for linear equilibrium isotherm, and also for an irreversible isotherm [5]. Neretnieks [6] also compared the performance of the system for these two different isotherms. Fornwalt and Hutchins [7] and Erskine and Schuliger [8] suggested a simplified graphical procedure to assess the effectiveness of multiple beds. Chen et al. [9] used a tanks-in series model with linear

mass transfer driving force. Asymptotic solutions to moving-bed exchange equations are discussed by Rhee and Amundson [10] considering the effect of axial dispersion and interphase mass transfer. They derived the existence conditions by using perturbation theory in a properly defined moving coordinate system. They illustrated the application of their solution by using the Langmuir isotherm. The continuous countercurrent arrangement has long been used in industry as a series of discrete bed stages, and the use of a single pulsed bed has also been described by (Perry and Chilton [11])

Although there may be serious difficulties in implementing the continuous countercurrent adsorber (Westermarck [12]), it nevertheless provides a convenient theoretical upper limit to the attainable separation. Liapis and Rippin [13] simulated binary adsorption in continuous countercurrent operation and also compared with other operation modes. Simulation studies were presented of three different modes of operating a two-component adsorption system. The efficiency with which an activated carbon adsorbent is utilized was compared for a single fixed bed, a periodic countercurrent system in which the adsorbent was equally distributed over two, four and six beds and a continuous countercurrent system.

A mathematical model of steady state continuous countercurrent adsorbers was presented by Ruthven et al. [14, 15] by considering axially dispersed plug flow for the bulk fluid and linear relation for equilibrium isotherm. By solving the dimensionless model analytically, a theoretical expression was derived for the Height Equivalent of a Theoretical Plate (HETP). Ching and Ruthven [16] have presented a steady state theoretical and experimental study for the separation of glucose-fructose mixture. The dispersion coefficient was calculated from a pulse chromatographic measurement. An equilibrium stage model and McCabe-Thiele diagram has also been drawn to describe the behavior. They reported that the overall countercurrent HETP was of order 8-12 cm so

that each column was equivalent to 10 theoretical stages. Later Ching and Ruthven [17] presented the same theoretical and experimental study for the transient response of the separation of glucose-fructose mixture. From experiment it was found that 27 hours of operation were required to approach steady state for the fructose profile and 12 hours for the glucose profile. Ching and Ruthven [18] published a theoretical and experimental study of a simulated countercurrent adsorption system for non-isothermal operation for glucose-fructose mixture. By comparing the results from previous work which was done under isothermal condition, the authors reported that the separation performance was significantly better. Ching et al. [19] developed an improved adsorption process for the production of high fructose syrup. The experiments were carried out at steady state for a linear isotherm. It was shown that by applying a temperature profile to the system, the concentration of the extract product in a countercurrent adsorption separation process might be increased relative to the maximum concentration attainable under isothermal conditions. Ching and Ruthven [20] have reported a theoretical and experimental study of the "sorbex" operation for the linear isotherm and dispersed plug flow model. They reported that under properly selected conditions product purities and recoveries of 85-95% could be obtained. Nemeth et al. [21] developed mathematical models of steady state countercurrent vapour adsorption and compared them for various assumptions of the shape of the isotherm. They studied both linear and nonlinear isotherms for a dispersed plug flow model. They solved their model by the integral equation technique.

The transient and steady state numerical and experimental study of a semi-continuous countercurrent adsorption unit for fructose-glucose separation was done by Hidajat et al. [22]. They adopted the linear isotherm and axial dispersed plug flow model for their study. For HETP, a chromatographic method was used. Under the experimental conditions used 60 hours of operation was required for fructose and about 37 hours for glucose to reach steady state. The theoretical predictions were in good agreement with the

experimental results under the limiting operating conditions. Analysis of the performance of a simulated countercurrent chromatographic system for fructose-glucose separation has been carried out by Ching and Ruthven [23]. They reported that HETP in the countercurrent system is higher than would be expected for an ideal plug flow system, showing that axial mixing is important. The theoretical analysis of the effect of subdivision of the adsorbent bed was studied by Hidajat et al. [24]. The unsteady state model and the linear equilibrium relation was chosen to develop the relationship. The authors suggested that subdivision of each section into more than two subsections will be economically justified only if product purity requirements are stringent.

Ching et al. [25] studied the multicomponent separation using a column switching chromatographic method. They used carbohydrate mixture as their system. It permitted continuous introduction of the feed and was designed to produce higher product concentration compared to a normal elution cyclic process. A fixed-bed model incorporating axial dispersion and a linear driving force for mass transfer was successfully used to estimate optimum operating conditions (switch times and fluid-flow rates).

A theoretical model of a simulated countercurrent adsorption system for non-linear equilibrium relationship was developed and solved by the method of orthogonal collocation (Hidajat and Ching [26]). They used monoethanolamine (MEA) - methanol (MOH) mixture as their system. They also reported a comparison between their theoretical and experimental results. It was found that the nonlinearity of the MEA isotherm imposed significant constraints on the allowable operating conditions. Continuous operation of a simulated counter-current adsorption process for separating a binary mixture with non-linear, interacting equilibrium relationships has been demonstrated experimentally by Ching et al. [27] Emphasis is placed on the optimization

of operating conditions for attaining high product purity and recovery when the isotherm is non-linear.

An unsteady state theoretical dispersed plug flow model that includes a mass-transfer resistance represented by a linear driving force approximation was presented for continuous counter-current adsorption system having nonlinear equilibrium isotherm and solved by orthogonal collocation method by Hassan et al. [28]. The model was used to investigate the effects of various parameters on the performance of the system. It was demonstrated that as the non-linearity changes, the optimal choice of bed length, feed and eluent flow rates, and switch times must be suitably adapted. Rahman et al. [29] extended the previous model to a "SORBEX" system. The effect of various process parameters on the performance of the system were investigated. The study revealed that the system performance and dynamics are strongly dependent on bed length, column diameter, feed and eluent flow rate, switch time and non-linearity of the isotherm. They concluded that there exists a set of optimum values of these process parameters that represents the proper combination for best performance. Recently Hassan et al. [30] developed a mathematical model for a simulated moving bed adsorption system using a more precise approach. In this approach appropriate equations and boundary conditions are written for each adsorption column as distinct from the section approach adopted by previous workers. The time-dependent boundary condition for each column are formulated and related to switching time. Both models predicted similar concentration profile at steady state and were shown to provide good representations of the experimental data for linear (glucose - fructose) and nonlinear (MEA - MOH) system. The study also revealed that the system performance and dynamics are strongly dependent on axial dispersion, eluent-to-feed ratio, bed length and switch time. It is observed that there exists a set of optimum values of all the parameters for best process performance. Recently Storty et al. [31] reported an optimal design procedure of the operating conditions involved in a simulated moving bed

unit. The characterization has been performed in the frame of the equilibrium theory with reference to the flow rate ratios. The space of the operating parameters i.e., mass flow rate ratios is divided into regions with different separation regimes of complete separation, pure extract, pure raffinate and no purity. They also reported a procedure for selecting the optimum switch time using a detailed model, which accounts for axial dispersion and mass transfer resistance. These results constitute a useful tool for determining the range of operating conditions to achieve an assigned separation requirement and then for selecting the optimal operating condition within this range. However, from their study it is not straightforward to arrive at the optimum values of the individual process parameters required for practical operations.

A brief summary of the published work in chronological order is given in Table 2.3.

2.3 CONCLUSIONS

Modelling and simulation of continuous counter-current adsorption systems is well established in the literature and has been shown to provide a good representation of experimental data. In both two section and four section models, the independent and dependent variables need to be identified. The effects of changes in the independent (manipulating) variables on the performance of the process are very strongly coupled thereby making it difficult to make intuitive predictions. The literature search reveals that there exists an optimum set of these independent variables. Experimental determination of this optimum set requires trial and error procedure which is time consuming and uneconomical. A systematic theoretical evaluation of these optimum set of values is yet to be accomplished.

REFERENCES

- (1) Ruthven, D. M., and Ching, C. B., "Counter-current and simulated counter-current adsorption separation processes", *Chem. Eng. Sci.*, 44(5), 1011-1038, (1989)
- (2) Storti, G., Masi, M., and Morbidelli, M., "Optimal design of SMB adsorption separation units through detailed modelling and equilibrium theory", NATO ASI Vimeiro, Portugal, Elsevier, (1988)
- (3) Amundson, N. R., and Kasten, P. R., "Analytical solutions for simple systems in moving bed adsorbers", *Ind. Eng. Chem.*, 44, 1704 (1952).
- (4) Neretnieks, I., "A mathematical model for continuous counter-current adsorption", *The Swedish Paper Journal*, 77, 407 (1974a).
- (5) Neretnieks, I., "Adsorption of components having a saturation isotherm", *Chem. Eng., Tech*, 46, 781 (1974b).
- (6) Neretnieks, I., "A simplified theoretical comparison of periodic counter-current adsorption", report DECHEMA, Frankfurt / Main., (B.R.D.) (Oct., 1974c).
- (7) Fornwalt, H. J., and Hutchins, R. A., "Purifying liquids with activated carbon", *Chem.Eng.*, 73, 155-164 (1968).
- (8) Erskine, D.B., and Schuliger, W.G., "Activated carbon processes for liquids", *Chem. Eng. Progr.*, 67, 41 (1971).
- (9) Chen, J. W., Cunningham, R. L., and Buege, J. A., "Computer simulation of plant-scale multicolumn adsorption process under periodic counter-current operation", *Ind. Eng. Chem., Proc. Design Develop.*, 11, 430 (1972).
- (10) Rhee, H. K., and Amundson, N. R., "Asymptotic solution to moving-bed exchange equation", *Chem. Eng. Sci.*, 28, 55-62 (1973).
- (11) Perry, J. H., and Chilton, C. H., *Chemical Engineers' Handbook*, McGraw-Hill Book Company, 5th ed., 16-20 (1973).
- (12) Westermark, M., "Purification of municipal wastewater by adsorption on granular activated carbon", Doctoral thesis, Dept. of Chem. Eng., Royal Inst. of Technology, Stockholm, Sweden (1975).
- (13) Liapis, A. I., and Rippin, D. W. T., "Simulation of binary adsorption in continuous counter-current operation in comparison with other operating models", *AICHE J.*, 25, 455-460 (1979).

- (14) Ruthven, D. M., Principles of Adsorption and Adsorptive Processes, John Wiley, New York (1984).
- (15) Ruthven, D. M., and Ching, C. B., "The axial dispersed plug-flow model for continuous counter-current adsorbents", *Can. J. Chem. Eng.*, 61, 881-883 (1983).
- (16) Ching, C. B., and Ruthven, D. M., "An experimental study of a simulated counter-current adsorption system-I. Isothermal steady state operation", *Chem. Eng. Sci.*, 40 (6) 877-885 (1985).
- (17) Ching, C. B., and Ruthven, D. M., "An experimental study of a simulated counter-current adsorption system-II. Transient response", *Chem. Eng. Sci.*, 40 (6), 887-891 (1985).
- (18) Ching, C. B., and Ruthven, D. M., "Experimental study of a simulated counter-current adsorption system-IV. Non-isothermal operation", *Chem. Eng. Sci.*, 41, 3063-3071 (1986).
- (19) Ching, C. B., Ho, C., and Ruthven, D. M., "An improved adsorption processes for the production of high fructose syrup", *AIChE*, 32, 1876-1880 (1986).
- (20) Ching, C. B., and Ruthven, D. M., "Separation of glucose and fructose by simulated counter-current adsorption", *AIChE Symp. Ser.*, 81 (242), 1-8 (1985).
- (21) Nemeth, J., Vasanits, E. V., and Virag, T., "Mathematical modelling of counter-current adsorption", *Int. J. Heat & Mass Transfer*, 28(4), 859-866 (1985).
- (22) Hidajat, K., Ching, C.B., and Ruthven, D.M., "Numerical simulation of a semi-continuous counter-current adsorption unit for fructose-glucose separation", *Chem. Eng. J.*, 33, B55-B61 (1986).
- (23) Ching, C. B., and Ruthven, D. M., "Analysis of the performance of a simulated counter-current chromatographic system for fructose-glucose separation", *Can. J. Chem. Eng.*, 62, 398-403 (1984).
- (24) Hidajat, K., Ching, C. B., and Ruthven, D. M., "Simulated counter-current adsorption processes: a theoretical study of the effect of sub-dividing the adsorbent bed", *Chem. Eng. Sci.*, 41, 2953-2956 (1986b).
- (25) Ching, C. B., Chu, K. H., and Hidajat, K., "Multicomponent separation using a column switching chromatographic method", *AIChE*, 40, 1843-1849 (1994).
- (26) Hidajat, K., and Ching, C. B., "Simulation of the performance of a continuous counter-current adsorption system by the method of Orthogonal collocation with nonlinear and interacting adsorption isotherms", *Trans I Chem. Eng.*, 68, 104-108 (1990).

- (27) Ching, C. B., Chu, K. H., Hidajat, R. and D. M. Ruthven, "Experimental study of a simulated counter-current adsorption system-VII. effects of nonlinear and interacting isotherms", *Chem. Eng. Sci.*, 48, 1343-1351 (1993).
- (28) Hassan, M. M., Rahman, A. K. M. S., and Loughlin, K. F., "Numerical simulation of unsteady continuous counter-current adsorption system with nonlinear adsorption isotherm", *Sep. Technol.*, 4, 15-26 (1994).
- (29) Rahman, A. K. M. S., Hassan, M. M., and Loughlin, K. F., "Unsteady state simulation of "Sorbex" system with nonlinear adsorption isotherms", *Sep. Technol.*, 4, 27-37 (1994).
- (30) Hassan, M. M., Rahman, A. K. M. S., and Loughlin, K. F., "Modelling of simulated moving bed adsorption system: a more precise approach", *Sep. Technol.*, 5, 77-89 (1995).
- (31) Storti, G., Baciocchi, R., M., and Morbidelli M., "Design of optimal operating conditions of simulated moving bed adsorptive separation units", *Ind. Eng. Chem. Res.*, 34, 288-301 (1995).
- (32) Hashimoto, K., Adach, S., Noujima, H., and Maruyama, H., "A new processes combining adsorption and enzyme reaction for the producing high fructose syrup", *Biotechnol. Bioeng.*, 25, 2371-2393 (1983).
- (33) Hashimoto, K., Adach, S., Noujima, H., and Maruyama, H., "Models for the separation of glucose / fructose mixture using a simulated moving-bed adsorber", *J. Chem. Eng. Japan*, 16, 400-406 (1983).
- (34) Ching, C. B., Ruthven, D. M., and Hidajat, R., "Experimental study of a simulated counter-current adsorption system-III. Sorbex Operation", *Chem. Eng. Sci.*, 40, 1411-1417 (1985).
- (35) Kubota, R., Hata, C., and Shinya, H., "Study of a SMB based on axial dispersion model", *Can. J. Chem. Eng.*, 66, (1988).
- (36) Liu, P.D., and Pigford, R. L., "Preparative separation of proteins by periodic counter-current sorption", *AICHE National Meeting, Houston*, (1987).
- (37) Carta, G., and Pigford, R. L., "Periodic counter-current operation of sorption processes applied to water desalination with thermally regenerable ion-exchange", *Ind. Eng. Chem. Fundam.*, 25, 677-685 (1986).
- (38) Barker, P.E., and Thawait, S., "Separation of fructose from carbohydrate mixtures by semi-continuous gas-liquid chromatography", *Chem. Ind.*, 7 November, 817-821 (1983).

- (39) Ching, C. B., Hidajat, K., Ho, C., and Ruthven, D. M., "Modelling of a simulated counter-current adsorption processes", *Reactive Polym.*, 6, 15-20 (1987).
- (40) Ching, C. B., Hidajat, K., Ho, C., and Ruthven, D. M., "Experimental study of a simulated counter-current adsorption system-V. Comparison of Resin and Zeolite adsorbents for fructose-glucose separation at high concentration", *Chem. Eng. Sci.*, 42, 2547-2555 (1987).
- (41) Ching, C. B., Ho, C., and Ruthven, D. M., "Experimental study of a simulated counter-current adsorption system-VI. Non-linear systems", *Chem. Eng. Sci.*, 43, 703-711 (1988).
- (42) Svedberg, U. G., "Numerical solution of multicolumn adsorption processes under periodic counter-current operation", *Chem. Eng. Sci.*, 31, 345-353 (1976).
- (43) Storti, G., Santacesaria, E., Morbidelli, M., and Carra, S., "Separation of Xylene on Y Zeolites in the vapour phase 3 choice of adsorbents", *Ind. Eng. Chem. Proc. Des. Dev.*, 24, 89-92 (1985).

NOMENCLATURE

D	molar flow rate of desorbent per unit column cross section
F	molar feed flow rate per unit cross section area of column
K	ratio constant
S	molar flow rate of adsorbed phase per unit column cross sectional area
x	solid phase concentration
x_F	solid phase concentration in feed
y	fluid phase concentration
y_D	fluid phase concentration in desorbent
y_E	fluid phase concentration in extract
y_F	fluid phase concentration in feed

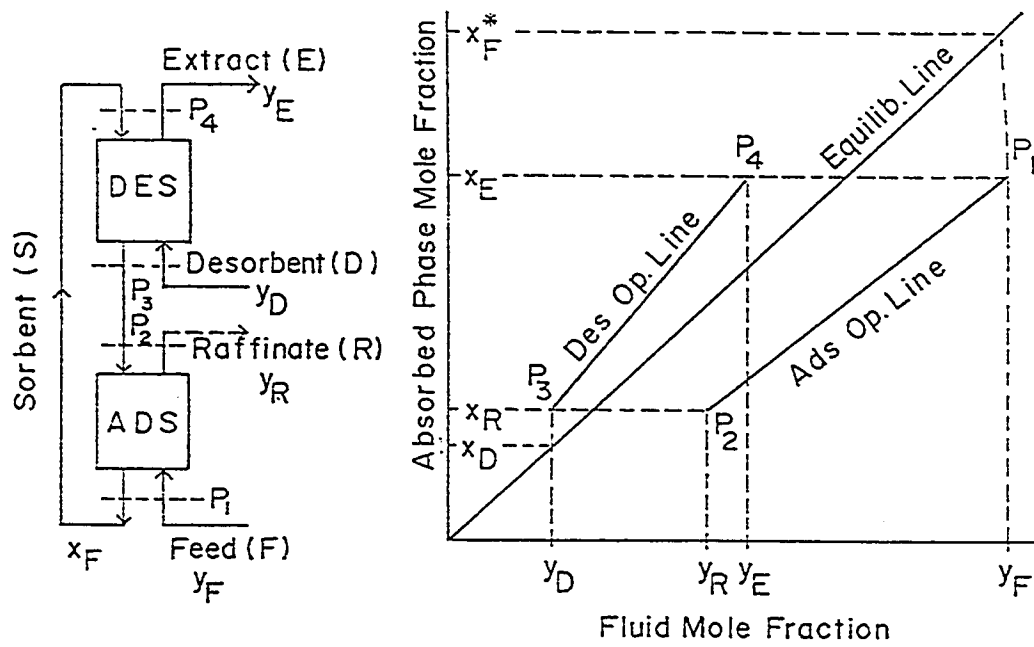


Figure 2.1 McCabe-Thiele analysis of a countercurrent system.

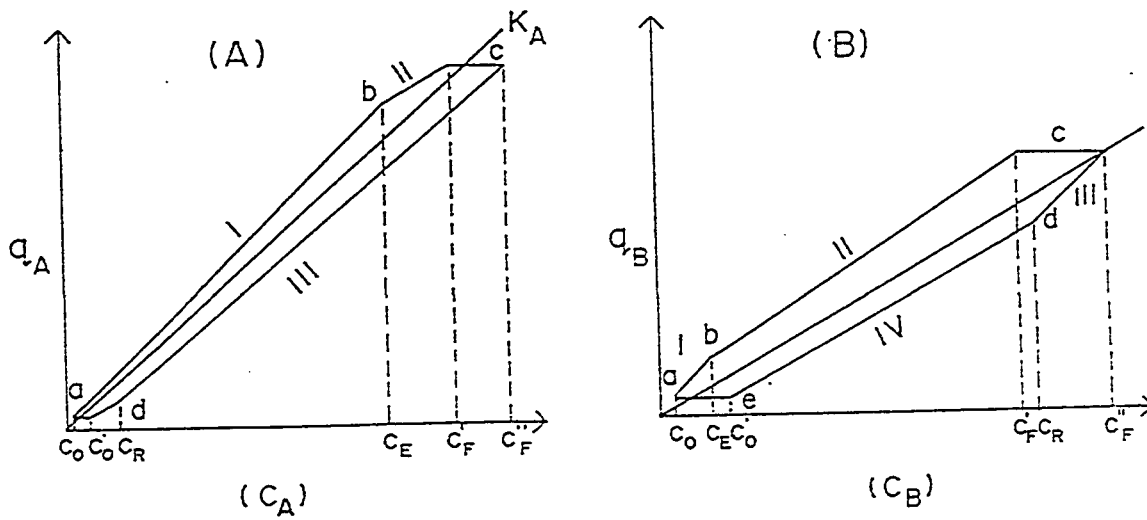
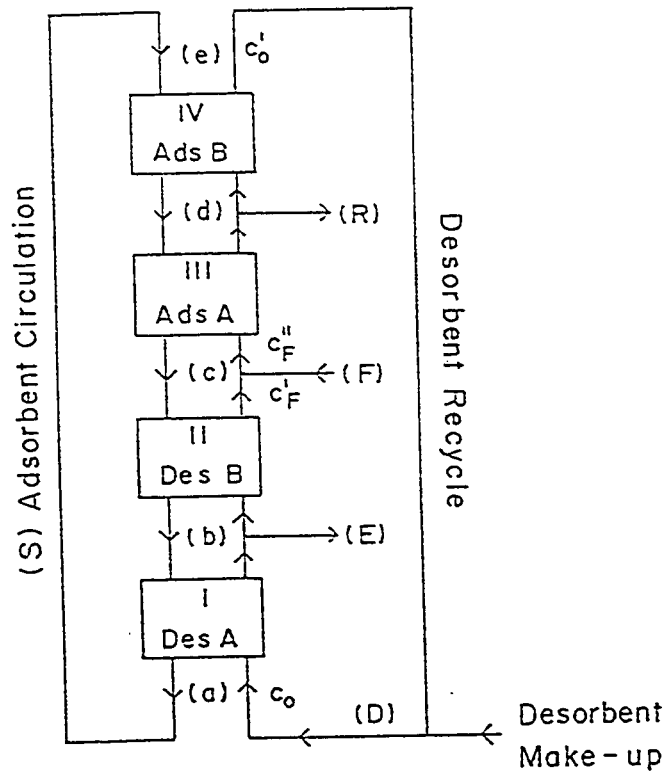


Figure 2.2 McCabe-Thiele analysis of "SORBEX" system

Table 2.1 Classification of models for countercurrent processes [1]

Representation of system	Representation of bed elements
(a) Continuous countercurrent	(a.1) Continuous
	(a.2) Mixing cell
(b) SMB (direct simulation of port switching)	(b.1) Continuous
	(b.2) Mixing cell

Table 2.2 Examples of the application of various countercurrent models [1]

Model No	Comments	References
a.1.I	Equilibrium theory for "Sorbex" unit constant separation factor, plug flow	Storti et al. [2]
a.1.II	Equivalent countercurrent model linear system, plug flow	Hashimoto et al. [32,33]
	Equivalent countercurrent model linear system, dispersed plug flow (analytical solution)	Ching and Ruthven [20,16]
	Extension of this model to " Sorbex " system	Ching et al. [34]
	Axial dispersed plug flow model applied to sorbitol-glucose separation	Kubota et al. [35]
	Equivalent countercurrent model with intraparticle diffusion (linear system)	Liu and Pigford [36]
a.2.I	comparison of equilibrium and continuous models for SMB system	Ching and Ruthven [20,16] Ching et al. [34]
b.1.II	Numerical simulation of SMB using continuous model for bed elements	Hashimoto et al. [32,33]
	Numerical simulation of SMB using continuous model for bed elements	Storti et al. [2]

Numerical simulation of SMB using mixing Carta and Pigford [37]
cell model-linear system

b.2.I Numerical simulation of SMB using mixing Barker and Thawait [38]
cell model-linear system

Numerical simulation of SMB using mixing Hidajat et al. [22,26]
cell model-linear system

Numerical simulation of SMB using mixing Ching et al. [39]
cell model-linear system

Numerical simulation of SMB using mixing Ching et al. [40,41]
cell model-non linear system

Table 2.3: Summary of the published work

Isotherm	Flow Model	Data	Year	Reference
Linear	Plug Flow	Theoretical	1952	Amudson & Kasten [3]
Linear	Plug Flow	Theoretical	1974	Neretnicks [4, 5, 6]
Linear	D.Plug Flow	Theoretical	1976	Svedberg [42]
Linear	Plug Flow	Experimental	1979	Liapis & Rippin [13]
Linear	D.Plug Flow	Theoretical	1983	Ruthven & Ching [15]
Linear	D.Plug Flow	Experimental	1985	Ching & Ruthven [20]
Linear	D.Plug Flow	Experimental	1985	Ching & Ruthven [16]
Linear	D.Plug Flow	Experimental	1985	Ching et al. [34]
Both	D.Plug Flow	Theoretical	1985	Nemeth et al. [21]
Linear	D.Plug Flow	Experimental	1986	Ching & Ruthven [18]
Linear	D.Plug Flow	Experimental	1986	Hidajat et al. [22, 24]
Linear	D.Plug Flow	Experimental	1986	Ching et al [19]
Non linear	D.Plug Flow	Experimental	1988	Ching et al. [41]
Both	D.Plug Flow	Both	1988	Ruthven & Ching [1]
Non linear	D.Plug Flow	Theoretical	1989	Storti et al. [43]
Non linear	D.Plug Flow	Both	1990	Hidajat & Ching [26]
Interacting	D.Plug flow	Experimental	1993	Ching et al. [27]
Non linear	D.Plug Flow	Theoretical	1994	Hassan et al. [28]
Non linear	D.Plug Flow	Theoretical	1994	Rahman et al. [29]
Non linear	D.Plug Flow	Theoretical	1995	Hassan et al. [30]
Non-linear	Equilibrium	Theoretical	1995	Storti et al. [31]

Chapter 3

Theoretical Model

3.1 INTRODUCTION

The problem of modelling a simulated moving bed (SMB) adsorption separation process has attracted a great deal of attention in recent years [1]. The approaches which have been followed may be classified according to whether the system is simulated directly or represented in terms of an equivalent true counter current system and whether the bed elements are represented by a continuous-flow model or as a cascade of mixing cells. The available theoretical models in the literature may be considered in these three categories and details of them are discussed in this section.

3.2 MODELLING AND SIMULATION OF SMB PROCESSES

3.2.1 Equivalent counter current model: dispersed plug flow model

The equivalent counter-current representation of a SMB adsorption process can be extended to provide the basis for a detailed mathematical model of the system. Assuming plug flow of the solid and axially dispersed plug flow of the fluid, the basic differential equation describing the system dynamics is

$$D_{L_j} \frac{\partial^2 c_{ij}}{\partial z_j^2} - V_j \frac{\partial c_{ij}}{\partial z_j} + \left(\frac{1-\varepsilon}{\varepsilon} \right) u \frac{\partial q_{ij}}{\partial z_j} = \frac{\partial c_{ij}}{\partial t} + \left(\frac{1-\varepsilon}{\varepsilon} \right) \frac{\partial q_{ij}}{\partial t} \quad (3.1)$$

The (Danckwerts) boundary conditions are:

$$\text{at } z_j = 0 \quad D_{L_j} \frac{\partial c_{ij}}{\partial z_j} \Big|_{z_j=0^+} = -V_j (c_{ij} \Big|_{z_j=0^+} - c_{ij} \Big|_{z_j=0^-}) \quad (3.2)$$

$$\text{at } z_j = L_{s_j} \quad \frac{\partial c_{ij}}{\partial z_j} = 0.0 \quad (3.3)$$

For linear equilibrium isotherms, the rate equation can be written as

$$\frac{\partial q_{ij}}{\partial t} = k [K c_{ij} - q_{ij}] \quad (3.4)$$

For Langmuir equilibrium isotherms, the rate equation can be written as

$$\frac{\partial q_{ij}}{\partial t} = k \left[\frac{b_i q_s c_{ij}}{1 + \sum_{i=1}^n b_i c_{ij}} - q_{ij} \right] \quad (3.5)$$

The models available in the literature are mostly limiting cases of the general model presented above.

Ruthven [2], and Ruthven & Ching [3] solved analytically the general model for steady state using linear equilibrium isotherm. They used glucose-fructose system in their experiment and a theoretical expression was derived for the Height Equivalent of a Theoretical Plate (HETP).

Ching and Ruthven [4] solved the above model under steady state condition for "SORBEX" system. They used linear equilibrium isotherm for their solution. They reported that under properly selected conditions product purities and recoveries of 85-95 % could be obtained.

A theoretical model for SMB with non-linear equilibrium isotherm was developed by Hidajat and Chng [5]. They solved the steady state model equations for non-linear MEA-MOH system by the method of orthogonal collocation. They also reported a comparison between their theoretical and experimental results. It was observed that system non-linearity imposes significant constraints on the allowable operating conditions.

Hassan et al. [6] solved the unsteady state model for axially dispersed plug flow system . They used both linear glucose-fructose system and non-linear MEA-MOH system. They investigated the effects of various process parameters on the performance of the system. It was reported that as the non-linearity changes, the optimal choice of the system variables must be suitably adapted.

Rahman et al. [7] solved the above axially dispersed plug flow model for "SORBEX" system. They used both Danckwert's boundary conditions and linear driving force relation in their model. The study revealed that system performance and dynamics are strongly dependent on process variables and as well as non-linearity of the system.

3.2.2 Equivalent counter current model: equilibrium stage model

Alternatively one may choose to represent the bed as equivalent to a certain number (n) of ideal equilibrium stages. For a linear system the fluid phase concentration ratio will then be given by the Kremser equation (Kremser [8], Souders and Brown [9]):

$$\frac{c_o - c_L}{c_o - c_L / K} = \frac{\gamma^{n+1} - \gamma}{\gamma^{n+1} - 1} \quad (3.6)$$

or

$$\frac{c_o}{c_L} = \frac{1}{\gamma - 1} [\gamma^{n+1} (1 - 1/K) + \gamma / K - 1] \quad (3.7)$$

A simple mass balance over the section gives

$$q_L = q_o + \left(\frac{L}{S}\right)(c_L - c_o) \quad (3.8)$$

For each section of the unit there is one equation of the form of equation (3.6) and one equation of the form of equation (3.8) relating the inlet and outlet concentrations. This gives in all a set of eight equations relating the 10 concentrations $q_o, q_I, q_{II}, c_o, c_I, c_{II}, c_{III}, c'_{III}$, and c_{IV} . Two additional equations are obtained from the mass balances over the feed point and for the circulating stream:

$$(D - E)c_{II} = (D - E + F)c'_{II}$$

$$(D - E + F - R)c_{IV} = Dc_o \quad (3.9)$$

With the flowrates, Peclet and Stanton numbers and equilibrium constants all defined the solution to this set of equations gives the steady state concentration profile through the

system. Since all equations are linear and equilibrium for each component is assumed independent, solution of the equation is straightforward.

The relationship between the two models may be derived by considering the HETP (height equivalent to a theoretical plate) Ruthven [2].

3.2.3 Equivalent counter current model: A more precise approach

The simulated continuous counter current system is shown in Figure 3.1. To simulate the solid phase movement, the feed input position is switched from one bed to another instead of recirculating the solid phase. This switching depends on the equilibrium and kinetic parameters of the system. Each time, with changing feed point and draw off position, material balance and boundary conditions are changed. After the feed location comes back to its original position at time $t = 0$, the system is considered to have completed one cycle.

The basic differential equations describing the system dynamics for i th component and j th bed can be written as

$$D_{L_j} \frac{\partial^2 c_{ij}}{\partial z_j^2} - V_j \frac{\partial c_{ij}}{\partial z_j} = \frac{\partial c_{ij}}{\partial t} + \left(\frac{1 - \epsilon}{\epsilon} \right) \frac{\partial q_{ij}}{\partial t} \quad (3.10)$$

For Langmuir equilibrium isotherms, the rate equation can be written as

$$\frac{\partial q_{ij}}{\partial t} = k \left[\frac{b_i q_s c_{ij}}{1 + \sum_{i=1}^n b_i c_{ij}} - q_{ij} \right] \quad (3.11)$$

Initial conditions: The initial condition of a bed at any particular time will be equal to the final condition of that bed at the previous switch time.

Boundary conditions: at $z = 0.0$

$$D_{L_j} \frac{\partial c_{ij}}{\partial z_j} \Big|_{z_j=0^+} = -V_j (c_{ij} \Big|_{z_j=0^+} - c_{ij} \Big|_{z_j=0^-}) \quad (3.12)$$

Boundary conditions at $z = L$

$$\frac{\partial c_{ij}}{\partial z_j} = 0.0 \quad (3.13)$$

Material balances for beds following the feed point and eluent point are:

$$c_{if} = \frac{V_{f-1} c_{i,f-1} \Big|_{z_{f-1}=L_{f-1}} + (V_f - V_{f-1}) c_{i,f}}{V_f} \quad (3.14)$$

$$c_{ie} = (c_{ie-1} \Big|_{z_{e-1}=L_{e-1}}) \frac{V_{e-1}}{V_e} \quad (3.15)$$

using the following dimensionless variables

$$C_{ij}' = \frac{c_{ij}}{c_f}; \quad Q_{ij}' = \frac{q_{ij}}{q_f}; \quad \tau = \frac{t}{L_1/V_1}; \quad Z_j = \frac{z_j}{L_1}$$

the above equations can be written following dimensionless form

$$\frac{\partial C_{ij}'}{\partial \tau} = F_j \left[\frac{1}{Pe_j} \frac{\partial^2 C_{ij}'}{\partial Z_j^2} - \frac{\partial C_{ij}'}{\partial Z_j} - \psi K_j \phi \frac{\partial Q_{ij}'}{\partial \tau} \right] \quad (3.16)$$

$$\frac{\partial Q_{ij}'}{\partial \tau} = \alpha \left[\frac{C_{ij}'}{1 + \sum_{i=1}^n \lambda_i (C_{ij}' - 1)} - Q_{ij}' \right] \quad (3.17)$$

Boundary conditions:

$$\text{at } Z_j = 0.0 \quad C_{ij}' = C_{ij}' \Big|_{Z_j=0.0} + \frac{1}{Pe_j} \frac{\partial C_{ij}'}{\partial Z_j} \Big|_{Z_j=0.0} \quad (3.18)$$

$$\text{at } Z_j = L_{sj} \quad \frac{\partial C_{ij}'}{\partial Z} = 0.0 \quad (3.19)$$

$$C_{i,j+1}' = C_{ij}' \Big|_{Z_{L_j}}, \quad j \neq f \text{ or } e \quad (3.20)$$

$$C_{if}' = \frac{V_{f-1} C_{i,f-1}' \Big|_{Z_{f-1}=L_{f-1}} + (V_f - V_{f-1})}{V_f} \quad (3.21)$$

$$C_{ie}' = (C_{ie-1}' \Big|_{Z_{e-1}=L_{e-1}}) \frac{V_{e-1}}{V_e} \quad (3.22)$$

Hassan et al. [10] solved the the above model to investigate the dynamics of each column. They studied the change in concentration profiles in each bed with number of cycles, for the linear glucose-fructose system and non-linear MEA-MOH system. They compared their results obtained for these systems with the experimental results of Ching et al. [4] and Hidajat et al. [5] respectively and found agree well. They also shown the change in concentration of a particular bed at steady state with number of switches both for linear and non-linear systems.

3.3 OPTIMIZATION METHODS

3.3.1 Introduction

Optimization can be defined as the technique used to improve the outcome of certain objectives. Recent advances in applied mathematics, operation research, and digital-computer technology enable many complex industrial problems in engineering and economics to be optimised successfully by the application of logical and systematic techniques. In mathematical terms, optimization usually involves maximizing or minimizing the objective function; for example, we may wish to maximize or minimize some economic or physical property which is of interest.

Many optimization functions possess more than one extremum. Hence we must recognize that the maximum or minimum which we may have found at some particular point is not necessarily the largest maximum or the smallest minimum in the entire region of interest. An extremum that exists at a point within some subregion R' of the region R is called a relative or local extremum; the greatest maximum (or the smallest minimum) in R is called an absolute or global maximum (or an absolute or global minimum).

3.3.2 The Objective Function

In order to consider attaining certain goals in an optimal manner, we must first define our objective quantitatively. We recognize that the desired objective must depend on certain variables, which are sometimes referred to as decision variables. In a standard optimization problem, an objective function is defined to represent some quantity, such as profit or cost, that we wish to optimise. The present problem deals with the separation of a liquid mixture into its components through a continuous countercurrent adsorption

process. This physical system is modelled by a set of ordinary differential equations. The objective function i.e., the recovery of one component is calculated from the solution of this set of model equations which are functions of several process variables. The goal is to achieve the optimum values of these variables for which the recovery of this component will be maximum.

3.3.3 Constraints

Sometimes the problem variables within a region are not entirely free, but must satisfy certain bounds or functional relationships. These auxiliary conditions are known as constraints. Usually the constraints represent either system limitations or the physical and economic laws that the variables must satisfy.

For example, the optimal design of a chemical reactor might involve the determination of some absolute temperature and absolute pressure that would maximize the yield of product. The objective function would represent the yield, and the independent variables are temperature and pressure. Clearly, the variables are bounded by the conditions that temperature and pressure must be greater than zero. In addition, we require that the pressure, temperature and density satisfy some equation of state. This is an equality constraint. There are inequality constraints which allows the variables to vary within a fixed bound.

More specifically, in the present problem optimization is carried out for maximum recovery of one component subjected to a specified purity of the other component. This is achieved by setting a purity band which will force the optimization routine to meet these constraints specifications.

3.3.4 Classification of Optimization Problem

Based on the nature of objective functions and constraints, optimization problems can be grouped into several categories. The optimization function can be univariate or multivariate; it can be linear or non-linear. Similarly the constraints can be linearly constrained or non-linearly constrained and for both cases it can be equality constrained or inequality constrained. Each type of function can have different types of constraints and exists in different categories. In a very simple way the optimization problem can be classified in the following different groups:

- (i) Unconstrained minimization problem
- (ii) Minimization with simple bounds
- (iii) Linearly constrained minimization
- (iv) Nonlinearly constrained minimization

The objective function of the present problem i.e., recovery is calculated from the solution of a set of nonlinear ordinary differential equations and falls into the category of nonlinear function. Similarly the constraints are also nonlinear and possess inequality behavior. In that context the present problem can be termed as nonlinearly inequality constrained minimization problem which fits into class iv above.

3.4 OPTIMALITY CONDITIONS

Optimization problems involve minimizing an objective function, subject to a set of constraints imposed on the variables. In essentially all problems of concern, the

constraints will be expressible in terms of relationships involving continuous functions of the variables.

The general problem class to be considered is known as nonlinearly constrained problem (NCP), and may be expressed in mathematical terms as [11]:

NCP	$\begin{aligned} & \text{minimize } F(x) \\ & \quad x \in \mathcal{R}^n \\ & \text{subject to } c_i(x) = 0, i = 1, 2, \dots, m'; \\ & \quad \quad \quad c_i(x) \geq 0, i = m' + 1, \dots, m. \end{aligned}$	(3. 23)
-----	---	---------

Any point x that satisfies all the constraints of NCP is said to be feasible. The set of all feasible points is termed the feasible region. A problem for which there are no feasible points is termed an infeasible problem.

In order to select an efficient method for solving a particular problem of the NCP, it is necessary to analyze and classify the problem in various ways. Before considering methods for solving problems, however, we must be able to define a “solution” of NCP. Firstly, we note that only feasible points may be optimal. Secondly, optimality of a point x^* is defined by its relationship with neighbouring points- in contrast, say, to seeking a point x where $F(x) = 0$. Formally, the set of relevant points is defined as follows. Let x^* denote a feasible point for problem NCP, and define $N(x^*, \delta)$ as the set of feasible points contained in a δ -neighbourhood of x^* .

Definition A. The point x^* is a strong local minimum of NCP if there exists $\delta > 0$ such that

A1. $F(x)$ is defined on $N(x^*, \delta)$; and

A2. $F(x^*) < F(y)$ for all $y \in N(x^*, \delta)$, $y \neq x^*$.

In the special circumstance when x^* is the only feasible point in $N(x^*, \delta)$, x^* is also considered to be a strong local minimum.

Definition B. The point x^* is a weak local minimum of NCP if there exists $\delta > 0$ such that

B1. $F(x)$ is defined on $N(x^*, \delta)$;

B2. $F(x^*) \leq F(y)$ for all $y \in N(x^*, \delta)$; and

B3. x^* is not a strong local minimum.

These definitions imply that x^* is not a local minimum if every neighbourhood of x^* contains at least one feasible point with a strictly lower function value.

In some applications, it is important to find the feasible point at which $F(x)$ assumes its least value. Such a point is termed the global minimum. It is usually not possible to find a global minimum except in special cases; however, this is rarely an impediment to the satisfactory solution of practical problems.

3.5 SOLUTION OF AN OPTIMIZATION PROBLEM

The solution of an optimization problem depends on the objective function and the constraints which must be satisfied in order to achieve the objective. In section 3.3.4 we discussed the different categories of the optimization problem. For example, in some cases for two different problems the functions may be the same but the constraints may differ. Further, the problem may contain equality constraints or inequality constraints which could be either linear or nonlinear. Based on these different categories there are different solution procedures which are available in the literature. IMSL mathematics

library has various subroutines which can solve different categories of optimization problems. Before selecting the appropriate subroutine to be used for solving the problem one must go through the details of the functions and constraints to make a suitable choice of the available subroutine.

3.5.1 Solution of a nonlinearly inequality constrained Optimization problem

The objective function of the present problem i.e., recovery is calculated from the simultaneous solution of a system of ordinary differential equations which represents the physical system of this problem. The constraints i.e., the specified purity band which allows the purity of the other component to vary within 10% of the desired purity are inequality constraints. In this problem we have two inequality constraints. To solve such an optimization problem IMSL subroutine NCONF [12] is used. The method is based on the iterative formulation and solution of quadratic programming subproblems by using a quadratic approximation of the Lagrangian and by linearizing the constraints. The optimization procedure can be described briefly in following steps:

Step 1: Count the number of variables in the objective function which will be optimized. In the present problem we have considered various cases with three, five and seven optimization variables. From these variables, we will need to construct the Hessian matrix. The size of the Hessian matrix depends on the number of optimization variables. For example three variables will generate a (3x3) Hessian matrix.

Step 2: A quadratic programming subproblem is obtained by using a quadratic approximation of the Lagrangian and by linearizing the constraints. That is,

$$\begin{aligned}
& \min \frac{1}{2} d^T B_k d + \nabla f(x_k)^T d \\
& d \in \mathfrak{R}^n \\
\text{subject to } & \nabla g_j(x_k)^T d + g_j(x_k) \geq 0 \quad j = m_e + 1, \dots, m \\
& x_l - x_k \leq d \leq x_u - x_k
\end{aligned}$$

where B_k is a positive definite approximation of the Hessian matrix and x_k is the current iterate. Here d is the solution of the subproblem, f and g are function and constraints respectively, and symbol ∇ refers to the gradient. Details of the solution procedure of the quadratic subproblem are given by Gill [11].

Step 3: The derivation of the quadratic programming subproblem holds only in a small neighbourhood of the optimum, and hence the significance of the subproblem is questionable when the iteration values is not close to optimum values. If feasibility is not maintained, then in order to decide whether the next iteration is a "better" point than the present, it is necessary to define a merit function that somehow balances the (usually) conflicting aims of reducing the objective function and satisfying the constraints. To find the merit function an augmented Lagrangian function is used.

Step 4: A line search is used to find a new point,

$$x_{k+1} = x_k + \lambda d_k \quad \lambda \in (0, 1)$$

If these new values satisfy the minimization criteria then that will give the result of the optimization problem otherwise the system will repeat the whole procedure.

REFERENCES

- (1) Ruthven, D. M., and Ching, C. B., "Counter-current and simulated counter-current adsorption separation processes", *Chem. Eng. Sci.*, 44(5), 1011-1038 (1989).
- (2) Ruthven, D. M., *Principles of Adsorption and Adsorptive Processes*, John Wiley, New York (1984).
- (3) Ruthven, D. M., and Ching, C. B., "The axial dispersed plug-flow model for continuous counter-current adsorbents", *Can. J. Chem. Eng.*, 61, 881-883 (1983).
- (4) Ching, C. B., and Ruthven, D. M., "Separation of glucose and fructose by simulated counter-current adsorption", *AIChE Symp. Ser.*, 81 (242), 1-8 (1985).
- (5) Hidajat, K., and Ching, C. B., "Simulation of the performance of a continuous counter-current adsorption system by the method of Orthogonal collocation with nonlinear and interacting adsorption isotherms", *Trans I Chem.Eng.*, 68, 104-108 (1990).
- (6) Hassan, M. M., Rahman, A. K. M. S., and Loughlin, K. F., "Numerical simulation of unsteady continuous counter-current adsorption system with nonlinear adsorption isotherm", *Sep. Technol.*, 4, 15-26 (1994).
- (7) Rahman, A. K. M. S., Hassan, M. M., and Loughlin, K. F., "Unsteady state simulation of "Sorbex" system with nonlinear adsorption isotherms", *Sep. Technol.*, 4, 27-37 (1994).
- (8) Kremser, A., *Nato. Petrol. News* 22(21), 42 (1930).
- (9) Souders, M. and Brown, G. C., "Fundamental design of absorbing and stripping columns for complex vapours", *Ind. Engng Chem.* 24, 519-527 (1932).
- (10) Hassan, M. M., Rahman, A. K. M. S., and Loughlin, K. F., "Modelling of simulated moving bed adsorption system: a more precise approach", *Sep. Technol.*, 5, 77-89 (1995).

- (11) Gill, P. E., Murray W., and Wright., M. H., Practical Optimization, Academic Press (London) Ltd. (1981).
- (12) IMSL Mathematic Library, Optimization, P 965-1103, (1995).

NOMENCLATURE

B_K	a positive definitive approximation of Hessian
b_i	Langmuir constant
C_{ij}	dimensionless sorbate concentration in fluid phase for component i in section j
c	fluid phase concentration
$c_{i,f}$	sorbate concentration of component i in feed stream
C_{ij}	sorbate concentration in fluid phase for component i in section j
C'_{ij}	dimensionless sorbate concentration in fluid phase for component i in section j
CI'_{ij}	dimensionless inlet concentration of fluid phase for component i at section j
c_o	concentration in the feed stream
C_L	fluid concentration at the outlet of counter current adsorber
D	desorbent flowrate expressed on equivalent counter current basis
D_{L_j}	axial dispersion coefficient (for flow in section j)
d_k	root of quadratic programming subproblem
e	eluent feed point
f	feed feed point
f, g	function and constraint used in equation (3. 24)
E	extract flowrate
F	feed flowrate
$F(x)$	optimization function
F_j	dimensionless factor, (V_j / V_1)
k	overall effective mass transfer coefficient
K	adsorption equilibrium constants for component i

L	liquid flow rate in equation (3. 8)
L	length of the adsorption column
$L_{s j}$	length of adsorption section j
n	number of ideal equilibrium stage in equation (3. 6)
n	number of components in equation
m	<i>a constant</i>
Pe_j	Peclet number in section j, $(V_j L_{s j} / D_{L j})$
q_0	solid phase concentration in equilibrium with feed concentration
$q_{i j}$	average solid phase concentration (of component i in section j)
q_{oi}	solid phase concentration in equilibrium with concentration of i in feed
Q'_{ij}	dimensionless solid phase concentration of component i at bed j
q_L	average sorbate concentration at the outlet of counter current adsorber
q_s	saturated solid phase concentration
R	raffinate flowrate
S	solid circulation rate
t	time
u	linear velocity of solid
V_j	fluid velocity in section j
V_I	fluid velocity in section 1
V_f, V_{f-1}	fluid velocity at the bed following / before the feed point
V_e, V_{e-1}	fluid velocity at the bed following / before the eluent point
x_k	present guess of the optimization variables
x_{k+1}	new value of the optimization variables
z_j	axial distance coordinate
Z_j	dimensionless axial distance coordinate

Greek Letters:

α	dimensionless mass transfer parameter, (kL / V_1)
ε	bed porosity
λ	value of the merit function used in optimization
λ_i	non-linearity parameter for component i , $(q_{i,f} / q_s)$
τ	dimensionless time
ϕ	nonlinear equilibrium factor, $1 - \sum_i \lambda_i$
ψ	ratio of packed bed to void bed ratio, $(1 - \varepsilon) / \varepsilon$
γ	ratio of downflow in solid to upflow in fluid

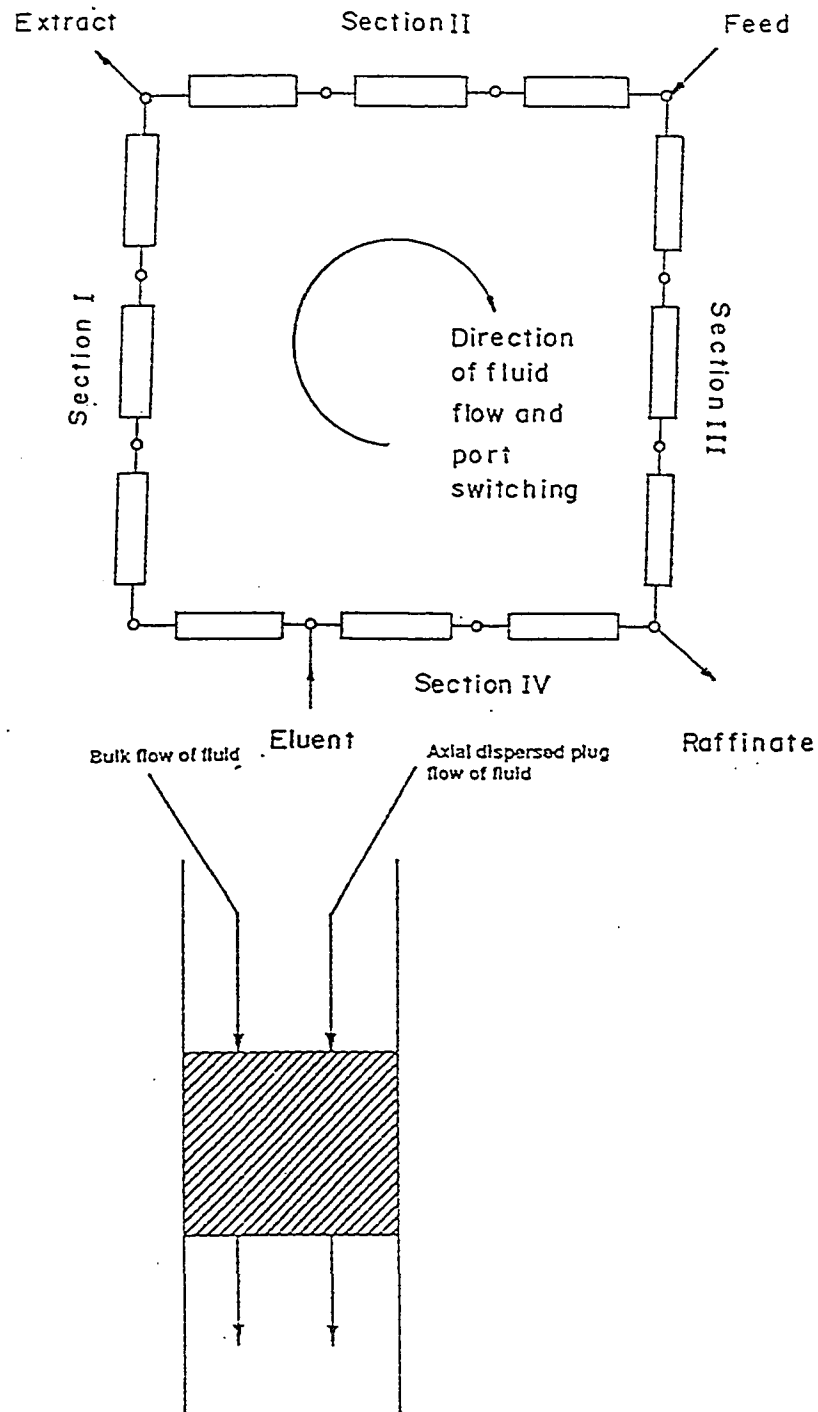


Figure 3.1 (a) Schematic diagram of the physical arrangement of columns and valves for the precise approach (b) Schematic diagram of the mass balances of the j th section for this model.

Chapter 4

Optimization of Continuous Countercurrent Adsorption system with non-linear Adsorption Isotherm

4.1 INTRODUCTION

Continuous countercurrent systems reduce the adsorbent requirement by maximizing the mass transfer driving force. The major problems of earlier versions of continuous countercurrent adsorption processes were associated with the recirculation of the solid adsorbent, which proved to be uneconomic. Such problems have been eliminated by the use of simulating moving bed systems. The continuous countercurrent contact is achieved by keeping the solid beds fixed while moving the fluid inlet and outlet points simultaneously at set time intervals in the direction of flow of the fluid phase as shown in Figure 4.1. Continuous countercurrent processes are now in extensive industrial use for several hydrocarbon separations [1], in the separation of glucose and fructose in the production of high fructose syrup [2], and in the separation of monoethanolamine and methanol [3].

The mathematical modelling of continuous countercurrent systems has also been reported by several investigators. Two basic approaches have been used in modelling these systems: (1) the system is considered as an equivalent countercurrent process

involving both fluid and solid velocities with fixed (time independent) boundary conditions, and (2) the system is modelled as a simulated countercurrent system consisting of various sections with each section comprised of a number of columns and where the boundary conditions change with switch time. Models for the first approach, the countercurrent operation [4-19] and for the second approach, the simulated countercurrent operation [4,15,16,20] have been presented in the literature. A reasonable representation of the actual process is depicted by both of the approaches. Indeed, the agreement between the theoretically predicted results and the experimentally observed data is excellent using either of the approaches thereby establishing the validity of the models. All previous studies show that the effect of various parameters are strongly coupled and, it is therefore, very difficult to predict the optimal choice of parameters in these systems. The situation is further complicated by the presence of nonlinearity of isotherm. For the case of linear isotherm Ching and Ruthven [12,13] show that an efficient separation of glucose and fructose occurs for a wide range of operating conditions provided that the ratio of downflow to upflow rates of fructose is greater than one and for glucose this ratio is less than one in both prefeed and post feed sections. However, this criteria was found to be insufficient for nonlinear systems [19]. Although the theoretical and experimental studies reveal the existence of an optimum set of operating variables, very little attention has been given towards the systematic evaluation of this optimum set of parametric values.

Experimental determinations of this optimum set requires a trial and error procedure which may become very time consuming and uneconomic. In the present study, therefore, a systematic theoretical evaluation of this optimum set of operating parameters are performed with the objective of obtaining maximum recovery of the less strongly adsorbed species in the raffinate for a specified concentration of the more strongly adsorbed species. Further, the best choice of optimum operating sets which yields high

recovery at an acceptable purity is determined. This numerical scheme is applied for glucose-fructose and monoethanolamine- methanol systems to investigate the effects of nonlinearity of isotherms.

4.2 THEORY

The numerical scheme for optimization of operating parameters consists of two parts: (i) the theoretical model and (ii) the optimization of process variables.

4.2.1 The Theoretical Model

The system described in Figure 4.1 may be considered as approximately equivalent to the hypothetical continuous countercurrent arrangement shown in Figure 4.2a. Assuming plug flow of solid and axially dispersed plug flow of fluid, the basic differential equation describing the system dynamics for i th component and j th section can be represented by the following set of equations:

$$D_{L_j} \frac{d^2 c_{ij}}{d z_j^2} - V_j \frac{d c_{ij}}{d z_j} - \left(\frac{1 - \epsilon}{\epsilon} \right) k_i (q_{ij}^* - q_{ij}) = 0 \quad (4.1)$$

For Langmuir type of equilibrium isotherm,

$$q_{ij}^* = \frac{b_i q_s c_{ij}}{1 + \sum_{i=1}^k b_i c_{ij}} \quad (4.2)$$

Boundary conditions

$$\text{at } z_j = 0 \quad D_L \frac{d c_{ij}}{d z_j} \Big|_{z_j=0^+} = -V_j (c_{ij} \Big|_{z_j=0^+} - c_{ij} \Big|_{z_j=0^-}) \quad (4.3)$$

$$\text{at } z_j = L_{s_j} \quad \frac{d c_{ij}}{d z_j} = 0.0 \quad (4.4)$$

where q_{i_j} is the solid concentration which is in equilibrium with the fluid phase concentration for component i in section j .

A mass balance over any section may be written as:

$$q_{ij} \Big|_{z=L_{s_j}} = q_{ij} \Big|_{z=0} + \left(\frac{Q_j}{S_j} \right) (c_{ij} \Big|_{z=L_{s_j}} - c_{ij} \Big|_{z=0}) \quad (4.5)$$

using the following dimensionless variables

$$C_{ij} = \frac{c_{ij}}{c_f}, \quad Q'_{ij} = \frac{q_{ij}}{c_f}, \quad Z_j = \frac{z_j}{L_{s_j}}, \quad \lambda_i = \frac{q_{ui}}{q_s}$$

Equation (1) - (2) can be written as

$$\frac{d^2 C_{ij}}{d Z_j^2} - (Pe_j + St) \frac{d C_{ij}}{d Z_j} + Pe_j \cdot St \left[(C_{ij} \Big|_{Z_j=1} - \alpha Q'_{ij} \Big|_{Z_j=1}) - (C_{ij} \Big|_{Z_j=0^+} - \alpha Q'_{ij} \Big|_{Z_j=0^+}) \right] = 0 \quad (4.6)$$

$$Q'_{ij} = K_i C_{ij} \left[\frac{1.0 - \sum \lambda_i}{1 + \sum \lambda_i (C_{ij} - 1.0)} \right] \quad (4.7)$$

The model equations are essentially similar to equations at steady state presented earlier by Hassan et al. [19] and are repeated here only for convenience.

4.2.2 Optimization of Process Variables

The continuous countercurrent system with two section configuration described in Figures 4.1 and 4.2a involves five independent variables: feed flow rate, F ; eluent flow rate, E ; switch time, τ ; column diameter, D ; and column length, L . These can be termed as the manipulating variables for this system. However, the model equations contains three dependent variables: fluid velocity in each section, V_j ; Peclet number in each section, Pe_j and solid velocity, u . These three dependent variables (V_j , Pe_j , u) are functions of the five manipulating variables (F , E , τ , D , L). The main objective is to find the optimum set of parameters values in this system, which yields maximum recovery of the less strongly adsorbable component (A) in the raffinate product subject to the constraints of a tightly specified concentration of strongly adsorbable component (B). The goal of the optimization function is to maximize recovery of A at the outlet of postfeed section using the following minimizing function

Minimize

$$F(x) = \frac{1}{\text{Recovery of A}} \quad (4.8)$$

where recovery is defined as

$$\text{Recovery} = \frac{\text{ConcA1}(M2) * \text{Raffinate flowrate}}{\text{ConcCoA} * \text{Feed flowrate}} \quad (4.9)$$

Here $\text{ConcA1}(M2)$ is the concentration of A at the exit of section 1 (post feed section) and ConcCoA is concentration of A in the feed. The above optimization function is subject to the following two constraints:

$$G(1) = 1.1 * \text{ConcBs} - \text{ConcB1}(M2) \quad (4.10)$$

$$G(2) = \text{ConcB1}(M2) - 0.9 * \text{ConcBs}$$

where $ConcB1(M2)$ is the calculated concentration of B at the outlet of the section 1(postfeed section) and $ConcBs$ is the desired concentration of B at the outlet and its value has to be specified or in other words

$$0.90 \leq \frac{ConcB1(M2)}{ConcBs} \leq 1.10.$$

The constraints, therefore, force the calculated concentrations values within the range of 90% to 110% of the specified values. The constraints provides a narrow bandwidth of acceptable concentrations in which the optimization is performed.

The algorithm of the optimization procedure is described in the flow-sheet given in the attached Figure 4.3. Method of orthogonal collocation has been used to obtain solution of the model equations using NEQNF subroutine of the IMSL library. The optimization function is solved by using NCONF subroutine of the IMSL library. A brief description of the procedure is given in section 3.5.1.

4.3 RESULTS AND DISCUSSION

The above optimization scheme was applied to evaluate the optimized set of parameters for systems with linear isotherm (Glucose-Fructose on Duolite C-204 resin) and nonlinear isotherm (Glucose-Fructose and Monoethanolamine-Methanol on Duolite C-204 resin).

Two different cases of optimization were carried out. In one case the length and diameter of the column were kept fixed at the experimental values reported by Ching and

Ruthven [12] and Hidajat and Ching [3]. This case would then yield the optimized set of parameters for the experimental set up used by these authors. In the other case, optimization is carried out by including the length and diameter as variables and, therefore, this would then represent a more general case.

The optimized parameters for glucose-fructose system for linear case ($\lambda_A = \lambda_B = 0$) with fixed column diameter and column length are presented in Table 4.1. The optimization was run for various fructose concentrations in the raffinate or (purity). The values of each variables (F, E, τ) represent the optimized values at the specified fructose concentration. It may be mentioned here that Run 2 corresponds to the experimental conditions (run 4) reported by Ching and Ruthven [12]. The corresponding steady state concentration profile is shown in Figure 4.4. Figure 4.5 shows at the optimal conditions, the recovery and purity of glucose in the raffinate at various fructose concentrations. It is observed that the recovery increases with the increase of fructose concentration in the raffinate but at the expense of lower purity. Based on a compromise between the purity and recovery, one may consider Run 6 in Table 4.1 as the optimal choice for operation which yields 99% recovery of glucose at a purity of 97.3%. The steady state concentration profile for this case is shown in Figure 4.6.

A comparison with Run 2, the experimentally reported case by Ching and Ruthven [12], shows that a small reduction in the feed rate and switch time would give a higher purity product with recovery as high as 99% [Run 6].

The optimized set of parameters for the Glucose-Fructose system with nonlinear isotherm are presented in Table 4.2 & 4.3. The corresponding recovery and purity plots are shown in Figure 4.5 for ($\lambda_A = 0.10$ & $\lambda_B = 0.17$) and ($\lambda_A = 0.20$ & $\lambda_B = 0.345$) cases. It is observed that for the case of ($\lambda_A = 0.10$ & $\lambda_B = 0.17$) the purity values are still

very close while the recovery is lower compared to those with the linear case (Table 4.1). However, as the nonlinearity increases to ($\lambda_A = 0.20$ & $\lambda_B = 0.345$) the purity are lower at the expense of higher recovery compared to both the linear case and ($\lambda_A = 0.10$ & $\lambda_B = 0.17$) case. This may be attributed to the interactions of the optimized parameters which are quite different for each case. Specifically, the feed rate is very different for linear and ($\lambda_A = 0.20$ & $\lambda_B = 0.345$) cases as shown in Table 4.3. Further, the optimal choice of operation indicated by the intersection of the recovery and purity curve is also different as shown in Figure 4.5.

The results for the general case, where the column diameter and length are also included as variables are shown in Table 4.4 to 4.6 for glucose-fructose system for various nonlinearity of isotherms.

For linear case ($\lambda_A = \lambda_B = 0$) Run 2 in Table 4.4 appears to be the optimal case. It is very interesting to note that the optimized values of all the variables (F,E, τ ,L) for this case is very close to the one reported by Ching and Ruthven [12] except the minute change in the diameter of the column. The corresponding steady state concentration profiles are shown in Figure 4.7. It may be further noted that the recovery remains fairly constant while the purity changes as the concentration of fructose in raffinate is changed.

The optimized values of the parameters for the general case are shown in Table 4.5 for ($\lambda_A = 0.10$ & $\lambda_B = 0.17$) and Table 4.6 for ($\lambda_A = 0.20$ and $\lambda_B = 0.345$) respectively. The influence of the nonlinearity parameters λ appears insignificant for both the recovery and purity values as shown in Figure 4.8. On the other hand, the values of the optimized parameters vary appreciably with λ as may be observed in Tables 4 to 6 for similar values of fructose concentration. Further, it may be noted that while an appreciable increase in recovery is observed at low fructose concentration for the case

where three parameters are optimized (Figure 4.5), it was not possible to obtain results in this region for the general case.

The results of the optimization for the nonlinear MEA-MOH system are listed in Table 4.7 with fixed column diameter (5.5 cm) and length (100 cm) which were used in the experiments carried out for four section system by Hidajat and Ching [3]. It may be mentioned here that it is very difficult to achieve good separation for this system. Indeed, the results reported earlier by Hassan et al. [19] showed no separation in the raffinate stream. Unfortunately, there is no experimental data available for two sections. However, the present optimization scheme has been able to find various set of optimized parameters for different MEA concentration in the raffinate. The steady state concentration profile for Run 4 are shown in Figure 4.9. The observed recovery of MOH is 100% but the purity obtained was quite low. The absolute values of concentration of the less strongly adsorbed species MOH in the raffinate is very low and the required optimized feed rate is also very small.

REFERENCES

- (1) de Rosset, A. J., Neuzil, R. W., and Korons, D., "Liquid column Chromatography as a predictive tool for continuous countercurrent adsorption separation", *Ind. Eng. Chem. Process Des. Dev.* 15, 261-266 (1976).
- (2) Neuzil, R. W., and Jensen, R. A., "Development of the SAREX process for separation of Saccharides", 85th National Meeting AIChE, Philadelphia, PA, U.S.A, June (1978).
- (3) Hidajat, K., and Ching, C. B., "Simulation of the performance of a continuous countercurrent adsorption system by the method of orthogonal collocation with nonlinear and interacting adsorption isotherms", *Trans.I. Chem. Eng.*, 68, 104-108 (1990).
- (4) Hidajat, K., Ching, C. B., and Ruthven, D. M., "Numerical simulation of a semi-continuous countercurrent adsorption unit for fructose-glucose separation", *Chem. Eng. J.*, 33, B55-B61 (1986).
- (5) Ching, C. B., Ruthven, D. M., and Hidajat, R., "Experimental study of a simulated countercurrent adsorption system-III. SORBEX Operation", *Chem. Eng. Sci.*, 40, 1411-1417 (1985).
- (6) Ching, C. B., Ho, C., and Ruthven, D. M., "An improved adsorption process for the production of high fructose syrup", *AIChEJ*, 32, 1876-1880 (1986).
- (7) Ching, C. B., Hidajat, K., Ho, C., and Ruthven, D. M., "Experimental study of a simulated countercurrent adsorption system-V. Comparison of Resin and Zeolite adsorbents for fructose-glucose separation at high concentration", *Chem. Eng. Sci.*, 42, 2547-2555 (1987).
- (8) Ching, C. B., Hidajat, K., Ho, C., and Ruthven, D. M., "Modelling of a simulated countercurrent adsorption processes", *Reactive Polym.*, 6, 15-20 (1987).
- (9) Ching, C. B., Ho, C., and Ruthven, D. M., "Experimental study of a simulated countercurrent adsorption system-VI. Non-linear systems", *Chem. Eng. Sci.*, 43, 703-711 (1988).
- (10) Ching, C. B., and Ruthven, D. M., "Analysis of the performance of a simulated countercurrent chromatographic system for fructose-glucose separation", *Can. J. Chem. Eng.*, 2, 398-403 (1984).
- (11) Ching, C. B., and Ruthven, D. M., "Separation of glucose and fructose by simulated countercurrent adsorption", *AIChE Symp. Ser.*, 81 (242), 1-8 (1985).

- (12) Ching, C. B., and Ruthven, D. M., "An experimental study of a simulated countercurrent adsorption system-I. Isothermal steady state operation", *Chem. Eng. Sci.*, 40 (6), 877-885 (1985).
- (13) Ching, C. B., and Ruthven, D. M., "An experimental study of a simulated countercurrent adsorption system-II. Transient response", *Chem. Eng. Sci.*, 40 (6), 887-891 (1985).
- (14) Ching, C. B., and Ruthven, D. M., "Experimental study of a simulated countercurrent adsorption system-IV. Non-isothermal operation", *Chem. Eng. Sci.*, 41, 3063-3071 (1986).
- (15) Hashimoto, K., Adach, S., Noujima, H. and Maruyama, H., "Models for the separation of glucose/fructose mixture using a simulated moving-bed adsorber", *J. Chem. Eng. Japan*, 16, 400-406 (1983).
- (16) Morbidelli, M., Storti, G., Paludetto, R. and Carra, S., "Mathematical models of moving beds and simulated moving-beds for adsorption: Analysis and Comparison", *Proceedings of the Second Engineering Foundation Conference on Fundamentals of Adsorption*. A.I. Liapis, Ed. New York: Engineering Foundation, 411 (1986).
- (17) Storti, G., Masi, M., and Carra, S., "Modelling and design of simulated moving-bed adsorption separation units", *Prep. Chromatography*1, 1-27, (1988).
- (18) Storti, G., Masi, M., and Carra, S. and Morbidelli, M., "Optimal design of multicomponent adsorption separation processes involving nonlinear equilibria", *Chem. Eng. Sci.*, 44, 6, 1329-1345 (1989).
- (19) Hassan, M. M., Rahman, A. K. M. S., and Loughlin, K. F., "Numerical simulation of unsteady continuous countercurrent adsorption system with non-linear adsorption isotherm", *Sep. Technol.*, 4, 15-26 (1994).
- (20) Hassan, M. M., Rahman, A. K. M. S., and Loughlin, K. F., "Modelling of simulated moving bed adsorption system: a more precise approach", *Sep. Technol.*, 7-89, (1995).

NOMENCLATURE

b_i	Langmuir constant
C_{ij}	dimensionless sorbate concentration in fluid phase for component i in section j
c_{ij}	sorbate concentration in fluid phase for component i in section j
c_0	concentration in the feed stream
D	diameter of column
D_{Lj}	axial dispersion coefficient (for flow in section j)
E	eluent flowrate
F	feed flowrate
k_i	overall effective mass transfer coefficient for component i
K_i	adsorption equilibrium constants for component i
L	length of the adsorption column
L_{sj}	length of adsorption section j
Pe_j	Peclet number in section j, $(v_j L_{sj} / D_{Lj})$
q_0	solid phase concentration in equilibrium with feed concentration
q_{ij}	average solid phase concentration (of component i in section j)
Q'_{ij}	dimensionless average solid phase concentration (of component i in section j)
Q'_{ij}	dimensionless equilibrium solid phase concentration (of component i in section j)
q_{oi}	solid phase concentration in equilibrium with concentration of i in feed
q_{ij}^*	equilibrium solid phase concentration (of component i in section j)
q_s	saturated solid phase concentration
Q_j	fluid flow rate in section j, $\varepsilon V_j A$

S_j	hypothetical adsorbent recirculation rate $(1-\varepsilon)uA$
St	Stanton number, $(k_i L_{s1} / u)$
u	linear velocity of solid, (L/τ)
V_j	fluid velocity in section j
z_j	axial distance coordinate
Z_j	dimensionless axial distance coordinate

Greek Letters:

α	dimensionless parameter, $(1-\varepsilon)u / \varepsilon v_j$
ε	bed porosity
λ_i	non-linearity parameter for component i, (q_{oi} / q_s)
τ	switch time

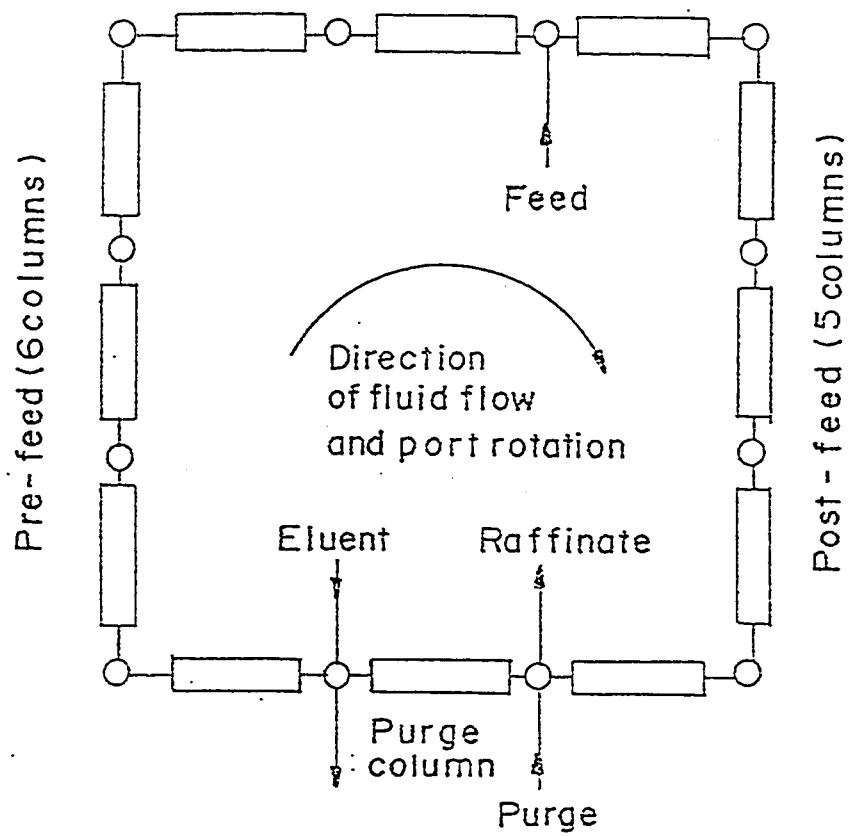


Figure 4.1 Schematic diagram of two section simulated moving bed

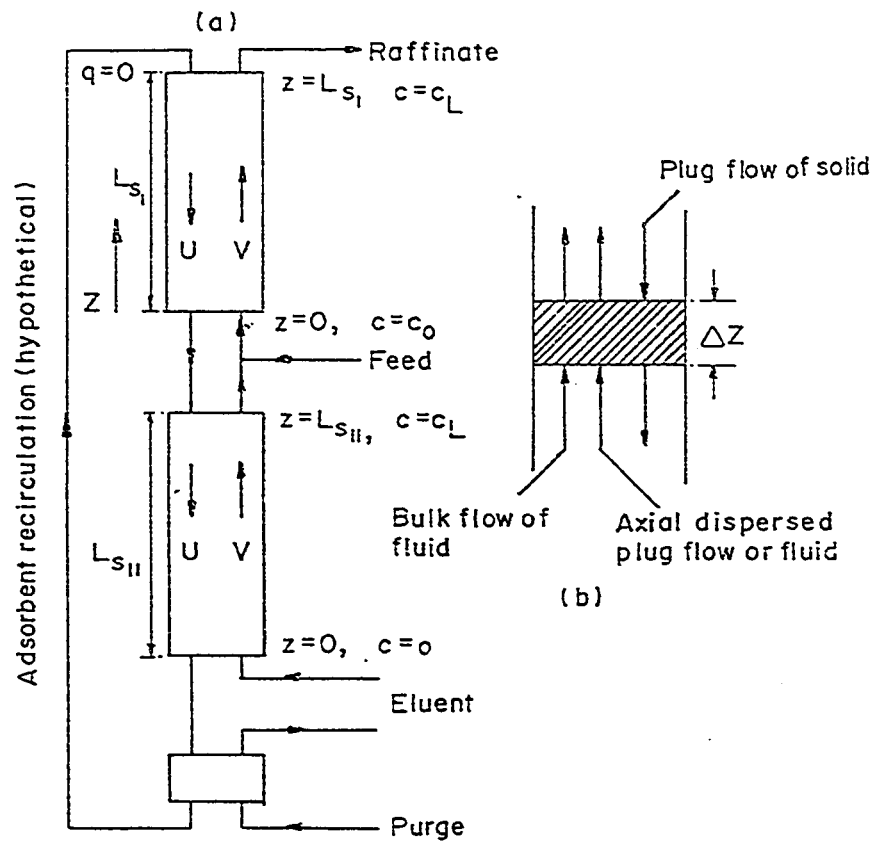


Figure 4.2 (a) Schematic diagram of two section equivalent countercurrent system (b) Schematic diagram of the mass balance of j th section for two section equivalent countercurrent system

FLOW DIAGRAM

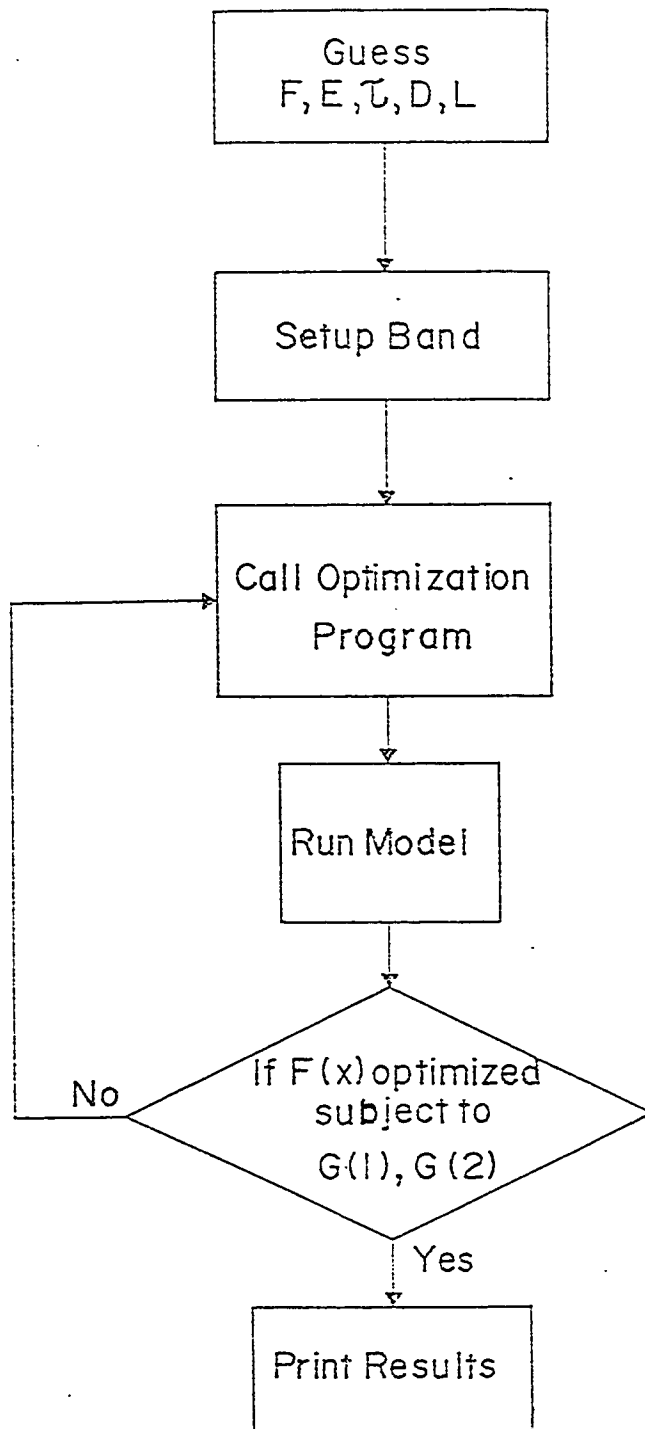


Figure 4.3 Flowsheet showing the algorithm of optimization procedure

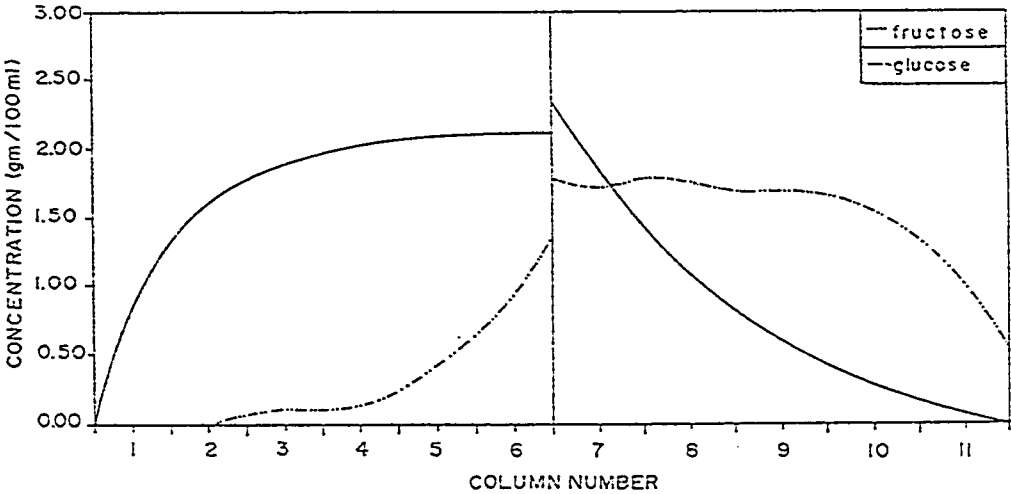


Figure 4.4 Concentration profile for the base case (Run 2 in Table 4.1)

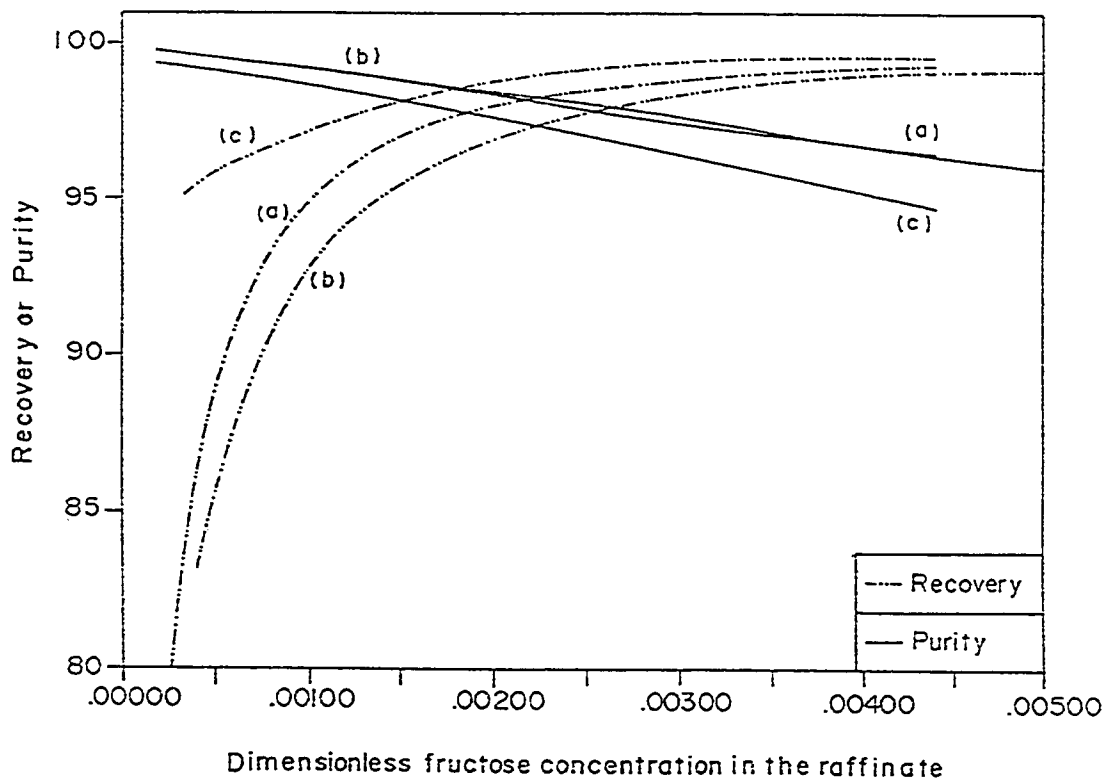


Figure 4.5 Plot of Recovery and Purity at various dimensionless Fructose concentrations in the raffinate for fixed length and diameter for (a) $\lambda_A = \lambda_B = 0$; (b) $\lambda_A = 0.1$ and $\lambda_B = 0.17$; and (c) $\lambda_A = 0.2$ and $\lambda_B = 0.345$

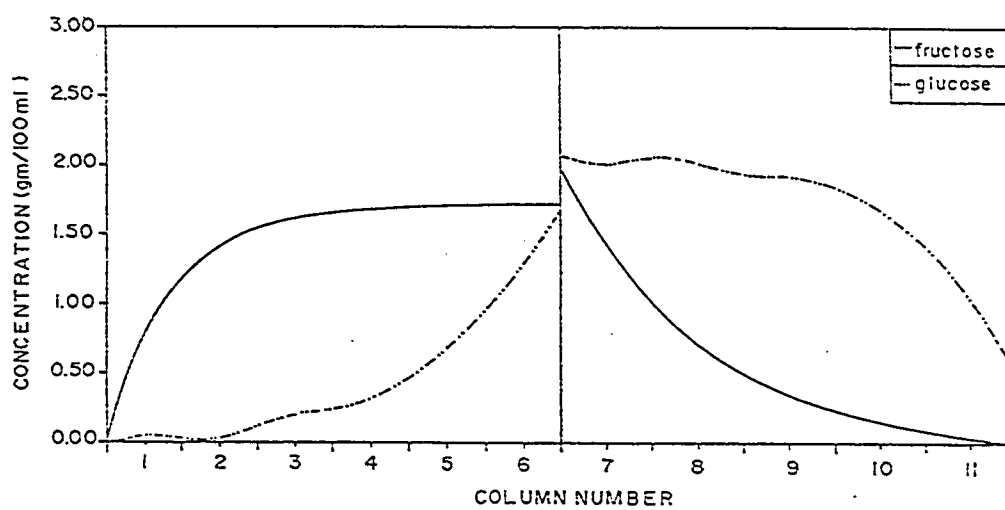


Figure 4.6 Concentration profile for optimal choice of operation (Run 6 in Table 4.1)

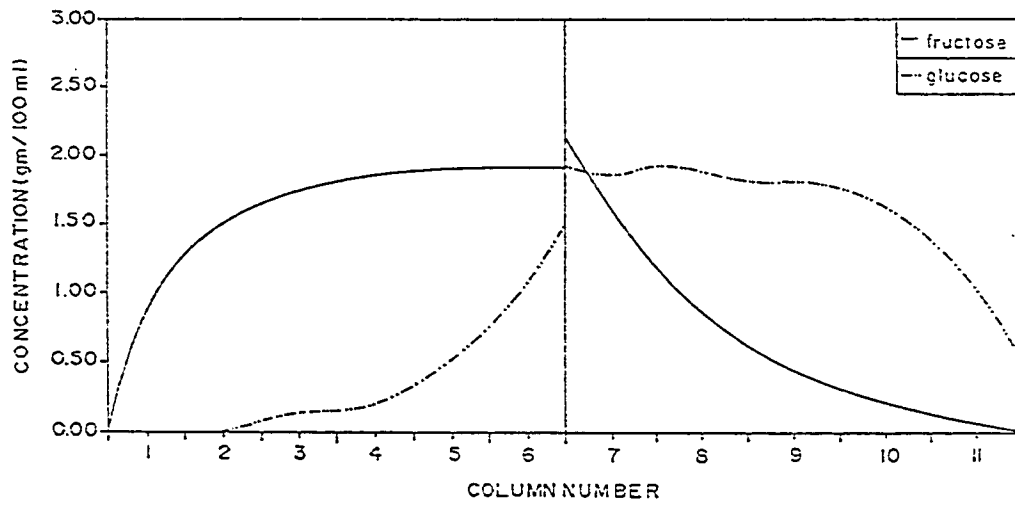


Figure 4.7 Concentration profile for the general case (Run 2 in Table 4.4)

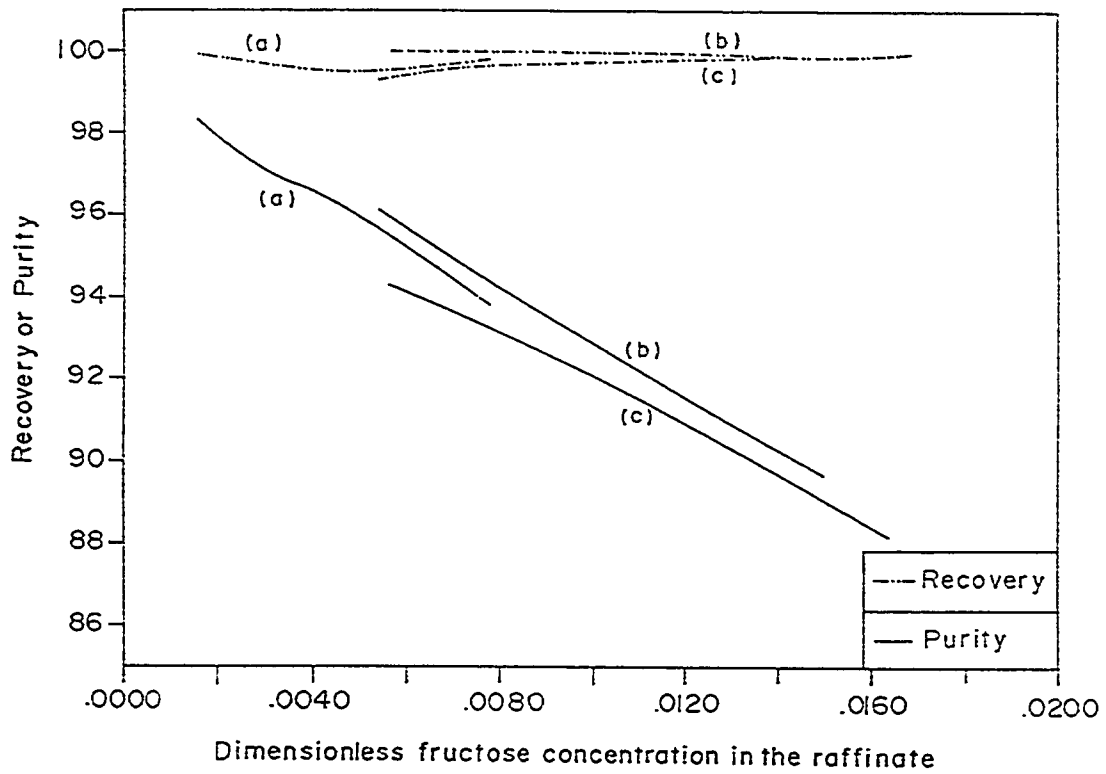


Figure 4.8 Plot of Recovery and Purity at various dimensionless Fructose concentrations in the raffinate for general case for (a) $\lambda_A = \lambda_B = 0$; (b) $\lambda_A = 0.1$ and $\lambda_B = 0.17$; and (c) $\lambda_A = 0.2$ and $\lambda_B = 0.345$

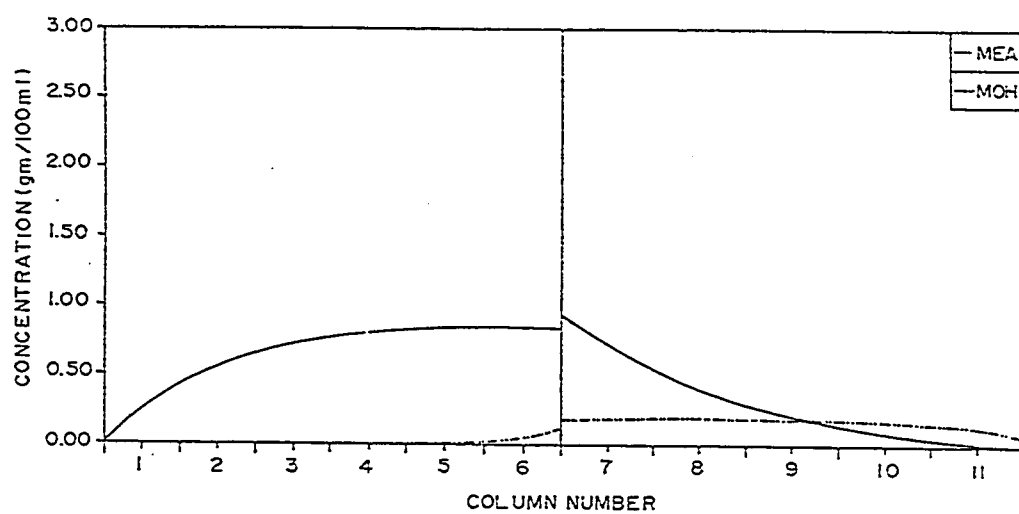


Figure 4.9 Concentration profile for MEA-MOH system (Run 4 in Table 4.7)

Table 4.1 Optimized parameters for glucose (A)-fructose (B) system for linear case ($\lambda_A = \lambda_B = 0$) with fixed column diameter (5.1 cm), length (100.00 cm): Feed composition: 5 % A, 5 % B; $K_A = 0.51$; $K_B = 0.88$; Configuration- Prefeed, Postfeed (6,5)[12]

Run No.	Feed rate (ml/min)	Eluent rate (ml/min)	Switch time (min)	Recovery	Purity	Concentration Ratio	Raffinate fructose concentration (Dimensionless)
1	7.51	110.01	15.07	99.8	93.1	11.9	0.0088
2	7.50	110.00	15.00	99.8	93.8	11.9	0.0078
3	7.48	109.99	14.89	99.7	94.8	11.9	0.0066
4	7.46	109.97	14.79	99.5	95.6	12.0	0.0056
5	7.44	109.95	14.65	99.3	96.5	12.0	0.0044
6	7.41	109.93	14.50	99.0	97.3	12.0	0.0032
7	7.37	109.90	14.29	98.2	98.2	12.1	0.0022
8	7.32	109.87	14.02	96.4	98.9	12.0	0.0014
9	7.15	109.75	13.15	75.4	99.8	9.90	0.0002

$$Purity = \frac{ConcAI(M2)}{ConcAI(M2) + ConcBI(M2)} ; Recovery = \frac{ConcAI(M2) * Raffinate\ flow\ rate}{ConcCoA * Feed\ flow\ rate} \text{ and Concentration Ratio} = \frac{ConcAI(M2)}{ConcCoA}$$

Table 4.2: Optimized parameters for glucose (A)-fructose (B) system for non-linear case ($\lambda_A = 0.10$ and $\lambda_B = 0.17$) with fixed column diameter (5.1 cm), length (100.00 cm): $K_A = 0.51$; $K_B = 0.88$; Configuration- Prefeed, Postfeed (6,5); [12].

Run No.	Feed (ml/min)	Eluent (ml/min)	Switch time(min)	Recovery	Purity	Concentration Ratio	Raffinate fructose concentration (Dimensionless)
1	7.31	109.90	14.22	99.4	95.4	12.2	0.0060
2	7.30	109.89	14.14	99.2	96.0	12.2	0.0050
3	7.04	102.91	14.96	99.1	97.2	12.6	0.0036
4	7.21	109.85	13.85	98.1	97.8	12.2	0.0028
5	7.20	109.85	13.77	97.7	98.1	12.2	0.0024
6	7.11	109.81	13.48	95.0	98.9	12.0	0.0014
7	7.05	109.78	13.22	90.7	99.3	11.6	0.0008
8	7.00	109.75	12.98	83.3	99.6	10.9	0.0004

Table 4.3: Optimized parameters for glucose (A)-fructose (B) system for non-linear case ($\lambda_A = 0.20$ & $\lambda_B = 0.345$) with fixed column diameter (5.1 cm), length (100.00 cm): $K_A = 0.51$; $K_B = 0.88$; Configuration- Prefeed, Postfeed (6,5); [12]

Run No.	Feed (ml/min)	Eluent (ml/min)	Switch time(min)	Recovery	Purity	Concentration Ratio	Raffinate fructose concentration (Dimensionless)
1	4.41	110.18	13.93	99.6	94.7	7.9	0.0044
2	4.31	110.14	13.60	98.8	97.6	7.8	0.0020
3	3.13	117.60	12.68	96.1	99.0	5.4	0.0006
4	2.14	116.76	12.87	95.3	99.3	3.7	0.0002

Table 4.4: Optimized parameters for glucose (A)-fructose (B) system for general case with linear isotherm ($\lambda_A = \lambda_B = 0$)
 Feed composition: 5 % A, 5 % B; $K_A = 0.51$; $K_B = 0.88$; Configuration- Prefeed, Postfeed (6,5) [12]

Run No.	Feed (ml/min)	Eluent (ml/min)	Switch time(min)	Diameter (cm)	Bed length (cm)	Recovery	Purity	Concentration Ratio	Raffinate fructose concentration (Dimensionless)
1	7.50	110.00	15.00	5.10	100.00	99.8	93.8	11.9	0.0078
2	7.50	110.00	14.99	5.14	100.00	99.5	96.1	12.0	0.0048
3	5.94	108.74	15.90	5.22	101.33	99.7	97.1	9.8	0.0030
4	5.72	104.98	18.46	5.42	105.39	99.9	98.3	9.9	0.0016

Table 4.5: Optimized parameters for glucose (A)-fructose (B) system for general case with non-linear isotherm ($\lambda_A = 0.10$ & $\lambda_B = 0.17$)
 $K_A = 0.51$; $K_B = 0.88$; Configuration- Prefeed, Postfeed (6,5) [12]

Run No.	Feed (ml/min)	Eluent (ml/min)	Switch time(min)	Diameter (cm)	Bed length (cm)	Recovery	Purity	Concentration Ratio	Raffinate fructose concentration (Dimensionless)
1	7.50	110.00	14.99	5.14	100.00	100.0	87.8	12.1	0.0168
2	7.50	110.00	14.99	5.16	100.00	99.9	89.2	12.1	0.0148
3	6.94	108.37	15.99	5.26	101.30	100.0	92.3	11.5	0.0096
4	5.54	106.76	17.41	5.38	102.54	100.0	94.3	9.5	0.0056

Table 4.6: Optimized parameters for glucose (A)-fructose (B) system for general case with non-linear isotherm ($\lambda_A = 0.20$ & $\lambda_B = 0.345$)
 $K_A = 0.51$; $K_B = 0.88$; Configuration- Prefeed, Postfeed (6,5) [12]

Run No.	Feed (ml/min)	Eluent (ml/min)	Switch time(min)	Diameter (cm)	Bed length (cm)	Recovery	Purity	Concentration Ratio	Raffinate fructose concentration (Dimensionless)
1	7.41	110.00	14.94	5.39	100.00	99.9	89.7	13.2	0.0150
2	7.41	110.00	14.94	5.42	100.00	99.7	93.2	13.3	0.0096
3	7.41	110.00	14.94	5.43	100.00	99.6	94.8	13.3	0.0072
4	7.40	110.00	14.93	5.45	100.00	99.4	95.7	13.4	0.0060
5	7.40	110.00	14.93	5.45	100.00	99.3	96.1	13.4	0.0054

Table 4.7: Optimized parameters for MOH (A)-MEA (B) system for non-linear isotherm ($\lambda_A = 0$ & $\lambda_B = 0.435$) with fixed column diameter (5.5 cm), length (100 cm): Feed composition: 10 % A, 20 % B; $K_A = 0.63$; $K_B = 0.24$; Configuration- Prefeed, Postfeed (6,5)[12]

Run No.	Feed (ml/min)	Eluent (ml/min)	Switch time(min)	Recovery	Purity	Concentration Ratio	Raffinate MEA concentration (gm/100ml)
1	0.71	130.62	19.66	100.00	66.6	0.90	0.043
2	0.72	130.76	19.42	100.00	73.3	0.90	0.032
3	0.73	130.91	19.27	100.00	77.2	0.90	0.026
4	0.64	131.00	18.74	100.00	89.6	0.80	0.009

Chapter 5

Optimization of "SORBEX" system with non-linear Adsorption Isotherm

5.1 INTRODUCTION

The SORBEX family of processes which have been developed by UOP [1] for a variety of industrially important separations operate on the same principle as the simulated moving bed system where the solid adsorbent recirculation is avoided by using a multiple column (or multiple section) fixed-bed system, with an appropriate sequence of column switching designed to simulate a counter flow. In this mode of operation, the countercurrent bed is divided into four sections; section I between desorbent inlet and extract withdrawal point, section II between extract and feed, section III between the feed and raffinate withdrawal points and section IV between raffinate and desorbent recirculation point and here desorption is achieved by adjusting correctly the flowrates in each section, rather than by using an isolated purge column [1-3]. Bieser and deRosset [4] successfully applied this mode of operation to the separation of glucose-fructose mixtures. The economic advantages of the SORBEX type of process is greatest for the separation of similar sorbates, often isomers, where differences in physical properties are too small to permit the economic application of more conventional processes such as distillation.

Many studies on the mathematical modeling of continuous countercurrent adsorption process have been reported in the literature. Both countercurrent modeling [5-22] and simulated countercurrent modeling [5, 17, 18, 21, 22] have been published in the literature. The experimentally obtained results agree quite well with theoretical predictions from both types of model, establishing the validity of these models.

Various process parameters are involved in the physical system of countercurrent adsorption systems. All previous studies have revealed that these process variables are strongly coupled and it is very difficult to predict the optimal choice of these variables. Very little attention has been given in the literature towards the systematic approach of predicting the optimum values of these process variables in countercurrent adsorption system. Storti et al. [23] reported an optimal design procedure of the operating conditions involved in a simulated moving bed unit. The characterization has been performed in the frame of the equilibrium theory with reference to the flow rate ratios. The space of the operating parameters, i.e., mass flow rate ratios is divided into regions with different separation regimes of complete separation, pure extract, pure raffinate and no purity. They also reported a procedure for selecting the optimum switch time using a detailed model, which accounts for axial dispersion and mass transfer resistance. These results constitute a useful tool for determining the range of operating conditions to achieve an assigned separation requirement and then for selecting the optimal operating condition within this range. However, from their study it is not straightforward to arrive at the optimum values of the individual process parameters required for practical operations. More recently Hassan et al. [24] presented a systematic theoretical evaluation of the optimum set of operating parameters for a two-section continuous countercurrent adsorption system. Their objective was to maximize the recovery of the less strongly adsorbable component (A) in the raffinate by fixing the concentration of strongly adsorbable component (B). The relevant parameters to be optimized are the feed flow

rate, eluent flow rate, switch time, length and diameter of the column. For various specified concentrations of B the optimum values of these parameters were presented in tabular form for several cases. The optimization had been carried out for systems with linear and non-linear isotherms. The optimization results indicate that the optimum values of parameters are significantly different for linear and non-linear isotherms. An optimal choice of operating variables corresponding to a compromise between recovery and purity was also suggested.

The extension of this optimization scheme for the more practical SORBEX system where products are withdrawn both at raffinate and extract points is of interest. In this system, therefore, optimization has to be performed for seven variables (feed flow rate, eluent flow rate, raffinate flow rate, extract flow rate, switch time, length and diameter of column). Further, one may be interested in maximizing the less strongly adsorbable component (A) in the raffinate or in maximizing the strongly adsorbable component (B) in the extract, thereby solving for two different objective functions. Because of the increasing number of optimization variables and choices of optimization objectives, the solution of the optimization program becomes very complex. In the present study, therefore, a systematic theoretical evaluation of the optimum set of operating parameters is performed for two different schemes: (a) maximization of recovery of less strongly adsorbable component (A) for a specified purity of (B) in the raffinate and (b) maximization of recovery of strongly adsorbable component (B) for a specified purity of A in the extract. The above optimization have been carried out by including and excluding the column length and diameters as process variables

5.2 THEORY

The numerical scheme for optimization of operating parameters consists of two parts: (i) the theoretical model and (ii) the optimization of process variables.

5.2.1 The Theoretical Model

The system described in Figure 1.4 may be considered as approximately equivalent to the hypothetical continuous countercurrent arrangement shown in Figure 1.5a. Assuming plug flow of solid and axially dispersed plug flow of fluid, the basic differential equation describing the system dynamics for i th component and j th section can be represented by the following set of equations:

$$D L_j \frac{d^2 c_{ij}}{d z_j^2} - V_j \frac{d c_{ij}}{d z_j} - \left(\frac{1-\varepsilon}{\varepsilon} \right) k_i (q_{ij}^* - q_{ij}) = 0 \quad (5.1)$$

For Langmuir type of equilibrium isotherm,

$$q_{ij}^* = \frac{b_i q_s c_{ij}}{1 + \sum_{i=1}^k b_i c_{ij}} \quad (5.2)$$

Boundary conditions

$$\text{at } z_j = 0 \quad D L_j \frac{d c_{ij}}{d z_j} \Big|_{z_j=0^-} = -V_j (c_{ij} \Big|_{z_j=0^-} - c_{ij} \Big|_{z_j=0^+}) \quad (5.3)$$

$$\text{at } z_j = L_{sj} \quad \frac{d c_{ij}}{d z_j} = 0.0 \quad (5.4)$$

where q_{ij} is the solid concentration which is in equilibrium with the fluid phase concentration for component i in section j .

Material balances:

Material balances at the inlet for each section are given by the following equations.

At the inlet of section IV

$$c_{i4} \Big|_{z_4=0^-} = c_{i3} \Big|_{z_3=L_3} \quad (5.5)$$

At the inlet of section III

$$c_{i3} \Big|_{z_3=0^-} = \frac{V_2 c_{i2} \Big|_{z_2=L_2} + (V_3 - V_2) c_{oi}}{V_3} \quad (5.6)$$

At the inlet of section II

$$c_{i2} \Big|_{z_2=0^-} = c_{i1} \Big|_{z_1=L_1} \quad (5.7)$$

At the inlet of section I

$$c_{i1} \Big|_{z_1=0^-} = (c_{i4} \Big|_{z_4=L_4}) \frac{V_4}{V_1} \quad (5.8)$$

A mass balance over any section may be written as:

$$q_{ij} \Big|_{z=L_j} = q_{ij} \Big|_{z=0} + \left(\frac{Q_j}{S_j} \right) (c_{ij} \Big|_{z=L_j} - c_{ij} \Big|_{z=0}) \quad (5.9)$$

Using the following dimensionless variables

$$C_{ij} = \frac{c_{ij}}{c_{oi}}, \quad Q_{ij} = \frac{q_{ij}}{q_{oi}}, \quad Z_j = \frac{z_j}{L_{s1}}, \quad \lambda_r = \frac{q_{oi}}{q_s}$$

Equations (5. 1) and (5. 2) can be written as

$$\frac{d^2 C_{ij}}{d Z_j^2} - (Pe_j + St) \frac{d C_{ij}}{d Z_j} + Pe_j \cdot St \left[(C_{ij} \Big|_{Z_j=l} - \alpha Q'_{ij} \Big|_{Z_j=l}) - (C_{ij} \Big|_{Z_j=l^+} - \alpha Q'_{ij} \Big|_{Z_j=l^+}) \right] = 0 \quad (5.10)$$

$$Q'_{ij} = K_i C_{ij} \left[\frac{1.0 - \sum \lambda_i}{1 + \sum \lambda_i (C_{ij} - 1.0)} \right] \quad (5.11)$$

The model equations are essentially similar to equations at steady state presented earlier by Hassan et al. [21] and are repeated here only for convenience.

5.2.2 Optimization of Process Variables

The continuous countercurrent system with four section configuration described in Figures 1.4 and 1.5a involves seven independent variables: feed flow rate, F ; eluent flow rate, EL ; raffinate flow rate, R ; extract flow rate, E ; switch time, τ ; column diameter, D ; and column length, L . These can be termed as the manipulating variables for this system. The model equations contains three dependent variables: fluid velocity in each section, V_j ; Peclet number in each section, Pe_j and solid velocity, u . These three dependent variables (V_j , Pe_j , u) are functions of (F , E , R , EL , τ , D , L) the seven manipulating variables. The objective is to find the optimum set of parameters values for the manipulating variables in this system by defining the objective functions for either of the following two cases: (a) maximization of recovery of the less strongly adsorbable component (A) for a specified concentration of B in the raffinate product and (b) maximization of recovery of strongly adsorbable component (B) for a specified concentration of A in the extract. The goal of the optimization scheme may be achieved by the minimization of the following functions:

Minimize

$$F(x) = \frac{1}{\text{Recovery of A or B}} \quad (5.12)$$

where recovery is defined as

$$\text{Recovery of A} = \frac{\text{ConcA3}(M2) * \text{Raffinate flow rate}}{\text{ConcoA}(\text{feed}) * \text{Feed flow rate}} \quad (5.13)$$

and

$$\text{Recovery of B} = \frac{\text{ConcB1}(M2) * \text{Extract flow rate}}{\text{ConcoB}(\text{feed}) * \text{Feed flow rate}} \quad (5.14)$$

Here $\text{ConcA3}(M2)$ is the concentration of A at the exit of section 3 (at raffinate withdrawal point), $\text{ConcB1}(M2)$ is the concentration of B at the exit of section 1 (at the extract withdrawal point), ConcoA and ConcoB are concentration of A and B in the feed respectively. The above optimization function is subject to the following two sets of constraints:

For case (a)

$$G(1) = 1.1 * \text{ConcBs} - \text{ConcB3}(M2) \quad (5.15)$$

$$G(2) = \text{ConcB3}(M2) - 0.9 * \text{ConcBs}$$

This implies that

$$0.90 \leq \frac{\text{ConcB3}(M2)}{\text{ConcBs}} \leq 1.10$$

For case (b)

$$G(1) = 1.1 * \text{ConcAs} - \text{ConcA1}(M2) \quad (5.16)$$

$$G(2) = \text{ConcA1}(M2) - 0.9 * \text{ConcAs}$$

This implies that

$$0.90 \leq \frac{\text{ConcA1}(M2)}{\text{ConcAs}} \leq 1.10$$

where $ConcB3(M2)$ and $ConcA1(M2)$ are the calculated concentration of B at raffinate point and calculated concentration of A at the extract point respectively whereas $ConcBs$ and $ConcAs$ are the desired concentration of B at raffinate and desired concentration of A at extract respectively and these values have to be specified. The constraints force the calculated concentrations values within the range of 90% to 110% of the specified values. The constraints provide a narrow bandwidth of acceptable concentrations in which the optimization is performed.

The algorithm of the optimization procedure is described in the flow-sheet given in Figure 5.1. Orthogonal collocation has been used to obtain the solution of the model equations using the NEQNF subroutine in the IMSL library. The optimization function is solved by using the NCONF subroutine in the IMSL library. A brief description of the procedure is available [24].

5.3 RESULTS AND DISCUSSIONS

The above optimization scheme was applied to evaluate the optimized set of parameters for systems with linear isotherm (Glucose-Fructose on Duolite C-204 resin) and nonlinear isotherm (Monoethanolamine-Methanol on Duolite C-204 resin).

The optimization were carried out for two different schemes: (a) maximization of recovery of the less strongly adsorbable component (A) for a specified concentration of (B) in the raffinate, i.e., optimization of raffinate and (b) maximization of recovery of the strongly adsorbable component (B) for a specified concentration of (A) in the extract, i.e., optimization of extract. For both schemes of optimization two different cases have been considered. In one case the length and diameter of the column were kept fixed at the experimental values reported by Ching et al. [7] and Hidajat et al. [6]. This case provides

the optimized set of parameters for their experimental set up. In the other case, which is considered as the more general case, the length and diameter have also been included as optimization variables.

The optimized parameters for scheme (a) (optimization of raffinate) for glucose-fructose system with fixed column length and diameter are presented in Table 5.1. The optimization was run for various fructose concentrations in the raffinate. The values of each variables (feed flow rate, eluent flow rate, switch time, extract flow rate and raffinate flow rate) given in the Table represent the optimized values at the specified raffinate fructose concentration. It may be mentioned that Run 1 corresponds to the experimental conditions (Run 2) reported by Ching et al. [7].

Graphically, the outcome of the optimization may be represented on a phase plane envelope with one limb representing the raffinate phase and one limb representing the extract phase. One of the limbs represents the optimized limb for a phase and the other limb represents the calculated values in the other phase, e.g. when the raffinate limb is the optimized limb the extract limb is the calculated phase and vice versa. Any point on the optimized limb is connected by a model tie line to a point on the calculated limb. Unlike phase equilibria studies, these model tie lines are not at equilibrium but rather result from the fact that when one phase is optimized there must be an output for the other phase resulting from a solution of the model and the two results are connected by a tie line. As in phase equilibrium studies for three components having one partially mixed pair, the model phase envelope has a pinch point and the envelope varies in size depending on the specified objective function rather than temperature.

The optimal conditions are shown in Figure 5.2 as a recovery vs. purity plot for glucose in the raffinate (the optimized limb indicated by the blank symbols) at various

fructose concentrations, and the corresponding calculated recovery vs. purity plot for fructose in the extract (the calculated limb indicated by the corresponding filled symbols). The symbols are connected by model tie lines. It is observed that the recovery increases with the increase of purity upto the maximum attainable recovery shown in the Figure. At this point optimized recovery of A is 93.1% and calculated recovery of B is 94.5%. This is found to be the pinch point for the system representing the optimum conditions for the operation. Beyond this point computation could not be carried out because the optimization solution after this point moves to the infeasible region.

The optimized parameters considering scheme (a) (optimization of raffinate) for glucose-fructose system for the general case are presented in Table 5.2. It is observed that for the same raffinate fructose concentration, while feed flow rate, eluent flow rate, switch time, extract flow rate and raffinate flow rate remains the same compared to fixed column length and diameter case, the switch time and diameter are reduced slightly for the general case. Run 1 in this case corresponds to the experimental results of Ching et al. [7]. The corresponding recovery vs. purity plots are shown in Figure 5.3. It is interesting to note that the plots for both fixed column length and diameter case (Figure 5.2) and general case (Figure 5.3) overlap each other. This indicates that the approach towards the attainment of the maximum / optimum recovery is the same for both cases.

The optimized parameters considering scheme (b) (optimization of extract) for glucose-fructose system with both fixed column length and diameter and general cases are presented in Table 5.3 and Table 5.4 respectively. The corresponding recovery vs. purity plots are shown in Figures 5.4 and 5.5 respectively. Optimization runs were carried out for various specified glucose concentration in the extract. The trend is similar to that observed for scheme (a). Again the limbs for the fixed column length and diameter case (Figure 5.4) and general case (Figure 5.5) overlap each other. From these plots the

optimized recovery of B is 94.5% and the corresponding calculated recovery of A is 93.1% which is the same pinch point as obtained from Figures 5.2 and 5.3 through optimization of raffinate. However the size of the phase envelope in Figures 5.4 and 5.5 is significantly different from that in Figures 5.2 and 5.3. As the temperature is not different, this can only be due to the specification of the objective function. The corresponding values of the optimized parameters are also the same as shown in Run 1 (Tables 5.1-5.4). This indicates that if either optimization of raffinate or optimization of extract is carried out, both will give the same pinch point for optimized recovery, and also the same set of optimized parameters. The pinch point is the same but the phase envelope is different. The concentration profiles for glucose and fructose in this system for the best set of optimum results (Run 1 in Table 5.1- 5.4) are shown in Figure 5.6.

In order to extend the applicability of the present optimization study for systems with nonlinear isotherm, the optimization has been carried out for monoethanolamine (MEA) - methanol (MOH) system on Duolite C-204 resin for both schemes.

The optimized parameters considering scheme (a) (optimization of raffinate) for MEA-MOH system with fixed column diameter and length and general cases are presented in Table 5.5 and Table 5.6 respectively. The corresponding recovery vs. purity plots are shown in Figures 5.7 and 5.8 respectively. The first point to note is that this system is no longer analogous to a three component one partially mixed pair system as for the fructose-glucose system. It can be characterized as analogous to a three component two partially mixed pair systems. The second point to note is that the system exhibits *solutropy*, i.e., a reversal of model tie lines is observed to occur. It is observed that in both the figures recovery increases with increasing purity upto a point which is considered as the optimum point after this point recovery decreases drastically with increases of purity. It may be mentioned that both the plots overlap one another as was observed for the linear

glucose-fructose system. In both cases the calculated recovery of MEA in the extract remains constant at 99.97% while the maximum recovery of MOH was about 94%.

The optimized parameters considering scheme (b) (optimization of extract) for MEA-MOH system with fixed column length and diameter and general cases are presented in Tables 5.7 and 5.8 respectively. The corresponding recovery vs. purity plots are shown in Figures 5.9 and 5.10 respectively. It is observed, that the qualitative nature is similar to that found for scheme (a). However, in this case the optimized recovery of MEA in the extract remains constant at 99.97% while the maximum calculated recovery of MOH in the raffinate was almost about 94% which was also found from results of scheme (a). This implies that both schemes will give identical results at optimum condition even when the system isotherm is nonlinear.

The maximum point for the recovery appears to be the point of *solutropy* where the reversal of the model tie lines occur, as may be observed by inspection of Figures 5.7 to 5.10 respectively. This is not definitively established as it was not possible to attain the maximum recovery points exactly in the optimization.

REFERENCES

- (1) Broughton, D. B., U. S. Patent 3, 291, 13 Dec. (1966).
- (2) Broughton, D. B. " Molex: case history of a process", Chem. Engng Prog., 64(8), 60-65 (1968).
- (3) Broughton, D. B., Neuzil, R. W., Pharis, J. M. and Brearley, C. S., " The parex process for recovering p-xylene." Chem. Engng Prog., 66(9), 70-75 (1970).
- (4) Bieser, H. J. and de Rosset, A. J., "Continuous countercurrent separation of saccharides with inorganic adsorbents.", 28th Starch Convention, Detmold F.R.G. (1977).
- (5) Hidajat, K., Ching, C. B. and Ruthven, D. M., "Numerical simulation of a semi-continuous countercurrent adsorption unit for fructose-glucose separation", Chem. Eng. J., 33, B55-B61 (1986).
- (6) Hidajat, K., and Ching, C. B., "Simulation of the performance of a continuous countercurrent adsorption system by the method of orthogonal collocation with nonlinear and interacting adsorption isotherms", Trans. I. Chem. Eng., 68, 104-108 (1990).
- (7) Ching, C. B., Ruthven, D. M., and Hidajat, R., "Experimental study of a simulated countercurrent adsorption system-III. SORBEX Operation", Chem. Eng. Sci., 40, 1411-1417 (1985).
- (8) Ching, C. B., Ho, C., and Ruthven, D. M., "An improved adsorption process for the production of high fructose syrup", AIChEJ, 32, 1876-1880 (1986).
- (9) Ching, C. B., Hidajat, K., Ho, C., and Ruthven, D. M., "Experimental study of a simulated countercurrent adsorption system-V. Comparison of Resin and Zeolite adsorbents for fructose-glucose separation at high concentration", Chem. Eng. Sci., 42, 2547-2555 (1987).
- (10) Ching, C. B., Hidajat, K., Ho, C., and Ruthven, D. M., "Modeling of a simulated countercurrent adsorption processes", Reactive Polym., 6, 15-20 (1987).
- (11) Ching, C. B., Ho, C., and Ruthven, D. M., "Experimental study of a simulated countercurrent adsorption system-VI. Non-linear systems", Chem. Eng. Sci., 43, 703-711 (1988).

- (12) Ching, C. B., and Ruthven, D. M., "Analysis of the performance of a simulated countercurrent chromatographic system for fructose-glucose separation", *Can. J. Chem. Eng.*, 62, 398-403 (1984).
- (13) Ching, C. B., and Ruthven, D. M., "Separation of glucose and fructose by simulated countercurrent adsorption", *AIChE Symp. Ser.*, 81 (242), 1-8 (1985).
- (14) Ching, C. B., and Ruthven, D. M., "An experimental study of a simulated countercurrent adsorption system-I. Isothermal steady state operation", *Chem. Eng. Sci.*, 40 (6), 877-885 (1985).
- (15) Ching, C. B., and Ruthven, D. M., "An experimental study of a simulated countercurrent adsorption system-II. Transient response", *Chem. Eng. Sci.*, 40, (6), 887-891 (1985).
- (16) Ching, C. B., and Ruthven, D. M., "Experimental study of a simulated countercurrent adsorption system-IV. Non-isothermal operation", *Chem. Eng. Sci.*, 41, 3063-3071 (1986).
- (17) Hashimoto, K., Adachi, S., Noujima, H. and Maruyama, H., "Models for the separation of glucose/fructose mixture using a simulated moving-bed adsorber", *J. Chem. Eng. Japan*, 16, 400-406 (1983).
- (18) Morbidelli, M., Storti, G., Paludetto, R., and Carra, S., "Mathematical models of moving beds and simulated moving-beds for adsorption: Analysis and Comparison", *Proceedings of the Second Engineering Foundation Conference on Fundamentals of Adsorption*. A.I. Liapis, Ed. New York: Engineering Foundation, 411 (1986).
- (19) Storti, G., Masi, M., and Carra, S., "Modeling and design of simulated moving-bed adsorption separation units", *Prep. Chromatography*, 1, 1-27 (1988).
- (20) Storti, G., Masi, M., and Carra, S., and Morbidelli, M., "Optimal design of multicomponent adsorption separation processes involving nonlinear equilibria", *Chem. Eng. Sci.*, 44, 6, 1329-1345 (1989).
- (21) Rahman, A. K. M., Hassan, M. M., and Loughlin, K. F., "Unsteady state simulation of SORBEX system with linear adsorption isotherm", *Sep. Technol.*, 4, 27-37 (1994).
- (22) Hassan, M. M., Shamsur Rahman, A. K. M., and Loughlin, K. F., "Modeling of simulated moving bed adsorption system: a more precise approach", *Sep. Technol.*, 77-89, (1995).

- (23) Storti, G., Baciocchi, R., M., and Morbidelli M., " Design of optimal operating conditions of simulated moving bed adsorptive separation units", *Ind. Eng. Chem. Res.*, 34, 288-301 (1995).
- (24) Hassan, M M., Loughlin, K. F., and Biswas., M. E., "Optimization of continuous countercurrent adsorption systems", *Sep. Tehnol.*, accepted, (1995).

NOMENCLATURE

b_{ij}	Langmuir constant
C_{ij}	dimensionless sorbate concentration in fluid phase for component i in section j
c_{ij}	sorbate concentration in fluid phase for component i in section j
c_{oi}	concentration in the feed stream
D	diameter of column
D_{Lj}	axial dispersion coefficient (for flow in section j)
E	eluent flowrate
F	feed flowrate
k_i	overall effective mass transfer coefficient for component i
K_i	adsorption equilibrium constants for component i
L	length of the adsorption column
$L_{s j}$	length of adsorption section j
Pe_j	Peclet number in section j, $(V_j L_{s1} / D_{Lj})$
q_{ij}	average solid phase concentration (of component i in section j)
Q'_{ij}	dimensionless average solid phase concentration (of component i in section j)
Q''_{ij}	dimensionless equilibrium solid phase concentration (of component i in section j)
q_{oi}	solid phase concentration in equilibrium with concentration of i in feed
q_{ij}^*	equilibrium solid phase concentration (of component i in section j)
q_s	saturated solid phase concentration
Q_j	fluid flow rate in section j, $\epsilon V_j A$

S	hypothetical adsorbent recirculation rate $(1-\varepsilon)uA$
St	Stanton number, $(k_i L_{Sj} / u)$
u	linear velocity of solid, (L/τ)
V_j	fluid velocity in section j
z_j	axial distance coordinate
Z_j	dimensionless axial distance coordinate

Greek Letters:

α	dimensionless parameter, $(1-\varepsilon)u / \varepsilon v_j$
ε	bed porosity
λ_i	non-linearity parameter for component i , (q_{oi} / q_s)
τ	switch time

FLOW DIAGRAM

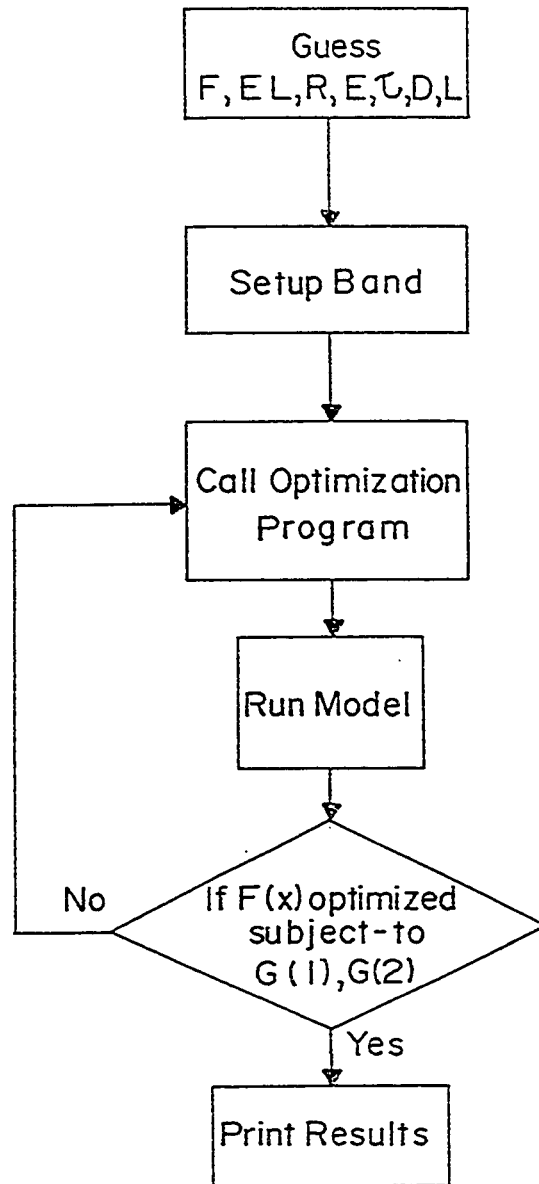


Figure 5.1 Flowsheet showing algorithm of optimization scheme

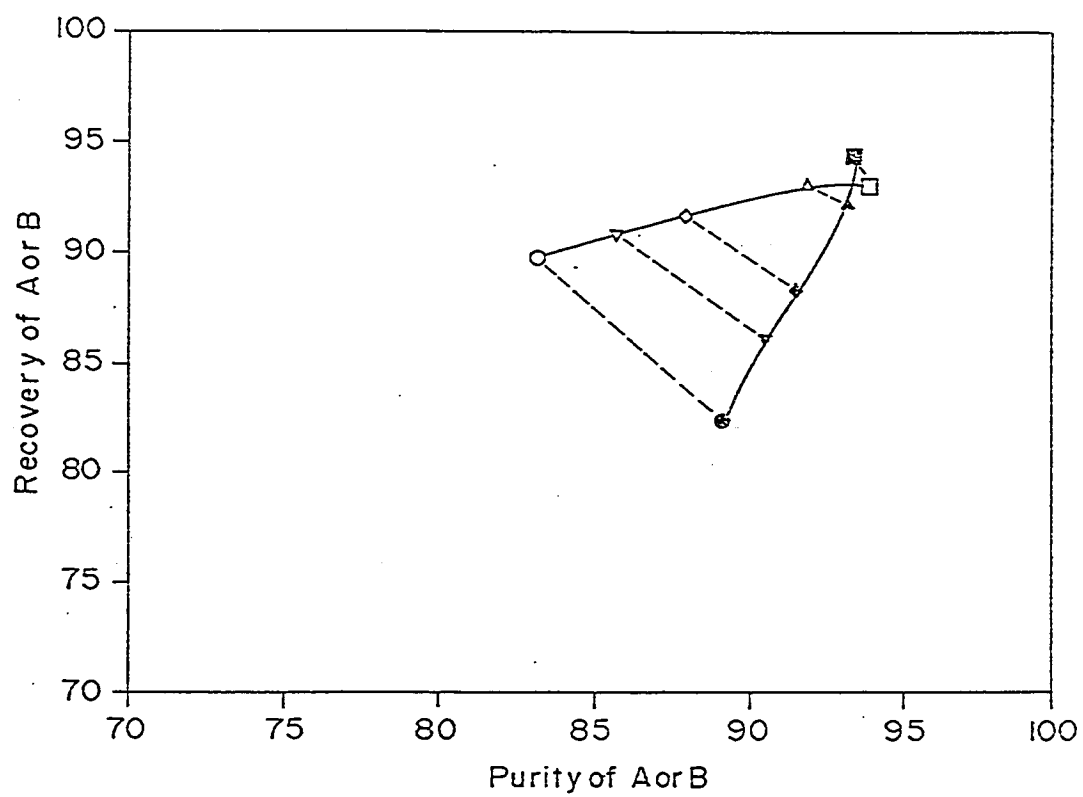


Figure 5.2 Recovery vs. purity plot considering scheme(a) for glucose-fructose system with fixed column length and diameter. ---- Model tie lines

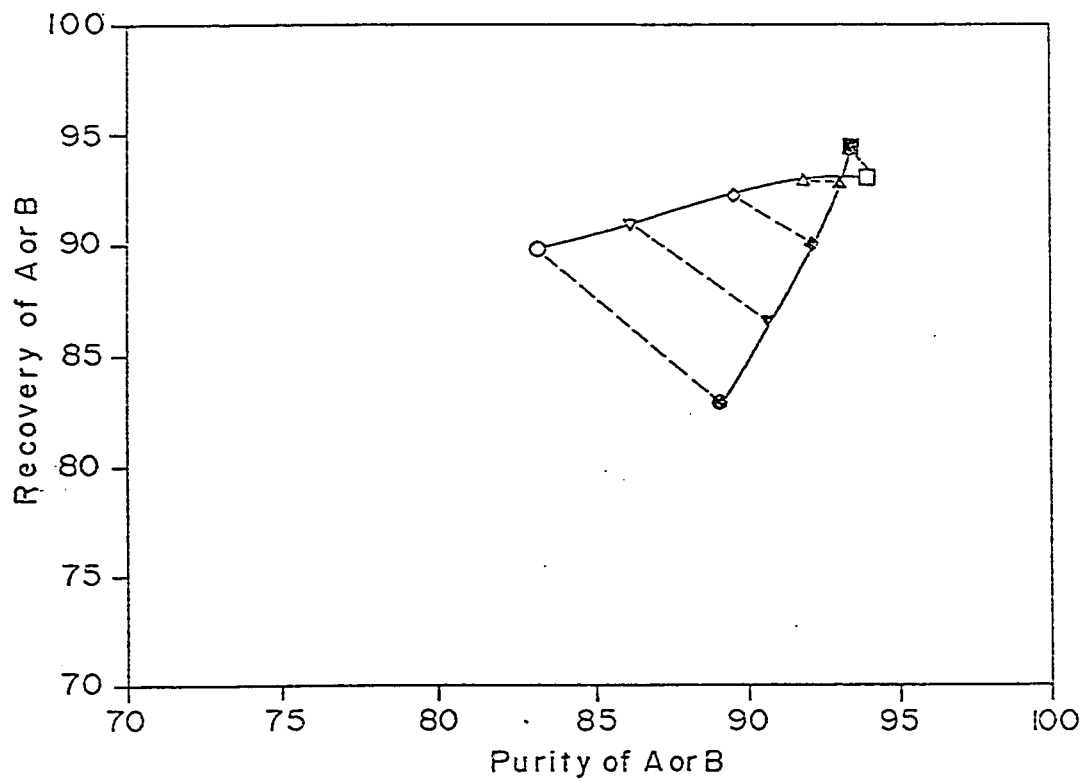


Figure 5.3 Recovery vs. purity plot considering scheme(a) for glucose-fructose system for general case. — Model tie lines

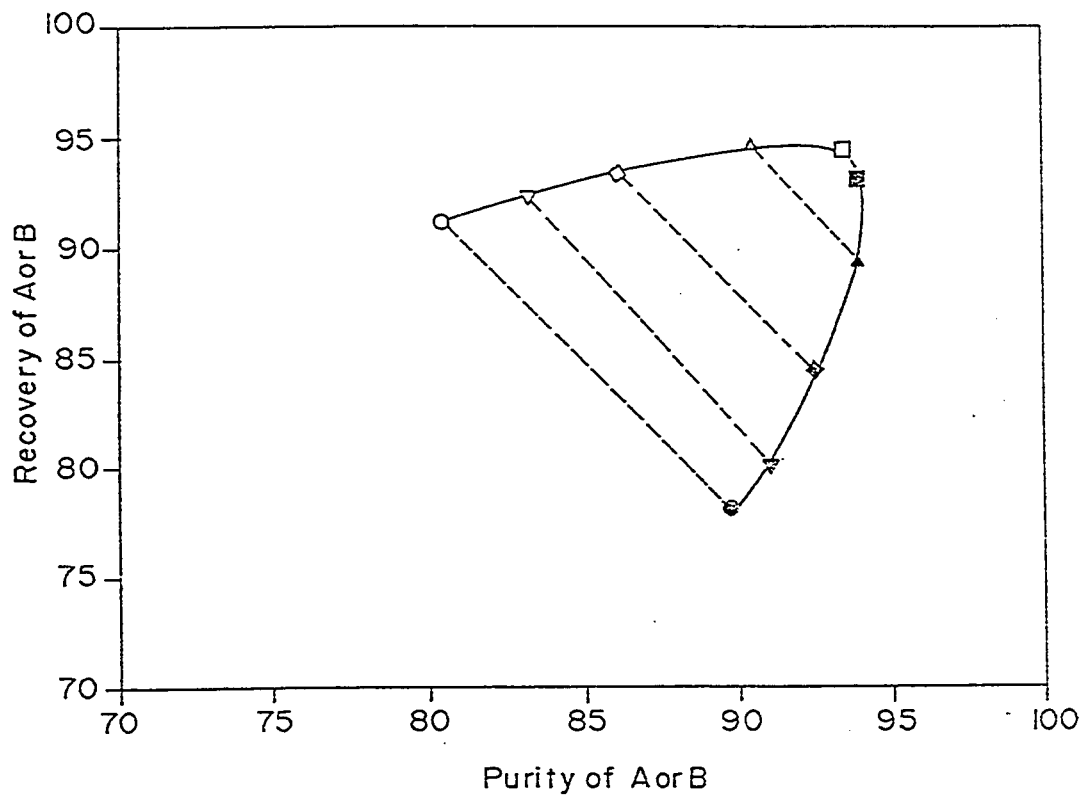


Figure 5.4 Recovery vs. purity plot considering scheme(b) for glucose-fructose system with fixed column length and diameter. ---- Model tie lines

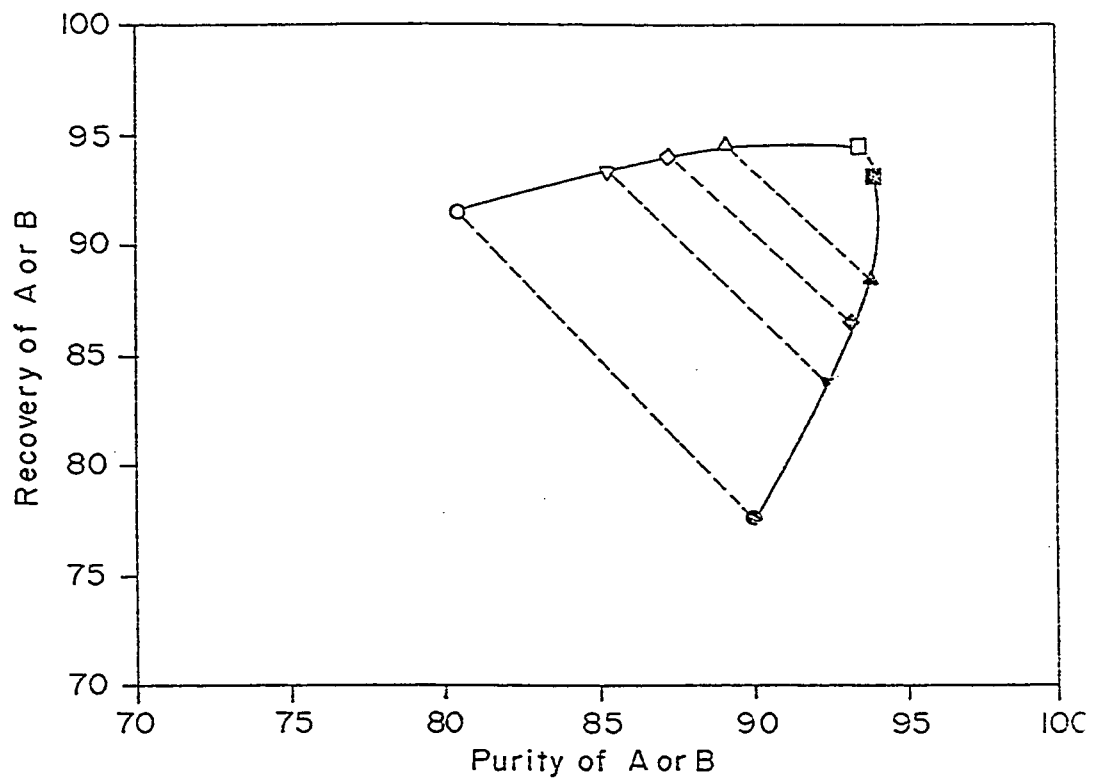


Figure 5.5 Recovery vs. purity plot considering scheme(b) for glucose-fructose system for general case. ---- Model tie lines

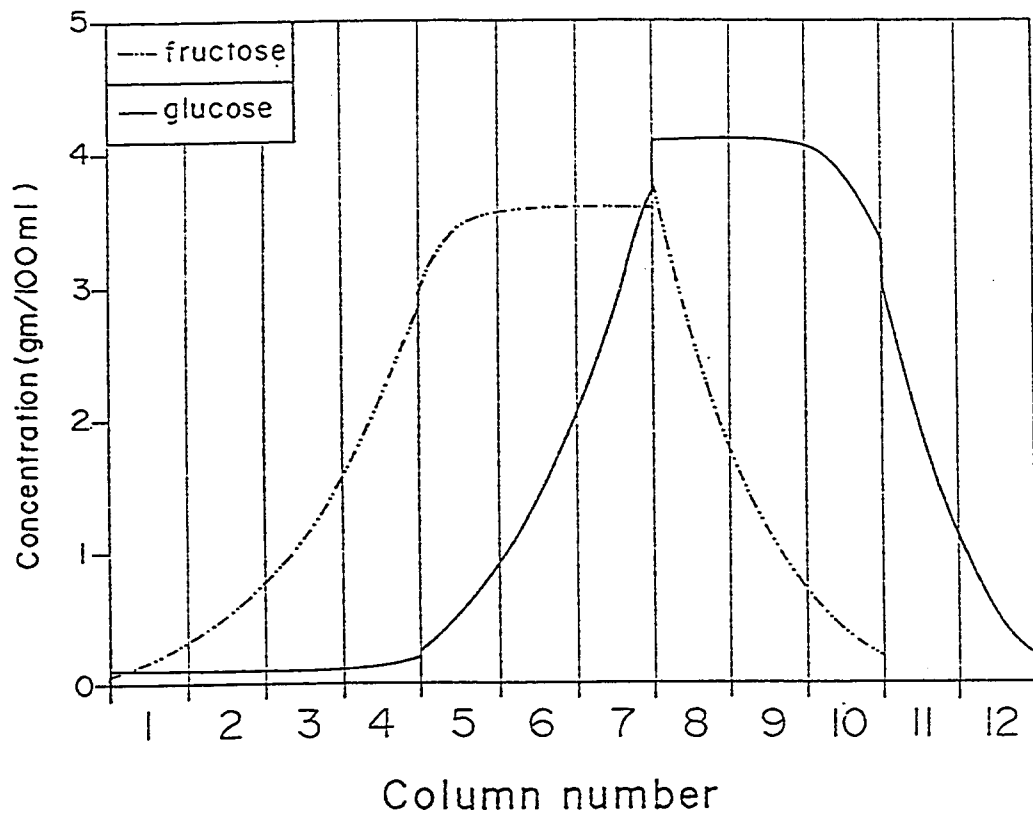


Figure 5.6 Concentration profiles for glucose fructose system for best case

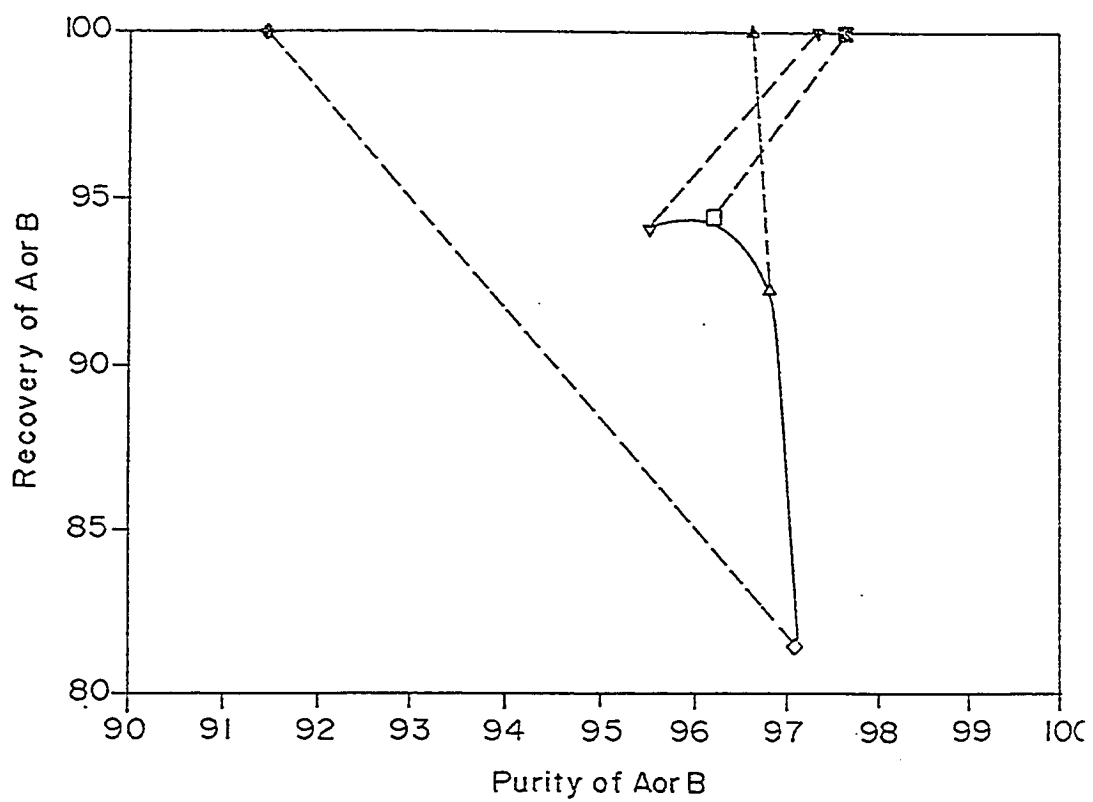


Figure 5.7 Recovery vs. purity plot considering scheme(a) for nonlinear MEA-MOH system with fixed column length and diameter. — Model tie lines

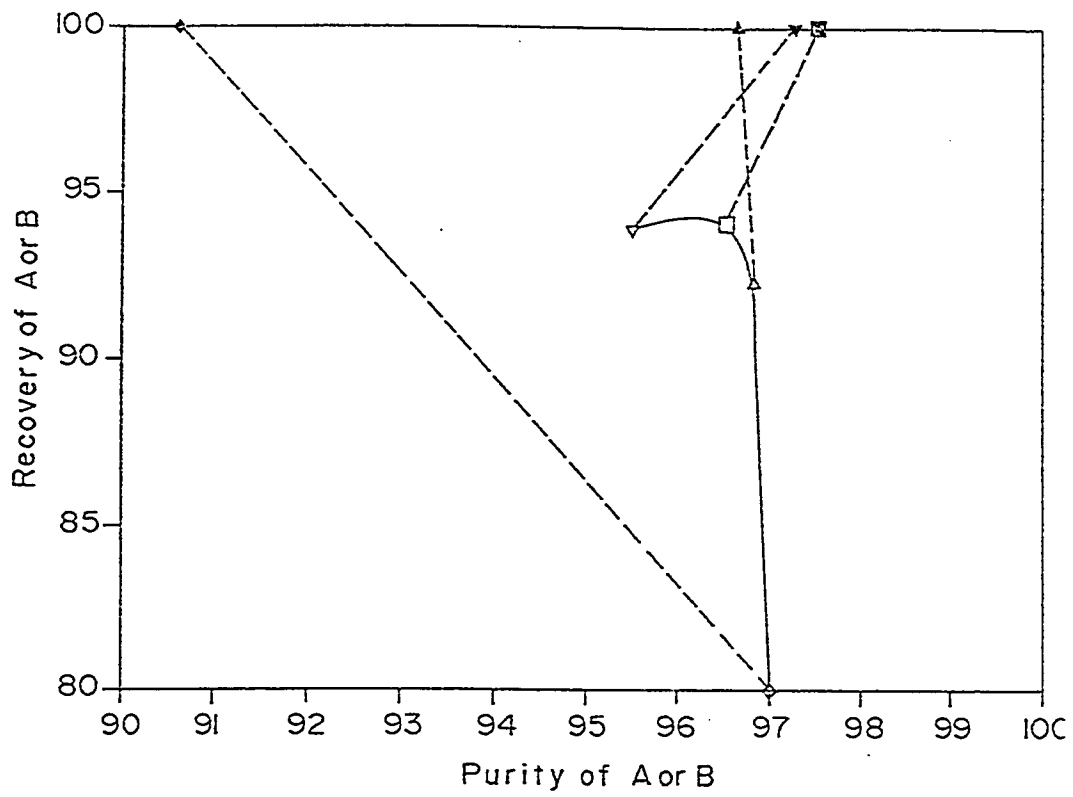


Figure 5.8 Recovery vs. purity plot considering scheme(a) for nonlinear MEA-MOH system for general case. — Model tie lines

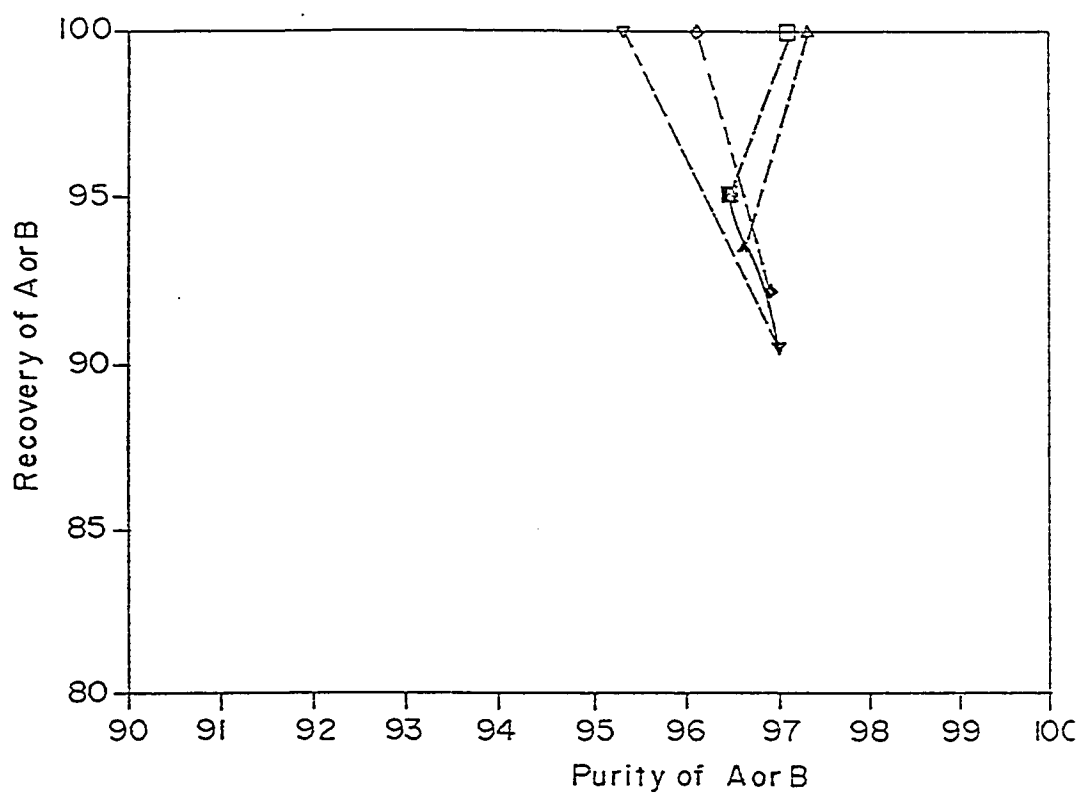


Figure 5.9 Recovery vs. purity plot considering scheme(b) for nonlinear MEA-MOH system with fixed column length and diameter. ---- Model tie lines

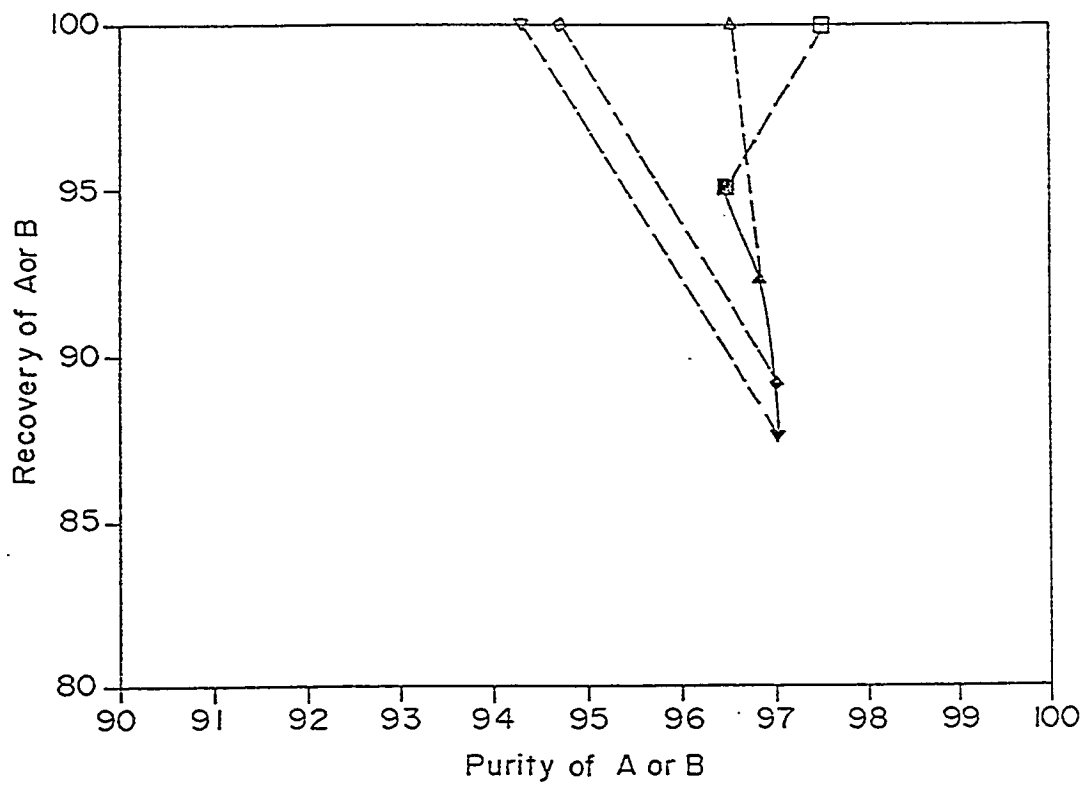


Figure 5.10 Recovery vs. purity plot considering scheme(a) for nonlinear MEA-MOH system for general case. — Model tie lines

Table 5.1 Optimized parameters for glucose (A)-fructose (B) system for raffinate optimization ($\lambda_A = \lambda_B = 0$); column diameter (5.1 cm), length(100.00 cm): Feed composition: 5 % A, 5 % B; $K_A = 0.51$; $K_B = 0.88$; Configuration- (4,3,3,2)

Run No.	Feed rate (ml/min)	Eluent rate (ml/min)	Switch time (min)	Extract flow rate (ml/min)	Raffinate flow rate (ml/min)	Raffinate recovery of A	Purity of A	Concentration Ratio	Raffinate fructose concentration (gm/100ml)
1	10.0	65.4	30.5	16.8	13.8	93.1	93.9	67.5	0.2206
2	10.0	65.4	31.2	16.8	13.8	93.1	91.8	67.4	0.2995
3	10.0	65.4	31.9	16.8	13.8	91.7	87.9	66.5	0.456
4	10.0	65.4	32.3	16.8	13.8	90.8	85.6	65.8	0.5516
5	10.0	65.4	32.6	16.8	13.8	89.8	83.1	65.1	0.662

$$\text{Purity} = \frac{\text{ConcA3}(M2)}{\text{ConcA3}(M2) + \text{ConcB3}(M2)}; \text{Recovery} = \frac{\text{ConcA3}(M2) * \text{Raffinate flow rate}}{\text{ConcCoA} * \text{Feed flow rate}}; \text{and Concentration Ratio} = \frac{\text{ConcA3}(M2)}{\text{ConcCoA}}$$

Table 5.2 Optimized parameters for glucose (A)-fructose (B) system for raffinate optimization ($\lambda_A = \lambda_B = 0$) for general case
 Feed composition: 5 % A, 5 % B; $K_A = 0.51$; $K_B = 0.88$; Configuration- (4,3,3,2)

Run No.	Feed rate (ml/min)	Eluent rate (ml/min)	Switch time (min)	Extract flow rate (ml/min)	Raffinate flow rate (ml/min)	Diameter of the column (cm)	Length of Column (cm)	Raffinate recovery of A	Purity of A	Concentration Ratio	Raffinate fructose concentration (gm/100ml)
1	10.0	65.4	30.5	16.8	13.8	5.10	100.00	93.1	93.9	67.5	0.2206
2	10.0	65.4	30.5	16.8	13.8	5.05	100.00	92.9	91.8	67.3	0.300
3	10.0	65.4	30.9	16.8	13.8	5.04	99.87	92.2	89.5	66.8	0.3913
4	10.0	65.4	30.8	16.8	13.8	5.00	99.89	90.9	86.1	65.9	0.533
5	10.0	65.4	31.5	16.8	13.8	5.02	99.68	89.8	83.2	65.1	0.6587

Table 5.3 Optimized parameters for glucose (A)-fructose (B) system for extract optimization ($\lambda_A = \lambda_B = 0$); column diameter (5.1 cm), length(100.00 cm): Feed composition: 5 % A, 5 % B; $K_A = 0.51$; $K_B = 0.88$; Configuration- (4,3,3,2)

Run No.	Feed rate (ml/min)	Eluent rate (ml/min)	Switch time (min)	Extract flow rate (ml/min)	Raffinate flow rate (ml/min)	Extract recovery of B	Purity of B	Concentration Ratio	Extract glucose concentration (gm/100ml)
1	10.0	65.4	30.5	16.8	13.8	94.5	93.4	56.3	0.200
2	10.0	65.4	29.5	16.8	13.8	94.6	90.4	56.3	0.300
3	10.0	65.4	28.9	16.8	13.8	93.3	86.1	55.5	0.4476
4	10.0	65.4	28.6	16.8	13.8	92.3	83.2	54.8	0.5546
5	10.0	65.4	28.3	16.8	13.8	91.2	80.4	54.3	0.6617

$$\text{Purity} = \frac{\text{ConcB1}(M2)}{\text{ConcA1}(M2) + \text{ConcB1}(M2)}; \text{Recovery} = \frac{\text{ConcB1}(M2) * \text{Extract flow rate}}{\text{ConcCoB} * \text{Feed flow rate}}; \text{and Concentration Ratio} = \frac{\text{ConcB1}(M2)}{\text{ConcCoB}}$$

Table 5.4 Optimized parameters for glucose (A)-fructose (B) system for extract optimization ($\lambda_A = \lambda_B = 0$) for general case
 Feed composition: 5 % A, 5 % B; $K_A = 0.51$; $K_B = 0.88$; Configuration- (4,3,3,2)

Run No.	Feed rate (ml/min)	Eluent rate (ml/min)	Switch time (min)	Extract flow rate (ml/min)	Raffinate flow rate (ml/min)	Diameter of the column (cm)	Length of Column (cm)	Extract recovery of B	Purity of B	Concentration Ratio	Extract glucose concentration (gm/100ml)
1	10.0	65.4	30.5	16.8	13.8	5.10	100.00	94.5	93.4	56.3	0.200
2	10.0	65.4	30.4	16.8	13.8	5.20	100.00	94.5	89.1	56.2	0.343
3	10.0	65.4	30.4	16.8	13.8	5.20	100.00	94.0	87.3	55.9	0.405
4	10.0	65.4	30.4	16.8	13.8	5.20	100.00	93.3	85.3	55.5	0.4767
5	10.0	65.4	31.4	16.8	13.8	5.30	100.00	91.5	80.4	54.5	0.6624

Table 5.5 Optimized parameters (raffinate optimization) for MOH (A)-MEA (B) system ($\lambda_A = 0$ & $\lambda_B = 0.435$); column diameter (5.5cm), length(100.00 cm): Feed composition: 10 % A, 20 % B; $K_B = 1.24$; Configuration- (4,3,3,2)

Run No.	Feed rate (ml/min)	Eluent rate (ml/min)	Switch time (min)	Extract flow rate (ml/min)	Raffinate flow rate (ml/min)	Raffinate recovery of A	Purity of A	Concentration Ratio	Raffinate MEA concentration (gm/100ml)
1	5.0	130.4	21.4	44.0	13.7	81.5	97.1	29.7	0.0887
2	5.0	130.4	21.8	44.0	13.7	92.3	96.8	33.7	0.111
3	5.0	130.4	22.3	44.0	13.7	94.5	96.2	34.5	0.135
4	5.0	130.4	22.7	44.0	13.7	94.1	95.5	34.3	0.1627

$$Purity = \frac{ConcA3(M2)}{ConcA3(M2) + ConcB3(M2)}; Recovery = \frac{ConcA3(M2) * Raffinate\ flow\ rate}{ConcCoA * Feed\ flow\ rate}; \text{ and Concentration Ratio} = \frac{ConcA3(M2)}{ConcCoA}$$

Table 5.6 Optimized parameters (raffinate optimization) for MOH (A)-MEA (B) system ($\lambda_A = 0$ & $\lambda_B = 0.435$) for general case: Feed composition: 10 % A, 20 % B; $K_A = 0.63$; $K_B = 1.24$; Configuration- (4,3,3,2)

Run No.	Feed rate (ml/min)	Eluent rate (ml/min)	Switch time (min)	Extract flow rate (ml/min)	Raffinate flow rate (ml/min)	Diameter of each column (cm)	Length of each column (cm)	Raffinate recovery of A	Purity of A	Concentration Ratio	Raffinate MEA concentration (gm/100ml)
1	5.0	130.4	22.1	44.0	13.7	5.6	100.0	79.6	97.0	29.0	0.088
2	5.0	130.4	22.1	44.0	13.7	5.5	100.0	92.3	96.8	33.7	0.1116
3	5.0	130.4	22.1	44.0	13.7	5.5	100.0	94.1	96.5	34.4	0.126
4	5.0	130.4	22.1	44.0	13.7	5.4	100.0	93.9	95.5	34.3	0.1609
5	5.0	130.4	22.1	44.0	13.7	5.4	100.0	92.8	95.0	33.9	0.1794

Table 5.7 Optimized parameters (extract optimization) for MOH (A)-MEA (B) system ($\lambda_A = 0$ & $\lambda_B = 0.435$); column diameter(5.5cm), length(100.00 cm): Feed composition: 10 % A, 20 % B; $K_A = 0.63$; $K_B = 1.24$; Configuration- (4,3,3,2)

Run No.	Feed rate (ml/min)	Eluent rate (ml/min)	Switch time (min)	Extract flow rate (ml/min)	Raffinate flow rate (ml/min)	Extract recovery of B	Purity of B	Concentration Ratio	Extract MOH(A) concentration (gm/100ml)
1	5.0	130.4	22.0	44.0	13.7	99.88	97.1	11.35	0.067
2	5.0	130.4	22.0	44.0	13.7	99.97	97.3	11.36	0.065
3	5.0	130.4	21.8	44.0	13.7	99.97	96.1	11.36	0.093
4	5.0	130.4	21.7	44.0	13.7	99.97	95.3	11.36	0.114

$$\text{Purity} = \frac{\text{ConcB1}(M2)}{\text{ConcA1}(M2) + \text{ConcB1}(M2)}; \text{Recovery} = \frac{\text{ConcB1}(M2) * \text{Extract flowrate}}{\text{ConcCoB} * \text{Feed flowrate}}; \text{and Concentration Ratio} = \frac{\text{ConcB1}(M2)}{\text{ConcCoB}}$$

Table 5.8 Optimized parameters (extract optimization) for MOH (A)-MEA (B) system ($\lambda_A = 0$ & $\lambda_B = 0.435$) for general case : Feed composition: 10 % A, 20 % B; $K_A = 0.63$; $K_B = 1.24$; Configuration- (4,3,3,2)

Run No.	Feed rate (ml/min)	Eluent rate (ml/min)	Switch time (min)	Extract flow rate (ml/min)	Raffinate flow rate (ml/min)	Diameter of each column (cm)	Length of each column (cm)	Extract recovery of B	Purity of B	Concentration Ratio	Extract MOH(A) concentration (gm/100ml)
1	5.0	130.4	22.1	44.0	13.7	5.5	100.0	99.97	97.5	11.36	0.0595
2	5.0	130.4	22.1	44.0	13.7	5.5	100.0	99.97	96.5	11.36	0.0842
3	5.0	130.4	22.1	44.0	13.7	5.6	100.0	99.97	94.7	11.36	0.1279
4	5.0	130.4	22.1	44.0	13.7	5.6	100.0	99.97	94.3	11.36	0.1393

Chapter 6

Conclusions and Recommendations

6.1 CONCLUSIONS

In doing the optimization of the continuous countercurrent adsorption systems the following important conclusions can be drawn for the two different cases considered:

6.1.1 Optimization of two-section continuous counter current adsorption systems

- The optimization scheme presented can successfully evaluate the optimum values of parameters for any specified concentration of the more strongly adsorbed species.
- The optimized values of parameters may become significantly different with the change in the nonlinearity of the isotherm.
- With the increase in the specified concentration of the more strongly adsorbed species in the raffinate, the purity decreases while the recovery increases and the cross over point of recovery and purity line can be regarded as a compromise between the recovery and purity.

6.1.2 Optimization of the SORBEX systems

- For both linear glucose-fructose and nonlinear MEA-MOH system recovery increases with increase in purity upto a maximum level of recovery which is

considered the best of all optimum sets and then for further increase in purity recovery decreases sharply.

- The approach towards the attainment of the maximum levels of recovery is same for fixed column length and diameter case and for general case in both linear and nonlinear systems.
- Either optimization of raffinate or optimization of extract is carried out, both of them will give the identical results of maximum recovery, purity and optimum values of process variables.
- The qualitative approach towards the maximum level of recovery is similar for both linear and nonlinear isotherm.

6.2 RECOMMENDATIONS FOR FURTHER STUDY

On the basis of results obtained from the present study, the following recommendations can be made for future work:

- In the present optimization a dispersed plug flow isothermal model is used which is reported in literature. But in some cases, due to high concentrations, the heat effects may become quite significant and the system may become nonisothermal. It is therefore recommended that this optimization may be extended to include the effect of nonisothermal condition.
- Experimental data has been reported in the literature for the system in the present study and therefore a local optimization could be attained quickly. However, for

unknown systems the present optimization could become difficult. A global optimization will therefore be required to solve such problems. Hence, the present study could be extended to global optimization.

- There are systems where both adsorption and reactions occurs simultaneously. In such a system reaction parameters are also important and also needs to be optimized. The present study can also be extended to such a reactive system.

APPENDIX A

(Computer program for two-section configuration)

```

C
C   COMPUTER PROGRAM TO SOLVE THE NONLINEAR INEQUALITY CONSTRAINT
C   OPTIMIZATION PROBLEM
C
C   THIS PROGRAM IS DONE FOR THE OPTIMIZATION OF TWO-SECTION
C   CONFIGURATION
C
C   -----
C   | DATA STRUCTURE SECTION |
C   -----
C
C   INTEGER IBTYPE, IPRINT, MMM, MAXITN, ME, NN
C   PARAMETER( IBTYPE=0, IPRINT=2, MMM=2, MAXITN=50, ME=0, NN=5, N=12)
C   REAL FVALUE, XX(NN), XGUESS(NN), XLB(NN), XUB(NN), XSCALE(NN)
C   DIMENSION A(2), C(2)
C   COMMON/DATA/QA1M2, QB1M2, PEM1, ALFA1, BETA1, V1
C   COMMON/DATA/CHAZ2, CHBZ2, PEM2, ALFA2, BETA2, V2
C   COMMON/BALL/MODNUM
C   COMMON/A/M2, XARRAY(12), CONCA1(12), CONCB1(12), CONCA2(12), CONCR2(12)
C   COMMON/AREA/PURITY, BANDWI
C   DIMENSION ZARRAY(10)
C   EXTERNAL MODEL, NCONF, WRRRN
C
C   XGUESS(1) = F IN ML/MIN
C   XGUESS(2) = E IN ML/MIN
C   XGUESS(3) = TAU IN MINUTES
C   XGUESS(4) = D IN CMS
C   XGUESS(5) = L IN CMS
C
C   DATA XGUESS/7.5,110.,15.,5.1,100./
C   DATA XSCALE/5*1.0E0/
C   DATA XLB /5.,90.,12.,5.1,100./
C   DATA XUB /40.0,120.,35.50,5.10,100./
C   DATA A/-0.7,0.3/
C   DATA C/-0.4,0.2/
C
C   SPECIFY FIGURE SIZE
C
C   XDIST=24.0
C   YDIST=20.0
C
C   -----
C   | FORMAT STATEMENTS |
C   -----
C
C   5   FORMAT(10X,7(F10.5))
C
C   -----
C   | INITIALISE THE PLOTTER AND GIVE NUMBER FOR OUTPUT |
C   -----
C
C   CALL PLOTS ( 0 , 0 , 1 )
C
C   -----
C   | MOVE THE PEN TO (5.0 , 5.0) , TO ENSURE THAT X=0 AND Y=0 |
C   | ARE BOTH 5 CMS AWAY FROM THE LIMITS OF THE PLOT , AND RESET |

```

```

C: | THE ORIGIN. DRAW BOUNDARIES OF FIGURE. |
C: -----
C:
C: CALL PLOT ( 3.0 , 8.0 , -3 )
C: CALL PLOT ( XDIST ,0.0 , 2)
C: CALL PLOT ( XDIST ,YDIST , 2)
C: CALL PLOT ( 0.0 ,YDIST , 2)
C: CALL PLOT ( 0.0 ,0.0 , 2)
C: XPOS=0.5*XDIST
C: CALL PLOT(XPOS,0.0, 3)
C: CALL PLOT(XPOS,YDIST,2)
C: CALL PLOT ( 0.0,YDIST, 3)
C: CALL PLOT ( 0.0,0.0 , 3)
C:
C: SET UP AXIS SIZE AND DIVISIONS
C:
C: XDVAL=0.5
C: YDVAL=0.25
C: XFIRST=0.0
C: XLAST=12.0
C: YFIRST=0.0
C: YLAST= 5.0
C:
C: -----
C: | SET UP SCALE FACTORS FOR X AND Y AXIS. |
C: | (CARD SCALE IS NOT NECESSARY ONCE YARRAY(NP+1) |
C: | AND YARRAY(NP+2) ARE DEFINED). |
C: -----
C:
C: NP=2
C: XARRAY(1)=XFIRST
C: XARRAY(2)=XLAST
C: CALL SCALE ( XARRAY(1),XDIST,NP, 1 )
C: XO=XARRAY(NP+1)
C: XS=XDVAL
C: CONCA1(1)=YFIRST
C: CONCA1(2)=YLAST
C: CALL SCALE(CONCA1(1),YDIST,NP,1)
C: YO=CONCA1(NP+1)
C: YS=YDVAL
C: WRITE(8,*)'ZERO VALUE OF X-AXIS ' ,XO
C: WRITE(8,*)'FINAL VALUE OF X-AXIS ' ,XLAST
C: WRITE(8,*)'LENGTH OF X-AXIS ' ,XDIST
C: WRITE(8,*)'INCREMENTAL VALUE OF X-AXIS ' ,XDVAL
C: WRITE(8,*)'ZERO VALUE OF Y-AXIS ' ,YO
C: WRITE(8,*)'FINAL VALUE OF Y-AXIS ' ,YLAST
C: WRITE(8,*)'LENGTH OF Y-AXIS ' ,YDIST
C: WRITE(8,*)'INCREMENTAL VALUE OF Y-AXIS ' ,YDVAL
C:
C: -----
C: | STARTING AT (0,0) , PLOT THE X-AXIS XDIST CMS LONG , |
C: | AT 0 DEGREES , PLACING THE ANNOTAION ON THE CLOCKWISE |
C: | SIDE OF THE AXIS , AND USING THE VALUES CALCULATED BY |
C: | 'SCALE' TO LABEL THE TICK MARKS. |
C: -----

```



```

C
C
C      CALL AXIS( 0.0 , 0.0 ,20H
@      @ ,0.,XFIRST,XS)
C      POSX=XDIST/2.-5.0
C      CALL SYMBOL(POSX,-1.6, 0.50,20H COLUMN NUMBER
@      @INTEQ,0.,20)
C
C      -----
C      | PLOT A SIMILAR Y-AXIS , YDIST CMS LONG , AT 90 DEGREES |
C      | WITH THE ANNOTATION ON THE COUNTER-CLOCKWISE SIDE.   |
C      -----
C
C      CALL AXIS ( 0.0,.0. 27H
+      + ,90. ,YFIRST, YS)
C      POSY=YDIST/2.-6.0
C      CALL SYMBOL(-1.5,POSY,0.50,33H      CONCENTRATION
+      + ,INTEQ,90.,33)
C
C      -----
C      | RESET NP+1 AND NP+2 POINTS SIMILAR FOR ALL SETS OF DATA |
C      -----
C
C      INPUT THE MODEL NUMBER
C
C      WRITE(8,*)'INPUT THE MODEL NUMBER'
C      WRITE(8,*)'1 STANDS FOR THE TWO BED MODEL'
C      WRITE(8,*)'2 STANDS FOR THE FOUR BED MODEL'
C      READ(8,*)MODNUM
C      GO TO(30,40),MODNUM
30  WRITE(8,*)' *****'
C      WRITE(8,*)' * USING TWO BED MODEL *'
C      WRITE(8,*)' *****'
C      GO TO 50
40  WRITE(8,*)' *****'
C      WRITE(8,*)' * USING FOUR BED MODEL *'
C      WRITE(8,*)' *****'
50  CONTINUE
C      WRITE(8,*)' SPECIFY PURITY DESIRED '
C      READ(8,*)PURITY
401 CONTINUE
C      XARRAY(NP+1)=XO
C      XARRAY(NP+2)=XS
C      CONCA1(NP+1)=YO
C      CONCA1(NP+2)=YS
C      CONCB1(NP+1)=YO
C      CONCB1(NP+2)=YS
C      CONCA2(NP+1)=YO
C      CONCA2(NP+2)=YS
C      CONCB2(NP+1)=YO
C      CONCB2(NP+2)=YS
C      WRITE(8,*)MODNUM
C
C      -----
C      | PLOT DATA POINTS |
C      -----

```

```

CALL GUESS(NN,XGUESS,XLB,XUB)
CALL NCONF(MODEL,MMM,ME,NN,XGUESS,IBTYPE,XLB,XUB,XSCALE,IPRINT,MAX
@ITN,XX,FVALUE)
DO 95 I=1,M2
ZARRAY(I)=6.+5.*XARRAY(I)
XARRAY(I)=6*XARRAY(I)
95 CONTINUE
WRITE(8,*)' COLUMN  CONCA2  CONCB2'
DO 100 I=1,M2
WRITE(8,96)XARRAY(I),CONCA2(I),CONCB2(I)
WRITE(6,*)XARRAY(I),CONCA2(I),CONCB2(I)
100 CONTINUE
WRITE(8,*)' COLUMN  CONCA1  CONCB1'
DO 101 I=1,M2
WRITE(8,96)ZARRAY(I),CONCA1(I),CONCB1(I)
WRITE(6,*)ZARRAY(I),CONCA1(I),CONCB1(I)
101 CONTINUE
96 FORMAT(5(2X,F6.3))
WRITE(8,*)'          LOWBND  VALUE  UPPBND'
DO 102 IK=1,5
102 WRITE(8,98)XLB(IK),XX(IK),XUB(IK)
98 FORMAT(5X,3(2X,F7.2))
PHI=CONCA1(M2)/1.*100.
WRITE(8,97)PHI
97 FORMAT(' CONCENTRATION RATIO  =',F6.1,'%')
REC=(CONCA1(M2)*V1/1.0/(V1-V2))*100.
WRITE(8,91)REC
91 FORMAT(' RECOVERY  =',F6.1,'%')
PUR=(CONCA1(M2)/(CONCA1(M2)+CONCB1(M2)))*100.
WRITE(8,92)PUR
92 FORMAT(' PURITY  =',F6.1,'%')
WRITE(8,93)V1,V2
93 FORMAT(5X,2(2X,F6.2))
C
NP=M2
WRITE(8,*)NP,M2
XARRAY(NP+1)=XO
XARRAY(NP+2)=XS
CONCA2(NP+1)=YO
CONCA2(NP+2)=YS
CONCB2(NP+1)=YO
CONCB2(NP+2)=YS
CONCA1(NP+1)=YO
CONCA1(NP+2)=YS
CONCB1(NP+1)=YO
CONCB1(NP+2)=YS
CALL FLINE (XARRAY,CONCA2,-NP,1,1,3)
CALL FLINE (XARRAY,CONCB2,-NP,1,1,7)
DO 580 I=1,M2
XARRAY(I)=ZARRAY(I)
580 CONTINUE
CALL FLINE (XARRAY,CONCA1,-NP,1,1,3)
CALL FLINE (XARRAY,CONCB1,-NP,1,1,7)
CALL NUMBER(XDIST-23.5,YDIST-3.-0.5*12,0.3,TEMP,0.0,-1)

```

```

CALL SYMBOL(XDIST-22.0,YDIST-2.9-0.5*12,0.3,IBCD,12.0.0,-1)
500 CONTINUE
CALL WRRRN('THE SOLUTION IS',NN,1,XX,NN,0)
C
CALL GRPSEG ('CCAOPTIM', 70, 70 )
C
C-----
C | TO CREATE AN OUTPUT FILE FOR THE GRAPH, USE THE LINE BELOW |
C-----
C
CONTINUE
1000 STOP
END
C
C*****
C # GUESS SUBROUTINE *
C*****

SUBROUTINE GUESS(NN,XX,XLB,XUB)
INTEGER NUMB
DIMENSION XX(NN),XLB(NN),XUB(NN)
13 WRITE (8,*) ' '
WRITE (8,*) ' '
WRITE (8,*) ' '
WRITE (8,*) ('-',I=1,60)
WRITE (8,11)'*', 'COEF.NO.', '*', ' VALUE', '*', 'XLB ', '*', 'XUB ', '*'
11 FORMAT(A,1X,A,1X,A,5X,A,5X,A,5X,A,7X,A,5X,A,6X,A)
WRITE (8,*) ('-',I=1,60)
WRITE (8,12) '*', '1', '*', XX(1), '*', XLB(1), '*', XUB(1), '*'
12 FORMAT (A,4X,A,5X,A,2X,F10.4,4X,A,2X,F10.4,4X,A,2X,F10.4,3X,A)
WRITE (8,*) ('-',I=1,60)
WRITE (8,12) '*', '2', '*', XX(2), '*', XLB(2), '*', XUB(2), '*'
WRITE (8,*) ('-',I=1,60)
WRITE (8,12) '*', '3', '*', XX(3), '*', XLB(3), '*', XUB(3), '*'
WRITE (8,*) ('-',I=1,60)
WRITE (8,12) '*', '4', '*', XX(4), '*', XLB(4), '*', XUB(4), '*'
WRITE (8,*) ('-',I=1,60)
WRITE (8,12) '*', '5', '*', XX(5), '*', XLB(5), '*', XUB(5), '*'
WRITE (8,*) ('-',I=1,60)
WRITE(8,*) ' * PRESS 1 IF YOU WANT TO CHANGE XLB'
WRITE(8,*) ' * PRESS 2 IF YOU WANT TO CHANGE XUB'
WRITE(8,*) ' * PRESS 3 IF YOU WANT TO CHANGE XX VALUES'
WRITE(8,*) ' * PRESS 4 IF YOU WANT TO RUN THE OPTIMIZATION'
READ(8,*)NUMB
IF(NUMB.GE.4) THEN
WRITE(8,25)
25 FORMAT(2X,'THE VALUES ARE THE SAME ')
ENDIF
IF(NUMB.EQ.1) THEN
WRITE(8,26)
26 FORMAT(1X,'ENTER THE NEW VALUES OF XLB')
READ(8,*)XLB(1),XLB(2),XLB(3),XLB(4),XLB(5)
WRITE (8,*)
WRITE (8,*)
WRITE (8,*)

```

```

WRITE (8,*)
GOTO 13
ENDIF
IF(NUMB.EQ.2) THEN
WRITE(8,27)
27 FORMAT(1X,'ENTER THE NEW VALUES OF XUB')
READ(8,*)XUB(1),XUB(2),XUB(3),XUB(4),XUB(5)
WRITE (8,*)
WRITE (8,*)
WRITE (8,*)
WRITE (8,*)
GOTO 13
ENDIF
IF(NUMB.EQ.3) THEN
WRITE(8,28)
28 FORMAT(1X,'ENTER THE NEW VALUES OF XX VALUES')
READ(8,*)XX(1),XX(2),XX(3),XX(4),XX(5)
WRITE (8,*)
WRITE (8,*)
WRITE (8,*)
WRITE (8,*)
GOTO 13
ENDIF
RETURN
END
*****
C * OUTPUT SUBROUTINE *
C *****

SUBROUTINE OUTPUT( )

C
C RETURN
C
C ENTRY OUTP( )
C
C RETURN
C
C ENTRY OUTPH( )
C RETURN
C END
C SUBROUTINE DOTTED(X,Y,N,KODE)
C
C DIMENSION X(1),Y(1)
C DIMENSION CODE(9),SLTH(10),CHLTH(9),LTYPE(12)
C DATA NTPES/12/
C DATA LTYPE/4,95,9424,13,14,55955424,6424,64259524,
2 64,248424,24249424,2/
C DATA CODE/0.01,0.02,0.03,0.05,0.10,0.15,0.20,0.25,0.35/
C
C -----
C | CALCOMP SCALING CONVENTIONS |
C -----
C
C X0=X(N+1)

```

```

      Y0=Y(N+1)
      DELTAX=X(N+2)
      DELTAY=Y(N+2)
C
C -----
C | SET INITIAL COORDINATES |
C -----
C
      XT=(X(1)-X0)/DELTAX
      YT=(Y(1)-Y0)/DELTAY
C
C -----
C | SET N1 TO KODE (IFKODE>0) OR LTYPE(-KODE) (IF KODE<0) |
C | OR BRANCH TO DRAW A SOLID LINE (IF KODE=0). |
C -----
C
      IF(KODE.EQ.0) GO TO 270
      N1=KODE
      IF(N1.GT.0) GO TO 110
      N1=-N1
      IF(N1.GT.NTYPES) GO TO 100
      N1=LTYPE(N1)
      GO TO 110
100  N1=14
C
C -----
C | FIND THE SEGMENTS IN THE PATTERN |
C -----
C
110  LIM=0
120  IF(N1.LE.0) GO TO 160
      N2=N1/10
      N0=N1-10*N2
      IF(N0.EQ.0) GO TO 140
      LIM=LIM+1
      SLTH(LIM)=CODE(N0)
140  N1=N2
      GO TO 120
160  I=1
      J=LIM
      STEP=SLTH(J)
      DS=0.0
      CALL PLOT(XT,YT,3)
      IUPDN=2
      GO TO 250
C
C -----
C | IF NO, THEN TAKE THE STEP |
C -----
C
      XC=STEP*COSN+XC
      YC=STEP*SINE+YC
      CALL PLOT(XC,YC,IUPDN)
      IUPDN=5-IUPDN
      J=J-1

```

```

IF(J.LE.0) J=LIM
DS=DS-STEP
STEP=SLTH(J)
GO TO 220

-----
! IF YES, THE STEP OVERSHOOTS THE TARGET !
-----

240 CALL PLOT(XT,YT,IUPDN)
STEP=STEP-DS
250 I=I+1
IF(I.GT.N) GO TO 290

-----
! SET NEW TARGET !
-----

XC=XT
YC=YT
XT=(X(I)-X0)/DELTAX
YT=(Y(I)-Y0)/DELTAY
DX=XT-XC
DY=YT-YC
DS=SQRT(DX*DX+DY*DY)
IF(DS.EQ.0.0) GO TO 250
COSN=DX/DS
SINE=DY/DS
GO TO 220

270 CALL PLOT(XT,YT,3)
DO 280 I=2,N
XT=(X(I)-X0)/DELTAX
YT=(Y(I)-Y0)/DELTAY
280 CALL PLOT(XT,YT,2)
290 RETURN
ENTRY SETDOT(CHLTH)
DO 320 I=1,9
320 CODE(I)=CHLTH(I)
RETURN
END
SUBROUTINE MODEL(MMH,ME,NN,XX,ACTIVE,F,G)

C
C
C *****
C
C PROGRAM TO SOLVE THE SYSTEMS OF ORDINARY DIFFERENTIAL EQUATIONS
C *****
C
C IMPLICIT REAL*8(A-H,O-Z)
C INTEGER ITMAX,N,MMH,ME,NN
C PARAMETER(N=40)
C REAL ERRREL,L,LS1,LS2,KR,XX(*),F,G(*)
C LOGICAL ACTIVE(*)
C INTEGER K,NOUT
C REAL FNORM,CA(N),CGUESS(N)
C COMMON/DATA/QA1M2,QB1M2,PEM1,ALFA1,BETA1,V1

```

```

COMMON/DATA/CHAZ2,CHBZ2,PEM2,ALFA2,BETA2,V2
COMMON  A(30,30),B(30,30),X(50)
COMMON  CHA1(50,50),CHA2(50,50)
COMMON/DATA/MM,EA,EB,GA,GB
COMMON/A/M2,XARRAY(12),CONCA1(12),CONCB1(12),CONCA2(12),CONCB2(12)
COMMON/AREA/PURITY,BANDWI
EXTERNAL FCN,NEQNF
C
C *****COLLOCATION PARAMETERS*****
C
C   MM IS THE NUMBER OF INTERNAL COLLOCATION POINTS FOR BED
C
C *****
C
C   MM=8
C   M1=MM+1
C   M2=MM+2
C   DO 1 I=1,N
C     CGUESS(I)=0.5
C 1 CONTINUE
C
C ***** IMSL VARIABLES *****
C
C   ERRREL=0.0001
C   ITMAX=100
C
C ***** PARAMETERS FOR THE PROBLEM *****
C   KR= 0.21
C   EPS = 0.4
C   LS1 = 5.* XX(5)
C   LS2 = 6.* XX(5)
C   U = XX(5) / XX(3)
C   AREA = ATAN(1.)*XX(4)**2
C   V1 = (XX(2)+XX(1))/EPS/AREA-U
C   V2 = XX(2)/EPS/AREA-U
C   PEM1 = V1*LS1/5./{(U+V1)}
C   PEM2 = V2*LS2/5./{(U+V2)}
C   ALFA1 = KR*LS1/U
C   ALFA2 = KR*LS2/U
C   BETA1 = (1.-EPS)/EPS*U/V1
C   BETA2 = (1.-EPS)/EPS*U/V2
C   CHAZ2=0.0
C   CHBZ2=0.0
C   EA=0.51
C   EB=0.88
C   GA=0.0
C   GB=0.0
C   QA1M2=0.0
C   QB1M2=0.0
C ***** END OF PARAMETERS *****
C ***** INPUT FOR X VALUE AND A & B MATRIX *****
C
C   X(1)=0.0
C   X(2)=0.0199
C   X(3)=0.1017

```

```

X(4)=0.2372
X(5)=0.4083
X(6)=0.5917
X(7)=0.7628
X(8)=0.8983
X(9)=0.9801
X(10)=1.0
A( 1, 1)= -0.7300000E+02
A( 1, 2)=  0.8122396E+02
A( 1, 3)= -0.1085292E+02
A( 1, 4)=  0.3924518E+01
A( 1, 5)= -0.2122025E+01
A( 1, 6)=  0.1464189E+01
A( 1, 7)= -0.1220595E+01
A( 1, 8)=  0.1228254E+01
A( 1, 9)= -0.1645377E+01
A( 1,10)=  0.1000000E+01
A( 2, 1)= -0.3123007E+02
A( 2, 2)=  0.2467235E+02
A( 2, 3)=  0.8362857E+01
A( 2, 4)= -0.2655769E+01
A( 2, 5)=  0.1383075E+01
A( 2, 6)= -0.9394300E+00
A( 2, 7)=  0.7770883E+00
A( 2, 8)= -0.7788235E+00
A( 2, 9)=  0.1041352E+01
A( 2,10)= -0.6326363E+00
A( 3, 1)=  0.8914467E+01
A( 3, 2)= -0.1786548E+02
A( 3, 3)=  0.4361442E+01
A( 3, 4)=  0.6224194E+01
A( 3, 5)= -0.2560891E+01
A( 3, 6)=  0.1602304E+01
A( 3, 7)= -0.1276352E+01
A( 3, 8)=  0.1255230E+01
A( 3, 9)= -0.1663792E+01
A( 3,10)=  0.1008874E+01
A( 4, 1)= -0.4527522E+01
A( 4, 2)=  0.7968484E+01
A( 4, 3)= -0.8741957E+01
A( 4, 4)=  0.1452117E+01
A( 4, 5)=  0.5440369E+01
A( 4, 6)= -0.2625140E+01
A( 4, 7)=  0.1902832E+01
A( 4, 8)= -0.1792652E+01
A( 4, 9)=  0.2331610E+01
A( 4,10)= -0.1408140E+01
A( 5, 1)=  0.2827012E+01
A( 5, 2)= -0.4792190E+01
A( 5, 3)=  0.4153551E+01
A( 5, 4)= -0.6282481E+01
A( 5, 5)=  0.3796436E+00
A( 5, 6)=  0.5451533E+01
A( 5, 7)= -0.3031485E+01
A( 5, 8)=  0.2598803E+01

```


A(5, 9)= -0.3255013E+01
A(5,10)= 0.1950627E+01
A(6, 1)= -0.1950627E+01
A(6, 2)= 0.3255013E+01
A(6, 3)= -0.2598803E+01
A(6, 4)= 0.3031485E+01
A(6, 5)= -0.5451533E+01
A(6, 6)= -0.3796436E+00
A(6, 7)= 0.6282481E+01
A(6, 8)= -0.4153551E+01
A(6, 9)= 0.4792190E+01
A(6,10)= -0.2827012E+01
A(7, 1)= 0.1408140E+01
A(7, 2)= -0.2331610E+01
A(7, 3)= 0.1792652E+01
A(7, 4)= -0.1902832E+01
A(7, 5)= 0.2625140E+01
A(7, 6)= -0.5440369E+01
A(7, 7)= -0.1452117E+01
A(7, 8)= 0.8741957E+01
A(7, 9)= -0.7968484E+01
A(7,10)= 0.4527522E+01
A(8, 1)= -0.1008874E+01
A(8, 2)= 0.1663792E+01
A(8, 3)= -0.1255230E+01
A(8, 4)= 0.1276352E+01
A(8, 5)= -0.1602304E+01
A(8, 6)= 0.2560891E+01
A(8, 7)= -0.6224194E+01
A(8, 8)= -0.4361442E+01
A(8, 9)= 0.1786548E+02
A(8,10)= -0.8914467E+01
A(9, 1)= 0.6326363E+00
A(9, 2)= -0.1041352E+01
A(9, 3)= 0.7788235E+00
A(9, 4)= -0.7770883E+00
A(9, 5)= 0.9394300E+00
A(9, 6)= -0.1383075E+01
A(9, 7)= 0.2655769E+01
A(9, 8)= -0.8362857E+01
A(9, 9)= -0.2467235E+02
A(9,10)= 0.3123007E+02
A(10, 1)= -0.1000000E+01
A(10, 2)= 0.1645377E+01
A(10, 3)= -0.1228254E+01
A(10, 4)= 0.1220595E+01
A(10, 5)= -0.1464189E+01
A(10, 6)= 0.2122025E+01
A(10, 7)= -0.3924518E+01
A(10, 8)= 0.1085292E+02
A(10, 9)= -0.8122396E+02
A(10,10)= 0.7300000E+02
B(1, 1)= 0.2664000E+04
B(1, 2)= -0.3677014E+04
B(1, 3)= 0.1371027E+04

B(1, 4)= -0.5398939E+03
 B(1, 5)= 0.2994208E+03
 B(1, 6)= -0.2088227E+03
 B(1, 7)= 0.1750064E+03
 B(1, 8)= -0.1765906E+03
 B(1, 9)= 0.2368676E+03
 B(1,10)= -0.1440000E+03
 B(2, 1)= 0.1604764E+04
 B(2, 2)= -0.2113392E+04
 B(2, 3)= 0.6171044E+03
 B(2, 4)= -0.1554826E+03
 B(2, 5)= 0.7536884E+02
 B(2, 6)= -0.4964141E+02
 B(2, 7)= 0.4043721E+02
 B(2, 8)= -0.4020394E+02
 B(2, 9)= 0.5355405E+02
 B(2,10)= -0.3250816E+02
 B(3, 1)= -0.9760654E+02
 B(3, 2)= 0.2809078E+03
 B(3, 3)= -0.3027434E+03
 B(3, 4)= 0.1461175E+03
 B(3, 5)= -0.3904258E+02
 B(3, 6)= 0.2051605E+02
 B(3, 7)= -0.1499477E+02
 B(3, 8)= 0.1410044E+02
 B(3, 9)= -0.1830096E+02
 B(3,10)= 0.1104639E+02
 B(4, 1)= 0.2502030E+02
 B(4, 2)= -0.5017196E+02
 B(4, 3)= 0.1035801E+03
 B(4, 4)= -0.1428103E+03
 B(4, 5)= 0.7941196E+02
 B(4, 6)= -0.2243509E+02
 B(4, 7)= 0.1276781E+02
 B(4, 8)= -0.1062952E+02
 B(4, 9)= 0.1304849E+02
 B(4,10)= -0.7781758E+01
 B(5, 1)= -0.1170179E+02
 B(5, 2)= 0.2103617E+02
 B(5, 3)= -0.2393912E+02
 B(5, 4)= 0.6868810E+02
 B(5, 5)= -0.1050539E+03
 B(5, 6)= 0.6357770E+02
 B(5, 7)= -0.1940544E+02
 B(5, 8)= 0.1257950E+02
 B(5, 9)= -0.1385540E+02
 B(5,10)= 0.8074191E+01
 B(6, 1)= 0.8074191E+01
 B(6, 2)= -0.1385540E+02
 B(6, 3)= 0.1257950E+02
 B(6, 4)= -0.1940544E+02
 B(6, 5)= 0.6357770E+02
 B(6, 6)= -0.1050539E+03
 B(6, 7)= 0.6868810E+02
 B(6, 8)= -0.2393912E+02

```

B( 6, 9)= 0.2103617E+02
B( 6,10)= -0.1170179E+02
B( 7, 1)= -0.7781758E+01
B( 7, 2)= 0.1304849E+02
B( 7, 3)= -0.1062952E+02
B( 7, 4)= 0.1276781E+02
B( 7, 5)= -0.2243509E+02
B( 7, 6)= 0.7941196E+02
B( 7, 7)= -0.1428103E+03
B( 7, 8)= 0.1035801E+03
B( 7, 9)= -0.5017196E+02
B( 7,10)= 0.2502030E+02
B( 8, 1)= 0.1104639E+02
B( 8, 2)= -0.1830096E+02
B( 8, 3)= 0.1410044E+02
B( 8, 4)= -0.1499477E+02
B( 8, 5)= 0.2051605E+02
B( 8, 6)= -0.3904258E+02
B( 8, 7)= 0.1461175E+03
B( 8, 8)= -0.3027434E+03
B( 8, 9)= 0.2809078E+03
B( 8,10)= -0.9760654E+02
B( 9, 1)= -0.3250816E+02
B( 9, 2)= 0.5355405E+02
B( 9, 3)= -0.4020394E+02
B( 9, 4)= 0.4043721E+02
B( 9, 5)= -0.4964141E+02
B( 9, 6)= 0.7536884E+02
B( 9, 7)= -0.1554826E+03
B( 9, 8)= 0.6171044E+03
B( 9, 9)= -0.2113392E+04
B( 9,10)= 0.1604764E+04
B(10, 1)= -0.1440000E+03
B(10, 2)= 0.2368676E+03
B(10, 3)= -0.1765906E+03
B(10, 4)= 0.1750064E+03
B(10, 5)= -0.2088227E+03
B(10, 6)= 0.2994208E+03
B(10, 7)= -0.5398939E+03
B(10, 8)= 0.1371027E+04
B(10, 9)= -0.3677014E+04
B(10,10)= 0.2664000E+04

```

```
WRITE(7,2001)
```

```
2001 FORMAT(5X, '*****VALUES OF THE PARAMETERS FOR THIS RUN*****'./)
```

```
WRITE(7,5001)
```

```
5001 FORMAT(5X, '                                POSTFEED          PREFEED './)
```

```
WRITE(7,2002) PEM1, PEM2
```

```
2002 FORMAT(5X, 'PECLET NUMBER      =' ,2(3X, E14.7))
```

```
WRITE(7,2003) ALFA1, ALFA2
```

```
2003 FORMAT(5X, 'ALFA1, ALFA2      =' ,2(3X, E14.7))
```

```
WRITE(7,2004) BETA1, BETA2
```

```
2004 FORMAT(5X, 'BETA              =' ,2(3X, E14.7))
```

```
WRITE(7,2005) V1, V2
```

```
2005 FORMAT(5X, 'VELOCITY          =' ,2(3X, E14.7))
```

```
WRITE(7,2011)
```

```

WRITE(7,2010)
2010 FORMAT(5X,'*****END OF THE PARAMETERS FOR THIS RUN*****',/,/)
2011 FORMAT(5X,' ',/,/)
C *****
R=(A(1,1)-PEM1)*A(M2,M2) - A(1,M2)*A(M2,1)
R1=A(M2,1)/R
R2=(A(1,1)-PEM1)/R
R3=A(1,M2)/R
R4=A(M2,M2)/R
C
P=(A(1,1)-PEM2)*A(M2,M2) - A(1,M2)*A(M2,1)
P1=A(M2,1)/P
P2=(A(1,1)-PEM2)/P
P3=A(1,M2)/P
P4=A(M2,M2)/P
C *****
DO 23 I=2,M1
DO 22 J=2,M1
CHIA1(J,I)={ (B(J,I)-(PEM1+0.0 )*A(J,I)) + ((B(J,I)-(PEM1+ 0.0 )*
,A(J,I))*{R3*A(M2,1)-R4*A(1,1)}) + ((B(J,M2)-(PEM1+ 0.0 )*A(J,M2))
,*{R1*A(1,1)-R2*A(M2,1)}) - PEM1*ALFA1*(R1*A(1,1)-R2*A(M2,1))}
C
CHAZ2(J,I)={ (B(J,I)-(PEM2+ 0.0 )*A(J,I)) + ((B(J,I)-(PEM2+ 0.0 )*
,A(J,I))*{P3*A(M2,1)-P4*A(1,1)}) + ((B(J,M2)-(PEM2+ 0.0 )*A(J,M2))
,*{P1*A(1,1)-P2*A(M2,1)}) - PEM2*ALFA2*(P1*A(1,1)-P2*A(M2,1))}
22 CONTINUE
23 CONTINUE
C *****
C
CALL NEQNF (FCN, ERRREL, N, ITMAX, CGUESS, CA, FNORM)
C
SUM4=0.0
SUM5=0.0
DO 556 I=2,M1
SUM4=SUM4 + (P3*A(M2,I) - P4*A(1,I))*CA(I+M2)
556 SUM5=SUM5 + (P1*A(1,I) - P2*A(M2,I))*CA(I+M2)
CA2I= SUM4 - P4*PEM2*CHAZ2
CA2E= SUM5 + P1*PEM2*CHAZ2
C
CHAZ1=
,(V2*((P1*A(1,2)-P2*A(M2,2))*CA(2+M2))+
,(P1*A(1,3)-P2*A(M2,3))*CA(3+M2))+
,(P1*A(1,4)-P2*A(M2,4))*CA(4+M2))+
,(P1*A(1,5)-P2*A(M2,5))*CA(5+M2))+
,(P1*A(1,6)-P2*A(M2,6))*CA(6+M2))+
,(P1*A(1,7)-P2*A(M2,7))*CA(7+M2))+
,(P1*A(1,8)-P2*A(M2,8))*CA(8+M2))+
,(P1*A(1,9)-P2*A(M2,9))*CA(9+M2))+
,P1*PEM2*CHAZ2}
,+ (V1-V2))/V1
C
SUM6=0.0
SUM7=0.0
DO 456 I=2,M1
SUM6=SUM6 + (P3*A(M2,I) - P4*A(1,I))*CA(I+3*M2)

```

```

456 SUM7=SUM7 + (P1*A(1,1) - P2*A(M2,1))*CA(1+3*M2)
   CB2I= SUM6 - P4*PEM2*CHBZ2
   CR2E= SUM7 + P1*PEM2*CHBZ2
C
   CHBZ1=
   ,(V2*((P1*A(1,2)-P2*A(M2,2))*CA(2+3*M2)+
   ,(P1*A(1,3)-P2*A(M2,3))*CA(3+3*M2)+
   ,(P1*A(1,4)-P2*A(M2,4))*CA(4+3*M2)+
   ,(P1*A(1,5)-P2*A(M2,5))*CA(5+3*M2)+
   ,(P1*A(1,6)-P2*A(M2,6))*CA(6+3*M2)+
   ,(P1*A(1,7)-P2*A(M2,7))*CA(7+3*M2)+
   ,(P1*A(1,8)-P2*A(M2,8))*CA(8+3*M2)+
   ,(P1*A(1,9)-P2*A(M2,9))*CA(9+3*M2)+
   ,P1*PEM2*CHBZ2)
   ,+ (V1-V2))/V1
C
   SUM2=0.0
   SUM3=0.0
   DO 555 I=2,M1
   SUM2=SUM2 + (R3*A(M2,I) - R4*A(1,I))*CA(I)
555 SUM3=SUM3 + (R1*A(1,I) - R2*A(M2,I))*CA(I)
   CA1I= SUM2 - R4*PEM1*CHAZ1
   CA1E= SUM3 + R1*PEM1*CHAZ1
C
   SUM8=0.0
   SUM9=0.0
   DO 355 I=2,M1
   SUM8=SUM8 + (R3*A(M2,I) - R4*A(1,I))*CA(1+2*M2)
355 SUM9=SUM9 + (R1*A(1,I) - R2*A(M2,I))*CA(1+2*M2)
   CB1I= SUM8 - R4*PEM1*CHBZ1
   CB1E= SUM9 + R1*PEM1*CHBZ1
C
   WRITE(7,5003)
5003 FORMAT(4X,'          CONCA2          CONCB2          CONCA1          CONCB1
   ',/)
   WRITE(7,5002)
5002 FORMAT(4X,'XVALUE          PREFEED          POSTFEED
   ',/)
C
   WRITE(7,1006) X(1),1.*CA2I,1.*CB2I,1.*CA1I,1.*CB1I
   XARRAY(1)=X(1)
   CONCA1(1)=CA1I*1.
   CONCB1(1)=CB1I*1.
   CONCA2(1)=CA2I*1.
   CONCB2(1)=CB2I*1.
   DO 1005 I=2,M1
   WRITE(7,1006) X(I),1.*CA(1+M2),1.*CA(1+3*M2),1.*CA(I),
   ,1.*CA(1+2*M2)
   XARRAY(I)=X(I)
   CONCA1(I)=CA(I)*1.
   CONCB1(I)=CA(1+2*M2)*1.
   CONCA2(I)=CA(1+M2)*1.
   CONCB2(I)=CA(1+3*M2)*1.
1005 CONTINUE
   WRITE(7,1006) X(M2),1.*CA2E,1.*CB2E,1.*CA1E,1.*CB1E

```

```

XARRAY(M2)=X(M2)
CONCA1(M2)=CA1E*1.
CONCB1(M2)=CB1E*1.
CONCA2(M2)=CA2E*1.
CONCB2(M2)=CB2E*1.
1006 FORMAT(/,4X,F6.4,4(2X,F10.6))
F=1.0/((CONCA1(M2)*V1/5.0/(V1-V2))*100.)
IF(ACTIVE(1)) G(1)= 1.1*PURITY-CONCB1(M2)
IF(ACTIVE(2)) G(2)= CONCB1(M2)-0.9*PURITY
RETURN
END

C
C*****
C
SUBROUTINE FCN(CA,F,N)
INTEGER N
REAL CA(N),F(N)
COMMON/DATA/QA1M2,QB1M2,PEM1,ALFA1,BETA1,V1
COMMON/DATA/CHA22,CIBZ2,PEM2,ALFA2,BETA2,V2
COMMON/DATA/MM,EA,EB,GA,GB
COMMON A(30,30),B(30,30),X(50)
COMMON CIA1(50,50),CIA2(50,50)
C
MM=8
M1=MM+1
M2=MM+2
C
R=(A(1,1)-PEM1)*A(M2,M2) - A(1,M2)*A(M2,1)
R1=A(M2,1)/R
R2=(A(1,1)-PEM1)/R
R3=A(1,M2)/R
R4=A(M2,M2)/R
C
P=(A(1,1)-PEM2)*A(M2,M2) - A(1,M2)*A(M2,1)
P1=A(M2,1)/P
P2=(A(1,1)-PEM2)/P
P3=A(1,M2)/P
P4=A(M2,M2)/P
C *****
DO 23 I=2,M1
DO 22 J=2,M1
C
CHA1(J,I)={(B(J,I)-(PEM1+ 0.0 ))*A(J,I)}+{(B(J,I)-(PEM1+0.0 ))*
+A(J,I)}*(R3*A(M2,I)-R4*A(1,I)))+{(B(J,M2)-(PEM1+ 0.0 ))*A(J,M2)}
+*(R1*A(1,I)-R2*A(M2,I)))-PEM1*ALFA1*(R1*A(1,I)-R2*A(M2,I))
C
CHA2(J,I)={(B(J,I)-(PEM2+ 0.0 ))*A(J,I)}+{(B(J,I)-(PEM2+ 0.0 ))*
+A(J,I)}*(P3*A(M2,I)-P4*A(1,I)))+{(B(J,M2)-(PEM2+ 0.0 ))*A(J,M2)}
+*(P1*A(1,I)-P2*A(M2,I)))-PEM2*ALFA2*(P1*A(1,I)-P2*A(M2,I))
22 CONTINUE
23 CONTINUE
C
DO 800 J=2,M1
C
CA(1)= 0.0
CA(10)= 0.0

```

```

CA(11)= 0.0
CA(20)= 0.0
CA(21)= 0.0
CA(30)= 0.0
CA(31)= 0.0
CA(40)= 0.0
F(1)= 0.0
F(10)= 0.0
F(11)= 0.0
F(20)= 0.0
F(21)= 0.0
F(30)= 0.0
F(31)= 0.0
F(40)= 0.0

```

```

F(J)= CHA1(J,2)*CA(2)+CHA1(J,3)*CA(3)+CHA1(J,4)*CA(4)+
,CHA1(J,5)*CA(5)+CHA1(J,6)*CA(6)+CHA1(J,7)*CA(7)+CHA1(J,8)*
,CA(8)+CHA1(J,9)*CA(9)-PEM1*
,(((V2*((P1*A(1,2)-P2*A(M2,2))*CA(2+M2)+
,(P1*A(1,3)-P2*A(M2,3))*CA(3+M2)+
,(P1*A(1,4)-P2*A(M2,4))*CA(4+M2)+
,(P1*A(1,5)-P2*A(M2,5))*CA(5+M2)+
,(P1*A(1,6)-P2*A(M2,6))*CA(6+M2)+
,(P1*A(1,7)-P2*A(M2,7))*CA(7+M2)+
,(P1*A(1,8)-P2*A(M2,8))*CA(8+M2)+
,(P1*A(1,9)-P2*A(M2,9))*CA(9+M2)+
,P1*PEM2*CHAZ2)
,+ (V1-V2)/V1)*
,(R4*(B(J,1)-(PEM1+ 0.0 ))*
,A(J,1))-R1*(B(J,M2)-(PEM1+ 0.0 )*A(J,M2))+PEM1*ALFA1*R1))+PEM1*
,ALFA1*(1.0-BETA1*(EA+GA*CA(J)))*CA(J)+BETA1*PEM1*ALFA1*QA1M2

```

```

F(J+2*M2)= CHA1(J,2)*CA(2+2*M2)+CHA1(J,3)*CA(3+2*M2)+
,CHA1(J,4)*CA(4+2*M2)+CHA1(J,5)*CA(5+2*M2)+
,CHA1(J,6)*CA(6+2*M2)+CHA1(J,7)*CA(7+2*M2)+CHA1(J,8)*
,CA(8+2*M2)+CHA1(J,9)*CA(9+2*M2)-PEM1*
,(((V2*((P1*A(1,2)-P2*A(M2,2))*CA(2+3*M2)+
,(P1*A(1,3)-P2*A(M2,3))*CA(3+3*M2)+
,(P1*A(1,4)-P2*A(M2,4))*CA(4+3*M2)+
,(P1*A(1,5)-P2*A(M2,5))*CA(5+3*M2)+
,(P1*A(1,6)-P2*A(M2,6))*CA(6+3*M2)+
,(P1*A(1,7)-P2*A(M2,7))*CA(7+3*M2)+
,(P1*A(1,8)-P2*A(M2,8))*CA(8+3*M2)+
,(P1*A(1,9)-P2*A(M2,9))*CA(9+3*M2)+
,P1*PEM2*CHBZ2)
,+ (V1-V2)/V1)*
,(R4*(B(J,1)-(PEM1+ 0.0 ))*
,A(J,1))-R1*(B(J,M2)-(PEM1+ 0.0 )*A(J,M2))+PEM1*ALFA1*R1))+PEM1*
,ALFA1*(1.0-BETA1*(EB+GB*CA(J+2*M2)))*CA(J+2*M2)+BETA1*PEM1*ALFA1*
,QB1M2

```

```

F(J+M2)= CHA2(J,2)*CA(2+M2)+
,CHA2(J,3)*CA(3+M2)+CHA2(J,4)*CA(4+M2)+
,CHA2(J,5)*CA(5+M2)+CHA2(J,6)*CA(6+M2)+
,CHA2(J,7)*CA(7+M2)+CHA2(J,8)*CA(8+M2)+

```

```

, CHA2(J,9)*CA(9+M2)-PEM2*CHAZ2*(P1*(B(J,1)-(PEM2+ 0.0 )*
.A(J,1))-P1*(B(J,M2)-(PEM2+ 0.0 )*A(J,M2))+PEM2*ALFA2*P1)+PEM2*
,ALFA2*(1.0-BETA2*(EA+GA*CA(J+M2)))*CA(J+M2)+
, BETA2*PEM2*ALFA2*
C
, (QA1M2-(1.0/BETA1))*
C
, ((R1*A(1,2) - R2*A(M2,2))*CA(2)+
, (R1*A(1,3) - R2*A(M2,3))*CA(3)+
, (R1*A(1,4) - R2*A(M2,4))*CA(4)+
, (R1*A(1,5) - R2*A(M2,5))*CA(5)+
, (R1*A(1,6) - R2*A(M2,6))*CA(6)+
, (R1*A(1,7) - R2*A(M2,7))*CA(7)+
, (R1*A(1,8) - R2*A(M2,8))*CA(8)+
, (R1*A(1,9) - R2*A(M2,9))*CA(9)+
, (R1*PEM1*
, ((V2*((P1*A(1,2)-P2*A(M2,2))*CA(2+M2)+
, (P1*A(1,3)-P2*A(M2,3))*CA(3+M2)+
, (P1*A(1,4)-P2*A(M2,4))*CA(4+M2)+
, (P1*A(1,5)-P2*A(M2,5))*CA(5+M2)+
, (P1*A(1,6)-P2*A(M2,6))*CA(6+M2)+
, (P1*A(1,7)-P2*A(M2,7))*CA(7+M2)+
, (P1*A(1,8)-P2*A(M2,8))*CA(8+M2)+
, (P1*A(1,9)-P2*A(M2,9))*CA(9+M2)+
, P1*PEM2*CHAZ2)
, + (V1-V2)/V1)) -
C
, ((V2*
C
, ((P1*A(1,2) - P2*A(M2,2))*CA(2+M2)+
, (P1*A(1,3) - P2*A(M2,3))*CA(3+M2)+
, (P1*A(1,4) - P2*A(M2,4))*CA(4+M2)+
, (P1*A(1,5) - P2*A(M2,5))*CA(5+M2)+
, (P1*A(1,6) - P2*A(M2,6))*CA(6+M2)+
, (P1*A(1,7) - P2*A(M2,7))*CA(7+M2)+
, (P1*A(1,8) - P2*A(M2,8))*CA(8+M2)+
, (P1*A(1,9) - P2*A(M2,9))*CA(9+M2)+
, P1*PEM2*CHAZ2)
C
, + (V1-V2)/V1))
C
F(J+3*M2)= CHA2(J,2)*CA(2+3*M2)+
, CHA2(J,3)*CA(3+3*M2)+CHA2(J,4)*CA(4+3*M2)+
, CHA2(J,5)*CA(5+3*M2)+CHA2(J,6)*CA(6+3*M2)+
, CHA2(J,7)*CA(7+3*M2)+CHA2(J,8)*CA(8+3*M2)+
, CHA2(J,9)*CA(9+3*M2)-PEM2*CHBZ2*(P1*(B(J,1)-(PEM2+ 0.0 )*
, A(J,1))-P1*(B(J,M2)-(PEM2+ 0.0 )*A(J,M2))+PEM2*ALFA2*P1)+PEM2*
, ALFA2*(1.0-BETA2*(EB+GB*CA(J+3*M2)))*CA(J+3*M2)+
, BETA2*PEM2*ALFA2*
C
, (QB1M2-(1.0/BETA1))*
C
, ((R1*A(1,2) - R2*A(M2,2))*CA(2+2*M2)+
, (R1*A(1,3) - R2*A(M2,3))*CA(3+2*M2)+
, (R1*A(1,4) - R2*A(M2,4))*CA(4+2*M2)+

```



```

, (R1*A(1,5) - R2*A(M2,5))*CA(5+2*M2)+
, (R1*A(1,6) - R2*A(M2,6))*CA(6+2*M2)+
, (R1*A(1,7) - R2*A(M2,7))*CA(7+2*M2)+
, (R1*A(1,8) - R2*A(M2,8))*CA(8+2*M2)+
, (R1*A(1,9) - R2*A(M2,9))*CA(9+2*M2)+
, (R1*PEM1*
, ((V2*((P1*A(1,2)-P2*A(M2,2))*CA(2+3*M2)+
, (P1*A(1,3)-P2*A(M2,3))*CA(3+3*M2)+
, (P1*A(1,4)-P2*A(M2,4))*CA(4+3*M2)+
, (P1*A(1,5)-P2*A(M2,5))*CA(5+3*M2)+
, (P1*A(1,6)-P2*A(M2,6))*CA(6+3*M2)+
, (P1*A(1,7)-P2*A(M2,7))*CA(7+3*M2)+
, (P1*A(1,8)-P2*A(M2,8))*CA(8+3*M2)+
, (P1*A(1,9)-P2*A(M2,9))*CA(9+3*M2)+
, P1*PEM2*CHBZ2)
, + (V1-V2)/V1)) -
C
, ((V2*
C
, ((P1*A(1,2) - P2*A(M2,2))*CA(2+3*M2)+
, (P1*A(1,3) - P2*A(M2,3))*CA(3+3*M2)+
, (P1*A(1,4) - P2*A(M2,4))*CA(4+3*M2)+
, (P1*A(1,5) - P2*A(M2,5))*CA(5+3*M2)+
, (P1*A(1,6) - P2*A(M2,6))*CA(6+3*M2)+
, (P1*A(1,7) - P2*A(M2,7))*CA(7+3*M2)+
, (P1*A(1,8) - P2*A(M2,8))*CA(8+3*M2)+
, (P1*A(1,9) - P2*A(M2,9))*CA(9+3*M2)+
, P1*PEM2*CHBZ2)
C
, + (V1-V2)/V1)))
800 CONTINUE
RETURN
END

```

APPENDIX B

(Computer program for four-section configuration)

```

C *****
C
C OPTIMIZATION PROGRAM FOR MAXIMIZATION OF LESS STRONGLY ADSORBABLE *
C COMPONENT IN THE RAFFINATE FOR BOTH LINEAR AND NON-LINEAR SYSTEM *
C
C THIS PROGRAM IS DONE FOR THE OPTIMIZATION OF FOUR-SECTION *
C CONFIGURATION *
C *****
C
C -----
C | DATA STRUCTURE SECTION |
C -----
C
C INTEGER IBTYPE, IPRINT, IMM, MAXITN, ME, NN
C PARAMETER (IBTYPE=0, IPRINT=2, IMM=2, MAXITN=100, ME=0, NN=7)
C REAL FVALUE, XX(NN), XGUESS(NN), XLB(NN), XUB(NN), XSCALE(NN)
C COMMON/DATA/PEM1, ALFA1, BETA1, V1, ALAMB1
C COMMON/DATA/PEM2, ALFA2, BETA2, V2, ALAMB2
C COMMON/DATA/PEM3, ALFA3, BETA3, V3
C COMMON/DATA/PEM4, ALFA4, BETA4, V4, Q41M2, Q42M2
C COMMON/BALL/MODNUM
C COMMON/A/M2, XARRAY(12), CONCA1(12), CONCB1(12), CONCA2(12), CONCB2(12)
C COMMON/A/CONCA3(12), CONCB3(12), CONCA4(12), CONCB4(12)
C COMMON/AREA/PURITY, BANDWI
C DIMENSION YARRAY(12), ZARRAY(12), XXARRAY(12)
C EXTERNAL MODEL, NCONF, WRRRN
C
C XGUESS(1) = F IN ML/MIN
C XGUESS(2) = EL IN ML/MIN
C XGUESS(3) = TAU IN MINUTES
C XGUESS(4) = D IN CMS
C XGUESS(5) = CL IN CMS
C XGUESS(6) = E IN CMS
C XGUESS(7) = RAF IN CMS
C
C VALUES FOR FIXED D & L (LINEAR GLUCOSE-FRUCTOSE SYSTEM)
C
C DATA XGUESS/10., 65.42, 30.5, 5.1, 100., 16.8, 13.8/
C DATA XSCALE/7*1.0E0/
C DATA XLB /8.00, 60.42, 28.5, 5.10, 100., 15.8, 12.8/
C DATA XUB /13.0, 70.42, 34.5, 5.10, 100., 17.8, 14.8/
C DATA XGUESS/10., 72.42, 30.5, 5.1, 100., 16.8, 13.8/
C DATA XSCALE/7*1.0E0/
C DATA XLB /8., 72.42, 25.5, 5.1, 100., 15.8, 12.8/
C DATA XUB /13.0, 72.42, 32.5, 5.10, 100., 17.8, 14.8/
C
C VALUES FOR GENERAL CASES (LINEAR GLUCOSE-FRUCTOSE SYSTEM)
C
C DATA XGUESS/10., 65.42, 30.5, 5.1, 100., 16.8, 13.8/
C DATA XSCALE/7*1.0E0/
C DATA XLB /8., 60.42, 28.5, 4.90, 95., 15.8, 12.8/
C DATA XUB /13.0, 70.42, 32.5, 5.30, 105., 17.8, 14.8/
C
C FA=5.0 !GLUCOSE(LESS STRONGLY ADSORBABLE SPECIES)
C FB=5.0 !FRUCTOSE(MORE STRONGLY ADSORBABLE SPECIES)

```

```

C
C VALUES FOR FIXED D & L (NON-LINEAR MEA-MOH SYSTEM)
C LINEAR A (MOH) & NON-LINEAR B (MEA)
C
C DATA XGUESS/5.0,130.4,22.11,5.50,100.,44.0,13.7/
C DATA XSCALE/7*1.0E0/
C DATA XLB /2.0,120.4,18.11,5.50,100.,40.0,12.7/
C DATA XUB /10.0,140.4,28.11,5.50,100.,50.0,14.7/
C
C VALUES FOR GENERAL CASES (NON-LINEAR MEA-MOH SYSTEM)
C
C DATA XGUESS/5.0,130.4,22.11,5.50,100.,44.0,13.7/
C DATA XSCALE/7*1.0E0/
C DATA XLB /2.0,120.4,18.11,5.00,95.,40.0,12.7/
C DATA XUB /10.0,140.4,28.11,6.00,105.,50.0,14.7/
C
C FA=10.0 !MOH (LESS STRONGLY ADSORBABLE SPECIES)
C FB=20.0 !MEA (MORE STRONGLY ADSORBABLE SPECIES)
C
C INPUT THE MODEL NUMBER
WRITE(8,*)'INPUT THE MODEL NUMBER'
WRITE(8,*)'1 STANDS FOR THE TWO BED MODEL'
WRITE(8,*)'2 STANDS FOR THE FOUR BED MODEL'
READ(8,*)MODNUM
GO TO(30,40),MODNUM
30 WRITE(8,*)' *****'
WRITE(8,*)' * USING TWO BED MODEL *'
WRITE(8,*)' *****'
GO TO 50
40 WRITE(8,*)' *****'
WRITE(8,*)' * USING FOUR BED MODEL *'
WRITE(8,*)' *****'
50 CONTINUE
WRITE(8,*)' SPECIFY PURITY DESIRED '
READ(8,*)PURITY
401 CONTINUE
WRITE(8,*)MODNUM
C
CALL GUESS(NN,XGUESS,XLB,XUB)
CALL NCONF(MODEL,MMH,ME,NN,XGUESS,IBTYPE,XLB,XUB,XSCALE,IPRINT,MAX
@ITH,XX,FVALUE)
DO 95 I=1,M2
XXARRAY(I)=10.+2.*XARRAY(I)
ZARRAY(I)=7.+3.*XARRAY(I)
YARRAY(I)=4.+3.*XARRAY(I)
XARRAY(I)=4.*XARRAY(I)
95 CONTINUE
WRITE(8,*)' COLUMN CONCA1 CONCB1'
DO 100 I=1,M2
WRITE(8,96)XARRAY(I),CONCA1(I),CONCB1(I)
WRITE(6,*)XARRAY(I),CONCA1(I),CONCB1(I)
100 CONTINUE
WRITE(8,*)' COLUMN CONCA2 CONCB2'
DO 101 I=1,M2
WRITE(8,96)YARRAY(I),CONCA2(I),CONCB2(I)

```

```

WRITE(6,*)YARRAY(1),CONCA2(1),CONCB2(1)
101 CONTINUE
WRITE(8,*)' COLUMN CONCA3 CONCB3'
DO 103 I=1,M2
WRITE(8,96)ZARRAY(1),CONCA3(1),CONCB3(1)
WRITE(6,*)ZARRAY(1),CONCA3(1),CONCB3(1)
103 CONTINUE
WRITE(8,*)' COLUMN CONCA4 CONCB4'
DO 104 I=1,M2
WRITE(8,96)XXARRAY(1),CONCA4(1),CONCB4(1)
WRITE(6,*)XXARRAY(1),CONCA4(1),CONCB4(1)
104 CONTINUE
96 FORMAT(5(2X,F6.3))

PHI=CONCA3(M2)/FA*100.
WRITE(8,97)PHI
WRITE(6,97)PHI
97 FORMAT(' CONCENTRATION RATIO =',F6.1,'%')
REC=((CONCA3(M2))*(V3-V4))/FA/(V3-V2)*100.
WRITE(8,91)REC
WRITE(6,91)REC
91 FORMAT(' RECOVERY =',F6.1,'%')
PUR=(CONCA3(M2)/(CONCA3(M2)+CONCB3(M2)))*100.
WRITE(8,92)PUR
WRITE(6,92)PUR
92 FORMAT(' PURITY =',F6.1,'%')
WRITE(8,93)V1,V2,V3,V4
WRITE(6,93)V1,V2,V3,V4
93 FORMAT(5X,4(2X,F6.2))
C
500 CONTINUE
CALL WRRRN('THE SOLUTION IS',NN,1,XX,NN,0)
1000 STOP
END
C *****
C * GUESS SUBROUTINE *
C *****

SUBROUTINE GUESS(NN,XX,XLB,XUB)
INTEGER NUMB
DIMENSION XX(NN),XLB(NN),XUB(NN)
13 WRITE (8,*) ' '
WRITE (8,*) ' '
WRITE (8,*) ' '
WRITE (8,*) ('-',I=1,60)
WRITE (8,11)'*', 'COEF. NO.', '*', ' VALUE', '*', 'XLB ', '*', 'XUB ', '*'
11 FORMAT(A,1X,A,1X,A,5X,A,5X,A,5X,A,7X,A,5X,A,6X,A)
WRITE (8,*) ('-',I=1,60)
WRITE (8,12) '*', '1', '*', XX(1), '*', XLB(1), '*', XUB(1), '*'
12 FORMAT (A,4X,A,5X,A,2X,F10.4,4X,A,2X,F10.4,4X,A,2X,F10.4,3X,A)
WRITE (8,*) ('-',I=1,60)
WRITE (8,12) '*', '2', '*', XX(2), '*', XLB(2), '*', XUB(2), '*'
WRITE (8,*) ('-',I=1,60)
WRITE (8,12) '*', '3', '*', XX(3), '*', XLB(3), '*', XUB(3), '*'
WRITE (8,*) ('-',I=1,60)

```

```

WRITE (8,12) ' *', '4', ' *', XX(4), ' *', XLB(4), ' *', XUB(4), ' *'
WRITE (8,*) ('-', I=1,60)
WRITE (8,12) ' *', '5', ' *', XX(5), ' *', XLB(5), ' *', XUB(5), ' *'
WRITE (8,*) ('-', I=1,60)
WRITE (8,12) ' *', '6', ' *', XX(6), ' *', XLB(6), ' *', XUB(6), ' *'
WRITE (8,*) ('-', I=1,60)
WRITE (8,12) ' *', '7', ' *', XX(7), ' *', XLB(7), ' *', XUB(7), ' *'
WRITE (8,*) ('-', I=1,60)
WRITE(8,*) ' * PRESS 1 IF YOU WANT TO CHANGE XLB'
WRITE(8,*) ' * PRESS 2 IF YOU WANT TO CHANGE XUB'
WRITE(8,*) ' * PRESS 3 IF YOU WANT TO CHANGE XX VALUES'
WRITE(8,*) ' * PRESS 4 IF YOU WANT TO RUN THE OPTIMIZATION'
READ(8,*) NUMB
IF (NUMB.GE.4) THEN
WRITE(8,25)
25 FORMAT(2X, 'THE VALUES ARE THE SAME ')
ENDIF
IF (NUMB.EQ.1) THEN
WRITE(8,26)
26 FORMAT(1X, 'ENTER THE NEW VALUES OF XLB')
READ(8,*) XLB(1), XLB(2), XLB(3), XLB(4), XLB(5), XLB(6), XLB(7)
WRITE (8,*)
WRITE (8,*)
WRITE (8,*)
WRITE (8,*)
GOTO 13
ENDIF
IF (NUMB.EQ.2) THEN
WRITE(8,27)
27 FORMAT(1X, 'ENTER THE NEW VALUES OF XUB')
READ(8,*) XUB(1), XUB(2), XUB(3), XUB(4), XUB(5), XUB(6), XUB(7)
WRITE (8,*)
WRITE (8,*)
WRITE (8,*)
WRITE (8,*)
GOTO 13
ENDIF
IF (NUMB.EQ.3) THEN
WRITE(8,28)
28 FORMAT(1X, 'ENTER THE NEW VALUES OF XX VALUES')
READ(8,*) XX(1), XX(2), XX(3), XX(4), XX(5), XX(6), XX(7)
WRITE (8,*)
WRITE (8,*)
WRITE (8,*)
WRITE (8,*)
GOTO 13
ENDIF
RETURN
END

```

```

C:
C: SUBROUTINE TO SOLVE THE MODEL EQUATIONS
C:
C: SUBROUTINE MODEL(MMM,ME,NN,XX,ACTIVE,F,G)
C:

```

```

*****
C
C   N HAS BEEN USED AS A PARAMETER
C
C   N=96
C
*****
C
C   INTEGER ITMAX,N,MMM,ME,NN
C   PARAMETER(N=96)
C   REAL ERRREL,L,LS1,LS2,LS3,LS4,XX(*),F,G(*)
C   LOGICAL ACTIVE(*)
C   INTEGER K,NOUT
C   REAL FNORM,CA(N),CGUESS(N)
C   COMMON/DATA/PEM1,ALFA1,BETA1,V1,ALAMBA
C   COMMON/DATA/PEM2,ALFA2,BETA2,V2,ALAMBB
C   COMMON/DATA/PEM3,ALFA3,BETA3,V3
C   COMMON/DATA/PEM4,ALFA4,BETA4,V4,QA4M2,QB4M2
C   COMMON A(30,30),B(30,30),X(50)
C   COMMON CHA1(50,50),CHA2(50,50)
C   COMMON CHA3(50,50),CHA4(50,50)
C   COMMON/A/M2,XARRAY(12),CONCA1(12),CONCB1(12),CONCA2(12),CONCB2(12)
C   COMMON/A/CONCA3(12),CONCB3(12),CONCA4(12),CONCB4(12)
C   COMMON/DATA/MM,EA,EB,GA,GB,QA10,QB10,CKR,PHA1
C   COMMON/AREA/PURITY,BANDWI
C   EXTERNAL FCN,NEQNF
C
C   FEED COMPOSITION FOR GLUCOSE-FRUCTOSE SYSTEM
C
C   FA=5.0    !GLUCOSE
C   FB=5.0    !FRUCTOSE
C
C   *****
C   FEED COMPOSITION FOR MEA-MOH SYSTEM
C   FA=10.0  !MOH
C   FB=20.0  !MEA
C   *****
C   CKR=0.21
C   CKR=0.63    ! FOR MEA-MOH SYSTEM
C   ESP=0.4
C   D=5.1
C   D=5.5      ! FOR MEA-MOH SYSTEM
C   AREA=ATAN(1.0)*XX(4)**2
C   XX(2)=65.42
C   XX(2)=130.4 ! FOR MEA-MOH SYSTEM
C   E=16.8
C   XX(6)=16.8
C   XX(6)=44.0 ! FOR MEA-MOH SYSTEM
C   XX(1)=10.0
C   XX(1)=5.0  ! FOR MEA-MOH SYSTEM
C   RAF=13.8
C   XX(7)=13.8
C   XX(7)=13.7 ! FOR MEA-MOH SYSTEM
C
C   LS1=4.*XX(5)

```

```

LS2=3.*XX(5)
LS3=3.*XX(5)
LS4=2.*XX(5)
U=XX(5)/XX(3)
C
V1=XX(2)/ESP/AREA-U
V2=(XX(2)-XX(6))/ESP/AREA-U
V3=(XX(2)-XX(6)+XX(1))/ESP/AREA-U
V4=(XX(2)-XX(6)+XX(1)-XX(7))/ESP/AREA-U
C
PEM1=V1*LS1/5./{(U+V1)}
PEM2=V2*LS2/5./{(U+V2)}
PEM3=V3*LS3/5./{(U+V3)}
PEM4=V4*LS4/5./{(U+V4)}
C
ALFA1=CKR*LS1/U
ALFA2=CKR*LS2/U
ALFA3=CKR*LS3/U
ALFA4=CKR*LS4/U
C
BETA1=(1.5*U)/V1
BETA2=(1.5*U)/V2
BETA3=(1.5*U)/V3
BETA4=(1.5*U)/V4
C
EQUILIBRIUM CONSTANT FOR GLUCOSE-FRUCTOSE SYSTEM WHERE
C A: GLUCOSE & B: FRUCTOSE
C
EA=0.50 !GLUCOSE
EB=0.88 !FRUCTOSE
C
C*****
C
EQUILIBRIUM CONSTANT FOR MEA-MOH SYSTEM WHERE
C A: MEA & B: MOH
C
EA=0.63 !A:MOH
EB=1.24 !B:MEA
C *****
GA=0.0
GB=0.0
ALAMBA=0.00
ALAMBB=0.435
ALAMBB=0.00 !FOR GLUCOSE-FRUCTOSE SYSTEM
PHAI=(1.0-ALAMBA-ALAMBB)
C ***** END OF PARAMETERS *****
QA10=0.001E-00
QB10=0.001E-00
C
C*****
C
ITER=1
IMAX=30
MM=10
NI=MM+1

```



```

M2=MM+2
DO 1 I=1,N
CGUESS(I)=0.5
CGUESS(I)=0.0 !FOR MEA-NOH SYSTEM
1 CONTINUE
***** IMSL VARIABLES *****
ERRREL=0.0001
ITMAX=100
***** INPUT FOR X VALUE AND A & B MATRIX *****
*
* THIS VALUES IS THE SAME AS PROG_A GIVEN IN APPENDIX A *
*
*****
P=(A(1,1)-PEM1)*A(M2,M2) - A(1,M2)*A(M2,1)
P1=A(M2,1)/P
P2=(A(1,1)-PEM1)/P
P3=A(1,M2)/P
P4=A(M2,M2)/P
Q=(A(1,1)-PEM2)*A(M2,M2) - A(1,M2)*A(M2,1)
Q1=A(M2,1)/Q
Q2=(A(1,1)-PEM2)/Q
Q3=A(1,M2)/Q
Q4=A(M2,M2)/Q
R=(A(1,1)-PEM3)*A(M2,M2) - A(1,M2)*A(M2,1)
R1=A(M2,1)/R
R2=(A(1,1)-PEM3)/R
R3=A(1,M2)/R
R4=A(M2,M2)/R
S=(A(1,1)-PEM4)*A(M2,M2) - A(1,M2)*A(M2,1)
S1=A(M2,1)/S
S2=(A(1,1)-PEM4)/S
S3=A(1,M2)/S
S4=A(M2,M2)/S
*****
DO 23 I=2,M1
DO 22 J=2,M1
CHA1(J,I)={(B(J,I)-(PEM1+ 0.0 )*A(J,I))+((B(J,1)-(PEM1+ 0.0 )*
,A(J,1))*(P3*A(M2,1)-P4*A(1,1)))+(B(J,M2)-(PEM1+ 0.0 )*A(J,M2))
,*(P1*A(1,1)-P2*A(M2,1)))-PEM1*ALFA1*(P1*A(1,1)-P2*A(M2,1))}
CHA2(J,I)={(B(J,I)-(PEM2+ 0.0 )*A(J,I))+((B(J,1)-(PEM2+ 0.0 )*
,A(J,1))*(Q3*A(M2,1)-Q4*A(1,1)))+(B(J,M2)-(PEM2+ 0.0 )*A(J,M2))
,*(Q1*A(1,1)-Q2*A(M2,1)))-PEM2*ALFA2*(Q1*A(1,1)-Q2*A(M2,1))}
CHA3(J,I)={(B(J,I)-(PEM3+ 0.0 )*A(J,I))+((B(J,1)-(PEM3+ 0.0 )*
,A(J,1))*(R3*A(M2,1)-R4*A(1,1)))+(B(J,M2)-(PEM3+ 0.0 )*A(J,M2))

```

```

      *(R1*A(1,1)-R2*A(M2,1))-PEM3*ALFA3*(R1*A(1,1)-R2*A(M2,1))
C
      CHA1(J,1)=((B(J,1)-(PEM4+ 0.0 )*A(J,1))+((B(J,1)-(PEM4+ 0.0 )*
      ,A(J,1))*(S3*A(M2,1)-S4*A(1,1)))+(B(J,M2)-(PEM4+ 0.0 )*A(J,M2))
      ,(S1*A(1,1)-S2*A(M2,1)))-PEM4*ALFA4*(S1*A(1,1)-S2*A(M2,1))
C22 CONTINUE
C23 CONTINUE
C
C *****
C
      CALL NEQNF(FCN,ERRREL,N,ITMAX,CGUESS,CA, FNORM)
C
C
      CHAZ1=(CA(83)*V4/V1)
      SUM2=0.0
      SUM3=0.0
      DO 555 I=2,M1
      SUM2=SUM2 + (P3*A(M2,1) - P4*A(1,1))*CA(I)
555 SUM3=SUM3 + (P1*A(1,1) - P2*A(M2,1))*CA(I)
      CA1I= SUM2 - P4*PEM1*CHAZ1
      CA1E= SUM3 + P1*PEM1*CHAZ1
C
      CHBZ1=(CA(95)*V4/V1)
      SUM8=0.0
      SUM9=0.0
      DO 355 I=2,M1
      SUM8=SUM8 + (P3*A(M2,1) - P4*A(1,1))*CA(I+M2)
355 SUM9=SUM9 + (P1*A(1,1) - P2*A(M2,1))*CA(I+M2)
      CB1I= SUM8 - P4*PEM1*CHBZ1
      CB1E= SUM9 + P1*PEM1*CHBZ1
C
      CHAZ2=CA(11)
      SUMA=0.0
      SUMB=0.0
      DO 556 I=2,M1
      SUMA=SUMA + (Q3*A(M2,1) - Q4*A(1,1))*CA(I+2*M2)
556 SUMB=SUMB + (Q1*A(1,1) - Q2*A(M2,1))*CA(I+2*M2)
      CA2I= SUMA - Q4*PEM2*CHAZ2
      CA2E= SUMB + Q1*PEM2*CHAZ2
C
      CHBZ2=CA(23)
      SUM6=0.0
      SUM7=0.0
      DO 456 I=2,M1
      SUM6=SUM6 + (Q3*A(M2,1) - Q4*A(1,1))*CA(I+3*M2)
456 SUM7=SUM7 + (Q1*A(1,1) - Q2*A(M2,1))*CA(I+3*M2)
      CB2I= SUM6 - Q4*PEM2*CHBZ2
      CB2E= SUM7 + Q1*PEM2*CHBZ2
C
      CHAZ3=((V2*CA(35)+(V3-V2))/V3)
      SUM10=0.0
      SUM11=0.0
      DO 666 I=2,M1
      SUM10=SUM10 + (R3*A(M2,1) - R4*A(1,1))*CA(I+4*M2)
666 SUM11=SUM11 + (R1*A(1,1) - R2*A(M2,1))*CA(I+4*M2)

```

```

CA3I= SUM10 - R4*PEM3*CHAZ3
CA3E= SUM11 + R1*PEM3*CHAZ3
CHBZ3=((V2*CA(47)+(V3-V2))/V3)
SUM13=0.0
SUM14=0.0
DO 777 I=2,M1
SUM13=SUM13 + (R3*A(M2,I) - R4*A(1,I))*CA(1+5*M2)
777 SUM14=SUM14 + (R1*A(1,I) - R2*A(M2,I))*CA(1+5*M2)
CB3I= SUM13 - R4*PEM3*CHBZ3
CB3E= SUM14 + R1*PEM3*CHBZ3
C
CHAZ4=CA(59)
SUM15=0.0
SUM16=0.0
DO 888 I=2,M1
SUM15=SUM15 + (S3*A(M2,I) - S4*A(1,I))*CA(1+6*M2)
888 SUM16=SUM16 + (S1*A(1,I) - S2*A(M2,I))*CA(1+6*M2)
CA4I= SUM15 - S4*PEM4*CHAZ4
CA4E= SUM16 + S1*PEM4*CHAZ4
C
CHBZ4=CA(71)
SUM17=0.0
SUM18=0.0
DO 999 I=2,M1
SUM17=SUM17 + (S3*A(M2,I) - S4*A(1,I))*CA(1+7*M2)
999 SUM18=SUM18 + (S1*A(1,I) - S2*A(M2,I))*CA(1+7*M2)
CB4I= SUM17 - S4*PEM4*CHBZ4
CB4E= SUM18 + S1*PEM4*CHBZ4
C
C ITERATION FOR THE INTERNAL LOOP
C
ERRORA=QA4M2-QA10
ERRORB=QB4M2-QB10
IF(ITER.GT.1)GO TO 342
FOLDA=ERRORA
FOLDB=ERRORB
342 CONTINUE
ITER= ITER + 1
IF(ABS(ERRORA).LE.0.001.AND.ABS(ERRORB).LE.0.001)GO TO 303
IF(ITER.GT.2)GO TO 341
QA10=0.0015
QB10=0.0015
GO TO 23
341 CONTINUE
IF(ITER.GT.3)GO TO 343
DERIVA=(ERRORA-FOLDA)/(0.0005)
DERIVB=(ERRORB-FOLDB)/(0.0005)
343 CONTINUE
IF(ITER.GT.IMAX) GO TO 203
QA10N=QA10-(ERRORA/DERIVA)
QB10N=QB10-(ERRORB/DERIVB)
344 CONTINUE
QA10=QA10N
QB10=QB10N
GO TO 23

```

```

203 CONTINUE
    WRITE(7,*) 'SOLUTION DID NOT CONVERGE'
303 CONTINUE
C
C ITERATION COMPLETED HERE
C
    WRITE(7,5003)
5003 FORMAT(4X, '          CONCA1          CONCB1          CONCA2          CONCB2
          ,',/)
C
    WRITE(7,1006) X(1), FA*CA11, FB*CB11, FA*CA21, FB*CB21
    XARRAY(1)=X(1)
    CONCA1(1)=CA11*FA
    CONCB1(1)=CB11*FB
    CONCA2(1)=CA21*FA
    CONCB2(1)=CB21*FB
    DO 1005 I=2,M1
    WRITE(7,1006) X(I), FA*CA(I), FB*CA(I+1*M2), FA*CA(I+2*M2),
    , FB*CA(I+3*M2)
    XARRAY(I)=X(I)
    CONCA1(I)=CA(I)*FA
    CONCB1(I)=CA(I+1*M2)*FB
    CONCA2(I)=CA(I+2*M2)*FA
    CONCB2(I)=CA(I+3*M2)*FB
1005 CONTINUE
    WRITE(7,1006) X(M2), FA*CA1E, FB*CB1E, FA*CA2E, FB*CB2E
    XARRAY(M2)=X(M2)
    CONCA1(M2)=CA1E*FA
    CONCB1(M2)=CB1E*FB
    CONCA2(M2)=CA2E*FA
    CONCB2(M2)=CB2E*FB
C
    WRITE(7,5004)
5004 FORMAT(4X, '          CONCA3          CONCB3          CONCA4          CONCB4
          ,',/)
    WRITE(7,1006) X(1), FA*CA31, FB*CB31, FA*CA41, FB*CB41
    XARRAY(1)=X(1)
    CONCA3(1)=CA31*FA
    CONCB3(1)=CB31*FB
    CONCA4(1)=CA41*FA
    CONCB4(1)=CB41*FB
    DO 2015 I=2,M1
    WRITE(7,1006) X(I), FA*CA(I+4*M2), FB*CA(I+5*M2), FA*CA(I+6*M2),
    , FB*CA(I+7*M2)
    XARRAY(I)=X(I)
    CONCA3(I)=CA(I+4*M2)*FA
    CONCB3(I)=CA(I+5*M2)*FB
    CONCA4(I)=CA(I+6*M2)*FA
    CONCB4(I)=CA(I+7*M2)*FB
2015 CONTINUE
    WRITE(7,1006) X(M2), FA*CA3E, FB*CB3E, FA*CA4E, FB*CB4E
    XARRAY(M2)=X(M2)
    CONCA3(M2)=CA3E*FA
    CONCB3(M2)=CB3E*FB
    CONCA4(M2)=CA4E*FA

```

```

      CONCB4(M2)=CB4E*FB
1006 FORMAT(/,1X,F6.4,1(2X,F10.6))
C:
C: DEFINING OPTIMIZATION FUNCTION & CONSTRAINTS HERE
C:
      F=1.0/(((CONCA3(M2))*(V3-V4))/FA/(V3-V2)*100.0)
      IF(ACTIVE(1)) G(1)=1.1*PURITY-CONCB3(M2)
      IF(ACTIVE(2)) G(2)=CONCB3(M2)-0.90*PURITY
C:
      WRITE(7,2007)QA10,QA4M2,QB10,QB4M2
2007 FORMAT(5X,1(3X,E14.7))
      RETURN
      END
C:
      SUBROUTINE FCN(CA,F,N)
      INTEGER N
      REAL CA(N),F(N)
      COMMON/DATA/PEM1,ALFA1,BETA1,V1,ALAMBA
      COMMON/DATA/PEM2,ALFA2,BETA2,V2,ALAMBB
      COMMON/DATA/PEM3,ALFA3,BETA3,V3
      COMMON/DATA/PEM4,ALFA4,BETA4,V4,QA4M2,QB4M2
      COMMON A(30,30),B(30,30),X(50)
      COMMON CHA1(50,50),CHA2(50,50)
      COMMON CHA3(50,50),CHA4(50,50)
      COMMON/DATA/MM,EA,EB,GA,GB,QA10,QB10,CKR,PIA1
C:
C: MM=10
      M1=MM+1
      M2=MM+2
C:
      P=(A(1,1)-PEM1)*A(M2,M2) - A(1,M2)*A(M2,1)
      P1=A(M2,1)/P
      P2=(A(1,1)-PEM1)/P
      P3=A(1,M2)/P
      P4=A(M2,M2)/P
C:
      Q=(A(1,1)-PEM2)*A(M2,M2) - A(1,M2)*A(M2,1)
      Q1=A(M2,1)/Q
      Q2=(A(1,1)-PEM2)/Q
      Q3=A(1,M2)/Q
      Q4=A(M2,M2)/Q
C:
      R=(A(1,1)-PEM3)*A(M2,M2) - A(1,M2)*A(M2,1)
      R1=A(M2,1)/R
      R2=(A(1,1)-PEM3)/R
      R3=A(1,M2)/R
      R4=A(M2,M2)/R
C:
      S=(A(1,1)-PEM4)*A(M2,M2) - A(1,M2)*A(M2,1)
      S1=A(M2,1)/S
      S2=(A(1,1)-PEM4)/S
      S3=A(1,M2)/S
      S4=A(M2,M2)/S
C:
C: *****

```

DO 23 I=2,M1
DO 22 J=2,M1

CHA1(J,I)={(B(J,I)-(PEM1+ 0.0)*A(J,I))+((B(J,I)-(PEM1+ 0.0)*
A(J,I))*{P3*A(M2,I)-P4*A(1,I)}))+((B(J,M2)-(PEM1+ 0.0)*A(J,M2))
*(P1*A(1,I)-P2*A(M2,I)))-PEM1*ALFA1*(P1*A(1,I)-P2*A(M2,I))}

CHA2(J,I)={(B(J,I)-(PEM2+ 0.0)*A(J,I))+((B(J,I)-(PEM2+ 0.0)*
A(J,I))*{Q3*A(M2,I)-Q4*A(1,I)}))+((B(J,M2)-(PEM2+ 0.0)*A(J,M2))
*(Q1*A(1,I)-Q2*A(M2,I)))-PEM2*ALFA2*(Q1*A(1,I)-Q2*A(M2,I))}

CHA3(J,I)={(B(J,I)-(PEM3+ 0.0)*A(J,I))+((B(J,I)-(PEM3+ 0.0)*
A(J,I))*{R3*A(M2,I)-R4*A(1,I)}))+((B(J,M2)-(PEM3+ 0.0)*A(J,M2))
*(R1*A(1,I)-R2*A(M2,I)))-PEM3*ALFA3*(R1*A(1,I)-R2*A(M2,I))}

CHA4(J,I)={(B(J,I)-(PEM4+ 0.0)*A(J,I))+((B(J,I)-(PEM4+ 0.0)*
A(J,I))*{S3*A(M2,I)-S4*A(1,I)}))+((B(J,M2)-(PEM4+ 0.0)*A(J,M2))
*(S1*A(1,I)-S2*A(M2,I)))-PEM4*ALFA4*(S1*A(1,I)-S2*A(M2,I))}

22 CONTINUE

23. CONTINUE

DO 800 J=2,M1

CA(1)= 0.0

CA(12)= 0.0

CA(13)= 0.0

CA(24)= 0.0

CA(25)= 0.0

CA(36)= 0.0

CA(37)= 0.0

CA(48)= 0.0

CA(49)= 0.0

CA(60)= 0.0

CA(61)= 0.0

CA(72)= 0.0

CA(73)= 0.0

CA(84)= 0.0

CA(85)= 0.0

CA(96)= 0.0

F(1)= 0.0

F(12)= 0.0

F(13)= 0.0

F(24)= 0.0

F(25)= 0.0

F(36)= 0.0

F(37)= 0.0

F(48)= 0.0

F(49)= 0.0

F(60)= 0.0

F(61)= 0.0

F(72)= 0.0

F(73)= 0.0

F(84)= 0.0

F(85)= 0.0

```

F(96)= 0.0
QA4M2=
,(QA10 + (1.0/BETA1)*(CA(11) - (CA(83)*V4/V1))+
,(1.0/BETA2)*(CA(35) - (CA(11))))+
,(1.0/BETA3)*(CA(59) - ((V2*CA(35)+(V3-V2))/V3))+
,(1.0/BETA4)*(CA(83)-CA(59)))
QB4M2=
,(QB10 + (1.0/BETA1)*(CA(23) - (CA(95)*V4/V1))+
,(1.0/BETA2)*(CA(47) - (CA(23))))+
,(1.0/BETA3)*(CA(71) - ((V2*CA(47)+(V3-V2))/V3))+
,(1.0/BETA4)*(CA(95)-CA(71)))
C
C *****BED1*****
F(J)= CHA1(J,2)*CA(2)+CHA1(J,3)*CA(3)+CHA1(J,4)*CA(4)+
,CHA1(J,5)*CA(5)+CHA1(J,6)*CA(6)+CHA1(J,7)*CA(7)+CHA1(J,8)*
,CA(8)+CHA1(J,9)*CA(9)+
,CHA1(J,10)*CA(10)+CHA1(J,11)*CA(11)-PEM1*
,(CA(83)*V4/V1)*
,(P4*(B(J,1)-(PEM1+ 0.0 ))*A(J,1))
,-P1*(B(J,M2)-(PEM1+0.0 ))*A(J,M2))+PEM1*ALFA1*P1)+PEM1*ALFA1*
,(1.0-BETA1*(EA*
,(1.0 / (1.+ ALAMBA*(CA(J)-1.) + 0.0 *(CA(J+1*M2)-1.)))
,))*CA(J)+BETA1*PEM1*ALFA1*
,(QA10 + (1.0/BETA1)*(CA(11) - (CA(83)*V4/V1)))
C
F(J+1*M2)= CHA1(J,2)*CA(2+1*M2)+CHA1(J,3)*CA(3+1*M2)+
,CHA1(J,4)*CA(4+1*M2)+CHA1(J,5)*CA(5+1*M2)+
,CHA1(J,6)*CA(6+1*M2)+CHA1(J,7)*CA(7+1*M2)+CHA1(J,8)*
,CA(8+1*M2)+CHA1(J,9)*CA(9+1*M2)+
,CHA1(J,10)*CA(10+1*M2)+CHA1(J,11)*CA(11+1*M2)-PEM1*
,(CA(95)*V4/V1)*
,(P4*(B(J,1)-(PEM1+ 0.0 ))*A(J,1))
,-P1*(B(J,M2)-(PEM1+0.0 ))*A(J,M2))+PEM1*ALFA1*P1)+PEM1*ALFA1*
,(1.0-BETA1*(EB*
,(PHA1/(1.+ ALAMBA*(CA(J)-1.) + ALAMBB*(CA(J+1*M2)-1.)))
,))*CA(J+1*M2)+BETA1*PEM1*ALFA1*
,(QB10 + (1.0/BETA1)*(CA(23) - (CA(95)*V4/V1)))
C
C *****BED2*****
F(J+2*M2)= CHA2(J,2)*CA(2+2*M2)+CHA2(J,3)*CA(3+2*M2)+
,CHA2(J,4)*CA(4+2*M2)+CHA2(J,5)*CA(5+2*M2)+
,CHA2(J,6)*CA(6+2*M2)+CHA2(J,7)*CA(7+2*M2)+CHA2(J,8)*
,CA(8+2*M2)+CHA2(J,9)*CA(9+2*M2)+
,CHA2(J,10)*CA(10+2*M2)+CHA2(J,11)*CA(11+2*M2)-PEM2*
,(CA(11))*
,(Q4*(B(J,1)-(PEM2+ 0.0 ))*A(J,1))
,-Q1*(B(J,M2)-(PEM2+0.0 ))*A(J,M2))+PEM2*ALFA2*Q1)+PEM2*ALFA2*
,(1.0-BETA2*(EA*
,(1.0 / (1.+ ALAMBA*(CA(J+2*M2)-1.) + 0.0 *(CA(J+3*M2)-1.)))
,))*CA(J+2*M2)+BETA2*PEM2*ALFA2*
,(QA10 + (1.0/BETA1)*(CA(11) - (CA(83)*V4/V1))+
,(1.0/BETA2)*(CA(35) - (CA(11))))
C
F(J+3*M2)= CHA2(J,2)*CA(2+3*M2)+CHA2(J,3)*CA(3+3*M2)+
,CHA2(J,4)*CA(4+3*M2)+CHA2(J,5)*CA(5+3*M2)+

```

```

, CHA2(J,6)*CA(6+3*M2)+CHA2(J,7)*CA(7+3*M2)+CHA2(J,8)*
, CA(8+3*M2)+CHA2(J,9)*CA(9+3*M2)+
, CHA2(J,10)*CA(10+3*M2)+CHA2(J,11)*CA(11+3*M2)-PEM2*
, (CA(23))*
, (Q4*(B(J,1)-(PEM2+ 0.0 )*A(J,1))
, -Q1*(B(J,M2)-(PEM2+0.0 )*A(J,M2))+PEM2*ALFA2*Q1)+PEM2*ALFA2*
, (1.0-BETA2*(EB*
, (PHA1/(1.+ ALAMBA*(CA(J+2*M2)-1.) + ALAMBB*(CA(J+3*M2)-1.)))
, ))*CA(J+3*M2)+BETA2*PEM2*ALFA2*
, (QB10 + (1.0/BETA1)*(CA(23) - (CA(95)*V4/V1))+
, (1.0/BETA2)*(CA(47) - (CA(23))))
C: ****BED3*****
F(J+4*M2)= CHA3(J,2)*CA(2+4*M2)+CHA3(J,3)*CA(3+4*M2)+
, CHA3(J,4)*CA(4+4*M2)+CHA3(J,5)*CA(5+4*M2)+
, CHA3(J,6)*CA(6+4*M2)+CHA3(J,7)*CA(7+4*M2)+CHA3(J,8)*
, CA(8+4*M2)+CHA3(J,9)*CA(9+4*M2)+
, CHA3(J,10)*CA(10+4*M2)+CHA3(J,11)*CA(11+4*M2)-PEM3*
, ((V2*CA(35)+(V3-V2))/V3)*
, (R4*(B(J,1)-(PEM3+ 0.0 )*A(J,1))
, -R1*(B(J,M2)-(PEM3+0.0 )*A(J,M2))+PEM3*ALFA3*R1)+PEM3*ALFA3*
, (1.0-BETA3*(EA*
, (1.0/(1.+ ALAMBA*(CA(J+4*M2)-1.) + 0.0 *(CA(J+5*M2)-1.)))
, ))*CA(J+4*M2)+BETA3*PEM3*ALFA3*
, (QA10 + (1.0/BETA1)*(CA(11) - (CA(83)*V4/V1))+
, (1.0/BETA2)*(CA(35) - (CA(11))))+
, (1.0/BETA3)*(CA(59) - ((V2*CA(35)+(V3-V2))/V3)))
C
F(J+5*M2)= CHA3(J,2)*CA(2+5*M2)+CHA3(J,3)*CA(3+5*M2)+
, CHA3(J,4)*CA(4+5*M2)+CHA3(J,5)*CA(5+5*M2)+
, CHA3(J,6)*CA(6+5*M2)+CHA3(J,7)*CA(7+5*M2)+CHA3(J,8)*
, CA(8+5*M2)+CHA3(J,9)*CA(9+5*M2)+
, CHA3(J,10)*CA(10+5*M2)+CHA3(J,11)*CA(11+5*M2)-PEM3*
, ((V2*CA(47)+(V3-V2))/V3)*
, (R4*(B(J,1)-(PEM3+ 0.0 )*A(J,1))
, -R1*(B(J,M2)-(PEM3+0.0 )*A(J,M2))+PEM3*ALFA3*R1)+PEM3*ALFA3*
, (1.0-BETA3*(EB*
, (PHA1/(1.+ ALAMBA*(CA(J+4*M2)-1.) + ALAMBB*(CA(J+5*M2)-1.)))
, ))*CA(J+5*M2)+BETA3*PEM3*ALFA3*
, (QB10 + (1.0/BETA1)*(CA(23) - (CA(95)*V4/V1))+
, (1.0/BETA2)*(CA(47) - (CA(23))))+
, (1.0/BETA3)*(CA(71) - ((V2*CA(47)+(V3-V2))/V3)))
C: ****BED4*****
F(J+6*M2)= CHA4(J,2)*CA(2+6*M2)+CHA4(J,3)*CA(3+6*M2)+
, CHA4(J,4)*CA(4+6*M2)+CHA4(J,5)*CA(5+6*M2)+
, CHA4(J,6)*CA(6+6*M2)+CHA4(J,7)*CA(7+6*M2)+CHA4(J,8)*
, CA(8+6*M2)+CHA4(J,9)*CA(9+6*M2)+
, CHA4(J,10)*CA(10+6*M2)+CHA4(J,11)*CA(11+6*M2)-PEM4*
, (CA(59))*
, (S4*(B(J,1)-(PEM4+ 0.0 )*A(J,1))
, -S1*(B(J,M2)-(PEM4+0.0 )*A(J,M2))+PEM4*ALFA4*S1)+PEM4*ALFA4*
, (1.0-BETA4*(EA*
, (1.0/(1.+ ALAMBA*(CA(J+6*M2)-1.) + 0.0 *(CA(J+7*M2)-1.)))
, ))*CA(J+6*M2)+BETA4*PEM4*ALFA4*
, (QA10 + (1.0/BETA1)*(CA(11) - (CA(83)*V4/V1))+
, (1.0/BETA2)*(CA(35) - (CA(11))))+

```


, (1.0/BETA3)*(CA(59) - ((V2*CA(35)+(V3-V2))/V3))+
 ,(1.0/BETA4)*(CA(83)-CA(59)))

F(J+7*M2)= CHA4(J,2)*CA(2+7*M2)+CHA4(J,3)*CA(3+7*M2)+
 , CHA4(J,4)*CA(4+7*M2)+CHA4(J,5)*CA(5+7*M2)+
 , CHA4(J,6)*CA(6+7*M2)+CHA4(J,7)*CA(7+7*M2)+CHA4(J,8)*
 , CA(8+7*M2)+CHA4(J,9)*CA(9+7*M2)+
 , CHA4(J,10)*CA(10+7*M2)+CHA4(J,11)*CA(11+7*M2)-PEN4*
 ,(CA(71))*
 ,(S4*(B(J,1)-(PEN4+ 0.0)*A(J,1))
 ,-S1*(B(J,M2)-(PEN4+0.0)*A(J,M2))+PEN4*ALFA4*S1)+PEN4*ALFA4*
 ,(1.0-BETA4*(EB*
 ,(PHA1/(1.+ ALAMBA*(CA(J+6*M2)-1.) + ALAMBB*(CA(J+7*M2)-1.))
 ,))*CA(J+7*M2)+BETA4*PEN4*ALFA4*
 ,(QB10 + (1.0/BETA1)*(CA(23) - (CA(95)*V4/V1))+
 ,(1.0/BETA2)*(CA(47) - (CA(23)))+
 ,(1.0/BETA3)*(CA(71) - ((V2*CA(47)+(V3-V2))/V3))+
 ,(1.0/BETA4)*(CA(95)-CA(71)))

800 CONTINUE
 RETURN
 END

VITAE

Name: Mohammad Elias Biswas
Date & Place of Birth: November 25, 1966, Gopalganj, Bangladesh
Religion: Islam
Nationality: Bangladeshi
Marital Status: Married

Academic Achievements

March 1991 **B.S. in Chemical Engineering**
Bangladesh University of Engineering & Technology (BUET)
Dhaka, Bangladesh

Professional Experiences

Aug., 1992 To Oct 1993 **Bangladesh Council of Scientific & Industrial Research (BCSIR), Dhaka, Bangladesh.** Worked as a **Research Engineer** in the **Pilot Plant & Process Development Centre** .

July., 1992 To Aug 1992 **Bangladesh Gas Field Company Limited (BGFCL), B.Baria, Bangladesh.** Worked as a **Production Engineer**.

April., 1991 To June 1992 **Bangladesh University of Engineering & Technology (BUET), Dhaka, Bangladesh.** Worked as a **Teaching Assistant** in the **Chemical Engineering Department**.

Extra Curriculum Activities

Elected as **Vice President (V.P)** in the **Chemical Engineering Department, BUET, Dhaka, Bangladesh**

Research Publications

1. **M. M. Hassan, K. F. Loughlin, and M. E. Biswas, "Optimization of Continuous countercurrent Adsorption Systems", (Accepted) Separation Technology, 1995**
2. **M. M Hassan, S. A. Beg, and M. E. Biswas, "Modelling of Simultaneous Biodegradation and Adsorption for Reactors Packed with Activated Carbon", (submitted) Chemical Engineering Communication, 1995.**
3. **M. M. Hassan, K. F. Loughlin, and M. E. Biswas, "Optimization of SORBEX System with non-linear isotherm", (Submitted) Separation Technology, 1995**